SELECTIVE LASER SINTERING OF PHARMACEUTICAL PRINTLET FORMULATIONS

A Thesis

by

CYRUS ALEXANDER FUNKHOUSER

Submitted to the Office of Graduate and Professional Studies of
Texas A&M University
in partial fulfillment of the requirements for the degree of

MASTER OF SCIENCE

Chair of Committee,	Mathew Kuttolamadom
Committee Members,	Ziyaur Rahman
	Angie Hill Price
Head of Department,	Reza Langari

May 2021

Major Subject: Engineering

ABSTRACT

The purpose of this paper was to investigate the additive manufacturing of pharmaceutical medications through powder bed fusion (PBF), specifically selective laser sintering (SLS) with an objective to achieve printlets with competitive mechanical properties without compromising the drug's performance in an extended release study. Currently, pills/tablets are made through a combination of mechanical, pressing, and heat application processes in large standardized batches. Using additive manufacturing to make medications offers significant flexibility in personalization for the patient, Just-In-Time manufacture and delivery, and at the point of care, often in rural or underserved areas. SLS is a new method to manufacture pharmaceuticals, but one which has not been well-understood, especially in terms of process parameter effects on printlet quality and performance. In this study, the effects of process input variables related to temperature and laser energy density imparted, in conjunction with relative powder fractions and particle size distributions were studied against printlet quality and performance (both mechanical and pharmaceutical). Results show the fine balance needed to achieve structural integrity while not degrading the drug, and that controlling surface temperatures and particle sizes were the keys to printlet quality/performance.

ACKNOWLEDGEMENTS

Thank you to my committee, Dr. Kuttolamadom, Dr. Price, and Dr. Rahman, whose guidance before and during my time in the master's program has been crucial in my work.

Thank you to everyone at the Department of Pharmaceutical Research who taught me all the testing methods and assisted me with the equipment.

Thank you to Mr. Lewis and Mr. Hurst at ARL for granting me use of their SEM.

Finally, thank you to all my family and friends for your constant love and support.

CONTRIBUTORS AND FUNDING SOURCES

Contributors

This work was supervised by a thesis committee consisting of Dr. Mathew Kuttolamadom and Dr. Angie Hill Price of the Department of Engineering Technology and Industrial Distribution and Dr. Ziyaur Rahman of the Department of Pharmaceutical Research. I was granted use of the pharmaceutical testing equipment by Dr. Rahman.

Individuals who also aided in contribution to my thesis include Dr. Sogra F. Barakh Ali, Dr. Sathish Dharni, and Dr. Eman Mohamed of the Department of Pharmaceutical Research, as well as Mr. Daniel Lewis and Mr. Michael Hurst from Army Research Labs. The individuals from Department of Pharmaceutical Research assisted with training and use of the equipment. Dr. Ali also prepared the HPLC column carbamazepine and helped prepare the analytical method. The individuals from Army Research Labs assisted in training and operation of the SEM.

All other work conducted for the thesis was completed by the student independently.

Funding

This study was partially funded by T3, Texas A&M Triads for Transformation.

NOMENCLATURE

SLS	Selective Laser Sintering
CBZ	Carbamazepine
KDSR	Kollidon® SR
R. R.	Candurin® Ruby Red Sheen
AM	Additive Manufacturing
PBF	Powder Bed Fusion
USP	United States Pharmacopoeia
SEM	Scanning Electron Microscopy
XRD	X-Ray Diffraction
DOE	Design of Experiments
FTIR	Fourier-Transform Infrared Spectroscopy
NIR	Near-Infrared Spectroscopy
API	Active Pharmaceutical Ingredient
Printlet	A pharmaceutical tablet made in a 3D printer

TABLE OF CONTENTS

Page

LIST OF FIGURES

Page

LIST OF TABLES

Page

CHAPTER I

INTRODUCTION

Additive manufacturing is relatively new to the pharmaceutical industry when compared to other areas of medical manufacturing. Currently, only one drug, an anticonvulsant called SPRITAM, is FDA approved to be produced by additive manufacturing, which was approved in 2016 [1]. Although only SPRITAM is FDA approved, additive manufacturing shows potential to be worthwhile to explore in pharmacy, as additive manufacturing allows for the medication to be highly customized to cater towards each patient. This is especially important in the area of pediatrics, as some medications that are prescribed to a child may only be readily available in adult dosage amounts. In order to give the child, or any patient with the need for specialized prescription, the correct dosage, the readily available medication must be manipulated by means of partitioning, a process in which the drug is dissolved and reconstituted in a diluted form. This method poses a reliability issue on the accuracy of the dose partitioned. Additionally, if the medication is available in solid form, a different strength of the prescribed medication must be manufactured, but the mechanical presses used to manufacture medication are highly standardized to set dosage amounts in order to maintain a high efficiency, proving difficult to deviate from those dosages [2].

Additive manufacturing allows one to make customized dosages based on the powder mixture and size of tablet. These printed tablets, or printlets, can also be made immediately after the prescription is given, so the medication is not made beforehand, slowly expiring over time. It can be made and given on the same day as the prescription

is given because the 3D printers can be located at the point of care (hospitals, doctor's offices, etc.). It should be noted that the output of additive manufacturing is significantly lower than the conventional methods, such as the mechanical presses. The purpose of using additive manufacturing to manufacture medication is not to replace the current methods. Rather, the purpose of using additive manufacturing is to supplement these methods by taking the role of handling the specialized prescriptions.

The outcomes of this study were approached from both engineering and pharmaceutical viewpoints. In terms of engineering, the process parameters of using additive manufacturing, specifically selective laser sintering (SLS), are not well-understood. This study's outcomes provide insight on how the different process parameters present in SLS, and not in the conventional medication manufacture, can affect printlet performance. In terms of pharmacy, the focus was on exploring these process parameters in an extended drug release study, as prior studies involving SLS of pharmaceuticals are mostly centered around instant release studies.

CHAPTER II

BACKGROUND AND LITERATURE REVIEW

Pharmaceutical Manufacturing Overview

Tablets are currently manufactured in a mechanical process and then are measured against standards set by the United States Pharmacopoeia (USP). First, all components of the tablet must be thoroughly mixed. If a homogeneous mix of all the powders going into making the tablet cannot be achieved by mixing, granulation processes can be performed to mix the powders together. Failure to achieve a homogenous mixture can be caused by the powders not having good flowability. USP 1174, Powder Flow, provides guidance and tests to determine if the powder flowability is adequate enough to perform mixing without granulation processes [3]. The powders undergo either wet or dry granulation if mixing alone is insufficient at achieving a homogeneous mixture. Wet granulation [4] is the process of mixing the powder particles by using a granulating fluid to assist powder adhesion before the powder compression. Depending on the drug involved, different fluids may be used. If the drug and other powders are susceptible to hydrolysis, a solvent other than water may be used. Otherwise, water is commonly used as a granulating fluid, as it is non-toxic and non-flammable. After powder mixing and adhesion, the powder is dried, using hot air. Dry granulation [5] is the process of using pressure, whether through a press or a roller compactor to compress the powder together. The press is similar to the final compression of the powder to form the actual tablet, but in this case, the powder is broken up back into granules. These newly-formed granules are smaller, which

increases flowability. This process is desired if the drug is sensitive to heat or moisture. After the powder is properly mixed, it is compressed into the tablet. A lubrication fluid is commonly used to help the powder flow into the dies where it is pressed together by a force of 2 tons to form the tablet [6]. Lastly, a coating may be applied to the tablet, or the tablet may be left without a coating as the finished product. Once at the final compression stage, a tablet pressing machine can produce anywhere from 5,000 tablets/hour to over 200,000 tablets/hour [2], depending on the machine.

These tablets are subjected to quality control tests set by the USP [3]. Such tests include friability, disintegration, breaking force, dissolution, weight uniformity, and many other tests. Testing weight uniformity prevents incorrect dosages amounts from tablets with incorrect weights. The friability test is conducted to determine if the tablet holds its structure or breaks into smaller pieces when rubbed against other tablets or surfaces [7]. Hardness testing is a test conducted to determine pill's resistance to crushing to understand how it will withstand handling and transportation in manufacturing, distribution, and in the field [8]. The disintegration time test determines if the tablet disintegrates within a set time when placed in a solvent. Lastly, the dissolution test determines the rate at which the drug dissolves into the solvent. In this paper, the hardness and dissolution of the tablets made through SLS will be explored. However, it should be noted that while these are key critical quality attributes, there are many others that go into making a tablet acceptable.

Additive Manufacturing of Pharmaceuticals

Additive manufacturing has been explored as an alternative to the mechanical process for manufacturing pharmaceuticals. Currently, the only pharmaceutical approved by the FDA to be manufactured through additive manufacturing is Spritam [1], an anticonvulsant drug to prevent seizures, and it must be manufactured through the powder bed fusion (PBF) process known as binder jetting [9]. Binder jetting starts by having a layer of powder spread into the printing area. Next, a solvent, or the binder solution, is placed in the area where the printed part is desired in order to fuse the powder together. Then, another layer is placed, and the previous steps are repeated. The remaining powder around the fused powder acts as a support for the printlet. Once finished, the printlets are cured in a heating chamber to remove any unevaporated binder solution. This is the only process where the printlets are exposed to thermal energy, and the heat is low (under 50° C), as the heat is only applied to evaporate the binder solution. Binder jetting produces printlets with poor mechanical properties due to high porosity in the finished printlets [10]. However, the printlets produced disintegrate very rapidly, in under 15 seconds, when taken orally with no water. This low disintegration time is critical when the patient undergoes a seizure, as the quicker the printlet disintegrates, the quicker the drug can be absorbed by the body to stop handle the seizure.

In addition to binder jetting, other methods, such as stereolithography (SLA), have been explored to make pharmaceutical tablets [11]. SLA is a form of resin-printing where a liquid solution is heated by a laser to melt and form polymers layer by layer. The resin is placed into a tank with a platform. The laser's power is directed at the

platform, and the layer of the product is traced. Then, the platform moves one printing layer lower into the tank, resin covers the top of the printed layer, and the laser again traces the layer for the product. The process is repeated until the part is complete. These successes shows that additive manufacturing can be used to manufacture pharmaceuticals; however, other additive manufacturing methods (FDM, SLA, SLS) of other drugs require further direction and research in order to be approved by the FDA.

Selective Laser Sintering (SLS) of Polymers

SLS is a form of powder bed fusion (PBF). PBF is one of the seven categories in additive manufacturing (AM). SLS allows for AM without requiring a mold or supports. The SLS process can be broken down into three stages: powder recoating, energy input, and coalescence and cooling [12].

Powder recoating is the stage when a fresh layer of powder is evenly placed into the printer's powder vat where sintering occurs. Many factors go into effectively placing each new layer of powder. The first factor is good powder flowability. Both powder shape and size are important parameters when trying to achieve good flowability. The powder should have good sphericity, which is defined as the goal to have each particle as close to a perfect sphere as possible [13]. Having irregular and differently shaped particles leads to increased friction between the particles. This friction lowers the flow efficiency of the powder [14, 15]. In terms of flowability, powder size from 45 μm to 90 μm is suitable for SLS [16]. Fine particles are desired for good flowability, but when powder particles become smaller than 45 μm, they begin to

agglomerate, lowering their rheological properties, making an uneven layer. Particles that are too large are not really discussed from a flowability standpoint. Chatham [12] explains that this field prefers smaller particle sizes for other reasons, such as lack of fusion between layers and porosity in the final product. Similarly, to the powder in the mechanical process, if the powder chosen does not have good flowability, it must be properly prepared to suitable size and shape before printing. Another important factor of powder recoating is how the printer mechanism lays out the new layer. Currently, there are roller and blade mechanisms that spread new powder layers. The roller method is preferred and will be used in this study, as it creates a more even layer with lower surface roughness than a layer made by the blade [17]. It should also be noted that one appeal to using SLS is that the used powder can be recycled, as long as its properties have not degraded to where the flowability is compromised [18, 19].

The next stage of SLS is the energy input. The term stage should not be completely thought of as each stage is done chronologically. While this is mainly true, it should be noted that some parts of the energy input occur during the other two stages. In SLS, there are two forms of energy input: chamber heating and laser input. The chamber heating can also be referred to as the "bulk heating," whereas the laser is responsible for heating the material enough to achieve sintering. A number of factors go into both types of energy input. The chamber temperature should be very close to, but not over, the material's glass transition temperature, T_g [20]. There is a balance that must be achieved—having a high chamber temperature results in less of a temperature change needed from the laser to achieve layer fusion. Having a higher temperature results not

only in better fusion in the layer but also better fusion between layers. However, having a low chamber temperature avoids any unwanted fusion, branching, and powder degradation outside the laser area, caused by residual heat from previous layers and laser energy [19]. The chamber temperature is maintained by coils and lamps within the printer [21]. The other energy input is from the laser. After the chamber and powder are heated to the desired temperature, the laser is used in the area where the sintering is required. Different parameters go into the powder absorbing the laser's energy. The first and second parameters are powder size and shape. A smaller powder size needs less energy to begin melting, as many small particles have a larger surface area than one large particle. A larger surface area leads to more material exposed to the laser. The powder shape also affects how the laser's energy is distributed. Chatham [12] describes a phenomenon called "multiple scattering." It is stated that spherical particles offer a high number of paths and angles off which the laser can reflect onto other particles, rather than the laser's energy hitting the layer and immediately bouncing up and into the atmosphere. This helps with creating good fusion in each layer and between the layers. However, the powder does not absorb enough energy from the laser alone with this multiple scattering effect. Therefore, additives are put in the powder to better absorb the laser's energy. There are several additives that can be added to the powder mixture, such as carbon black [22], or some nontoxic alternatives are Candurin ® Gold Sheen (edible gold dust) or Candurin ® Ruby Red [23, 24]. Sufficient energy from the laser must be absorbed into the material to have enough surface energy to achieve molten flow. Attaining enough surface energy with an amorphous material can be difficult,

unreliable, and unpredictable, as amorphous material's change in viscosity due to temperature change is very gradual [25], whereas the viscosity change in semi-crystalline materials is more precise and predictable. Also, to attain the viscosity of a semi-crystalline polymer, an amorphous polymer must be heated to much higher temperatures. For these important sintering qualities, semi-crystalline polymers were chosen for this study. Once the powder's surface energy is high enough to achieve flow, fusion can occur. The more flow will lead to more fusion, which leads to less porous material with higher strength [26]. The mapping of laser application has been studied for PA 12 [27] to determine how the printlet quality is affected. PA 12 is a commonly-used powder in SLS of polymers [19]. This study concluded that the pathing the laser takes does not significantly affect the mechanical properties, except for the material toughness.

The final stage in SLS is the coalescence and cooling. This stage is further broken into two parts: individual layer cooling after laser exposure and completed printlet cooling after being removed from the heated chamber. The cooling after each layer is dependent on the laser speed and the chamber temperature. The longer the laser is in contact with the material, the more thermal energy the material absorbs. This leads to a higher cooling time for each layer when compared to having a smaller laser exposure time, as each layer cools towards the chamber temperature once the laser has finished its energy input [8]. The chamber temperature has the opposite effect on this interaction. The higher the chamber temperature, the more thermal energy the powder layer absorbs. This leads to a lower cooling time for each layer when compared to

having a cooler chamber temperature because, as mentioned, the layer after the laser's exposure cools towards the chamber temperature. Also, limiting the layer cooling with a high chamber temperature, one close to the powder melting point, slows crystallization rate. As each printlet layer solidifies and cools, the semi-crystalline polymer begins to grow crystal formations [15]. The crystals grow faster when the material is cooler. To achieve the best mechanical properties, inter-layer crystals, crystals growing from layer to layer, are desired. These crystals help avoid build-up of residual stress in the printlets [28]. Intra-layer crystals can cause non-uniform shrinkage, and the non-uniform shrinkage can cause layer warping and deformation, especially in the first few layers of the printlet.

Using SLS to Manufacture Pharmaceuticals: Previous Studies

To date, several [29-35] studies on the manufacture of pharmaceuticals by SLS have been conducted. Fina's first study [32] was conducted with very low to fair drug concentrations (5, 20, 35%) to determine if SLS could be used to manufacture pharmaceuticals without degradation of the drug. The conclusion was the tablets could be made without drug degradation with the parameters chosen. Fina conducted another study [34] focusing more on orally disintegrating tablets. These printlets' mechanical properties exhibited similar behavior to the Spritam, as the printlets dissolved in less than 4 seconds once taken orally. The rapid disintegration was a consequence of the porosity and poor strength of the printlets. Awad's first study [33] was to test just how customizable drug manufacture could be with SLS. In this study, two different powders

were used for the printlet. The printlet manufacture was split into two halves: one powder was used to manufacture the bottom half, and the second powder was used to manufacture the top half of the pellet. Awad's second study [31] also focuses on the precision and customizability of SLS to manufacture pharmaceutical printlets. In this study, printlets were manufactured with Braille and shape patterns on their top layers for visually impaired patients. Ali's study [29] began exploring the printing parameters needed to formulate the tablets with the best mechanical properties while still maintaining instant release capabilities without drug degradation. Allahham [30] conducted another study on orally disintegrating tablets manufactured through SLS. The final study [35] investigates the effect of thermal energy input on the printlets. It should be noted that none of the studies entirely focus on an extended release pharmaceutical tablet, and they do not account for the powder size distribution as a printer parameter beyond having all powder below 150 μm or lower, depending on the study.

Using SLS to Manufacture Pharmaceuticals: Appeals and Goals

The main appeal to using polymer SLS over other additive manufacturing, such as selective laser melting (SLM) or fused deposition modelling (FDM) is preservation of the drug or other active ingredients in the pharmaceutical products. SLM and FDM, for example, require completely melting the powder mixture to make products [36, 37]. Fully melting the powder mixture can degrade the drug and change its properties [38]. The SLS process, however, does not completely melt the powder mixture. Also, unlike in multi-jet fusion (MJF), SLS does not require a solvent mixture to be sprayed on each

layer. This is important, as every material in the manufacturing of pharmaceuticals must be non-toxic [39]. Also, the solvents take time to evaporate, increasing the amount of time needed to get the pharmaceuticals to patients; one of the main goals of using additive manufacturing to make pharmaceuticals is to quickly complete printlets, so patients may be given their medications the same day of receiving their prescriptions. Additionally, humid environments or other environments that cannot accommodate drying may not have suitable areas for printlets to dry if they were made with additive manufacturing processes that require solvent. The advantages with using SLS to manufacture pharmaceutical tablets have yielded successful studies, primarily with instant release tablets [29-35]

Using SLS to Manufacture Pharmaceuticals: Knowledge Gaps and Challenges

While SLS has its advantages and appeals to quickly manufacture highly customizable pharmaceuticals, there are knowledge gaps and challenges associated with using SLS. SLS with polymers is a relatively new process, so many parameters during the manufacturing process are either based on empirical data or not able to be controlled at all. For example, a term called the "glaze point" is sometimes used to determine what temperature to hold the chamber. The glaze point is the temperature when the powder mixture begins to "glisten and shimmer" and starts to melt in the chamber [12]. This glaze point is not a standardized term; it is determined by the operator at the time of printing. The glaze point is determined by one source of energy input, the chamber and surface heating. Another knowledge gap is understanding the balance between the

chamber heating and the other source of energy input, the laser. This balance must be achieved in order to produce printlets with good structural integrity without compromising the properties of the drug. Another challenge with SLS is attaining uniform layer cooling. The current chamber heaters do not keep the powder beds at a homogeneous temperature [40]. Also, the chamber temperature can vary during the printing process, which can influence the mechanical and pharmaceutical properties of the printlet. In addition to varying chamber temperature, the layer cooling after laser exposure is not controlled—the material simply starts cooling towards the chamber temperature until a new layer is put on top of it and the laser is used again. Many of the studies and works on polymer SLS are done with PA12, but different materials are used in this study, as PA12 is not safe for ingestion [41]. One final consideration not discussed until after this study's conclusion was the effect of humidity on the powder and the printing process. Though not taken into consideration until after the study was finished, differences in humidity can potentially affect how the powder flows, how it absorbs energy, and how it cools. Additionally, humidity may also have an effect on drug degradation.

CHAPTER III

MATERIALS AND METHODS

Materials

Kollidon® SR

Kollidon® SR (KDSR) was chosen for this study on extended release tablets. This polymer has been used in direct compression, hot-melt extrusion, wet granulation, sprays, and other methods [42], and when compared to other excipients, it proved to be a strong choice for extended release purposes [43]. KDSR is a copolymer, consisting of 80% polyvinyl acetone (PVAc) and 20% polyvinylpyrrolidone (povidone). KDSR, unlike Kollidon® VA64, is largely insoluble in water, inhibiting its ability to disintegrate quickly [44]. The PVAc is insoluble in water, and the povidone is soluble. This trait is essential when controlling drug release over an extended period of time, as the majority of the material holds its structure when placed in water, but the povidone dissolves, allowing for the active ingredient to navigate its way out of the melted PVAc structure. In addition to extended release properties, KDSR is appealing due to its good flowability. Though it has been extensively used in other methods of pharmaceutical manufacture, KDSR, along with extended release studies as a whole, has not been commonly used in SLS operations. KDSR meets the current standards to be accepted by the European Pharmacopeia, and a US-DMF has been filed [44]. KDSR has a melting point of 130 °C. Figure 1 and Figure 2 show how the powder appears normally, as well as in the SEM.

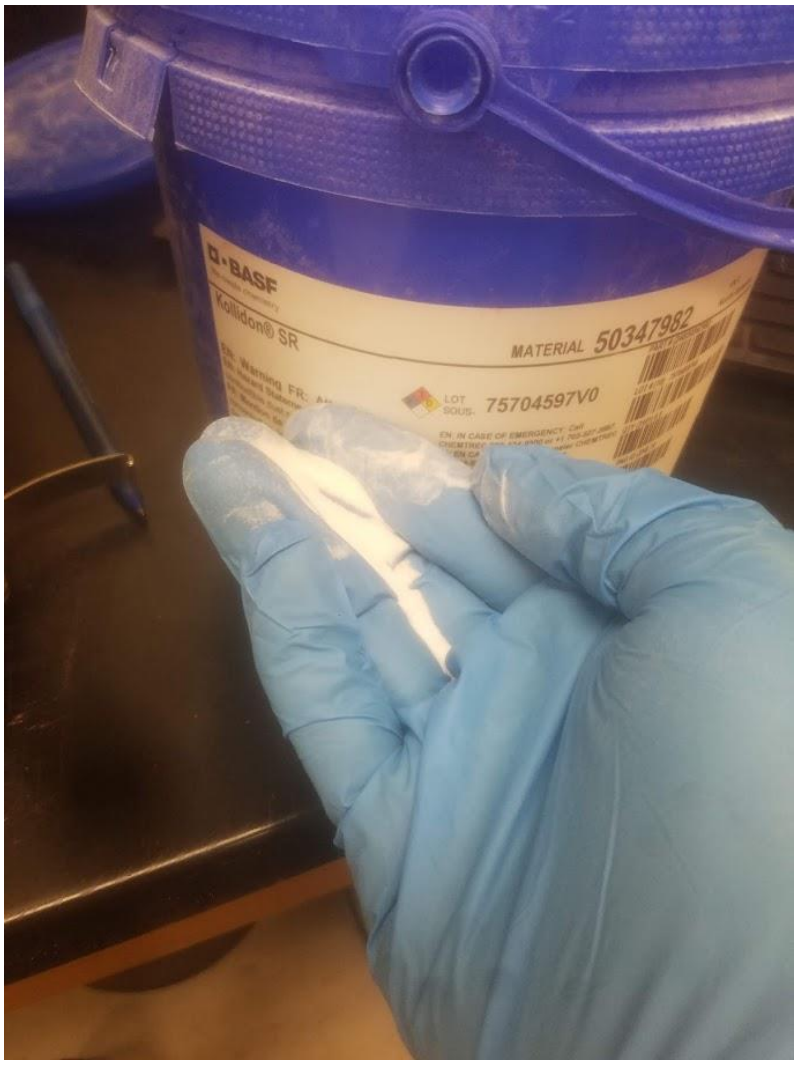

Figure 1: Kollidon® SR normal view

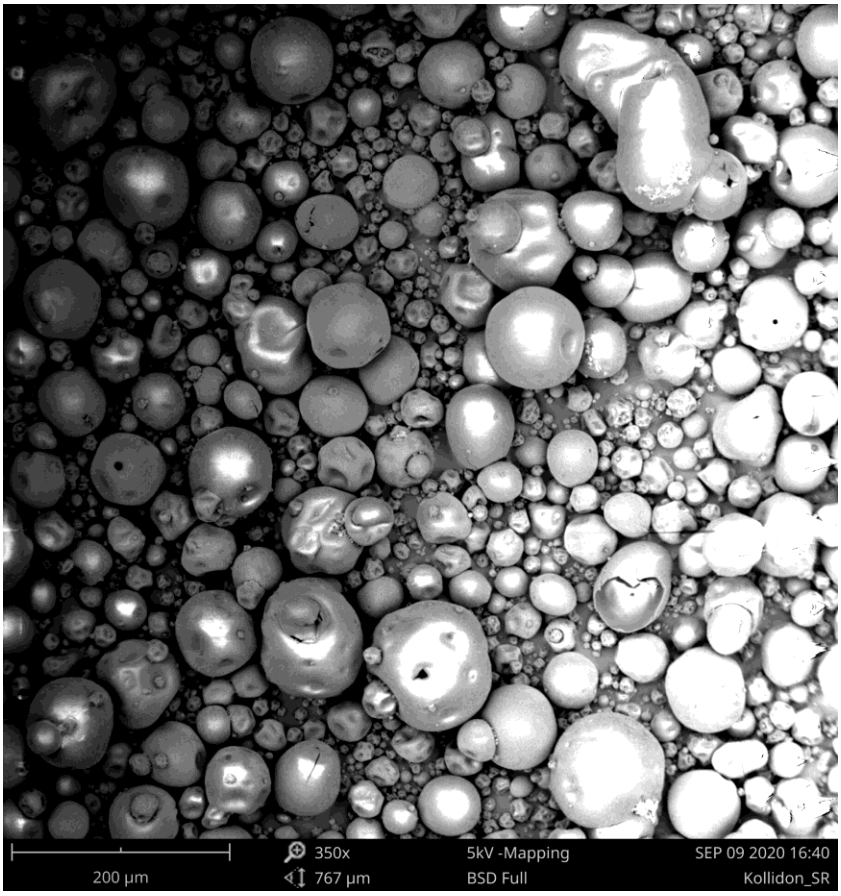

Figure 2: SEM Image of Kollidon® SR at 350x magnification

Carbamazepine (Drug/API)

Carbamazepine (CBZ), $C_{15}H_{12}N_2O$, was the active pharmaceutical ingredient (API) used for this study. CBZ is an anticonvulsant, used to prevent seizures, as well as treat bipolar disorders [45]. CBZ is a medication prescribed at twice a day at 50mg (for children), 100, 200, 300, or 400 mg doses, making it a good candidate for conducting an extended release study. Also, CBZ has already had extensive USP testing conducted on it at Texas A&M, so the methods for conducting the USP tests were already determined,

allowing the study to focus more on the additive manufacturing. Figure 3 and Figure 4 show how the powder appears normally, as well as in the SEM.

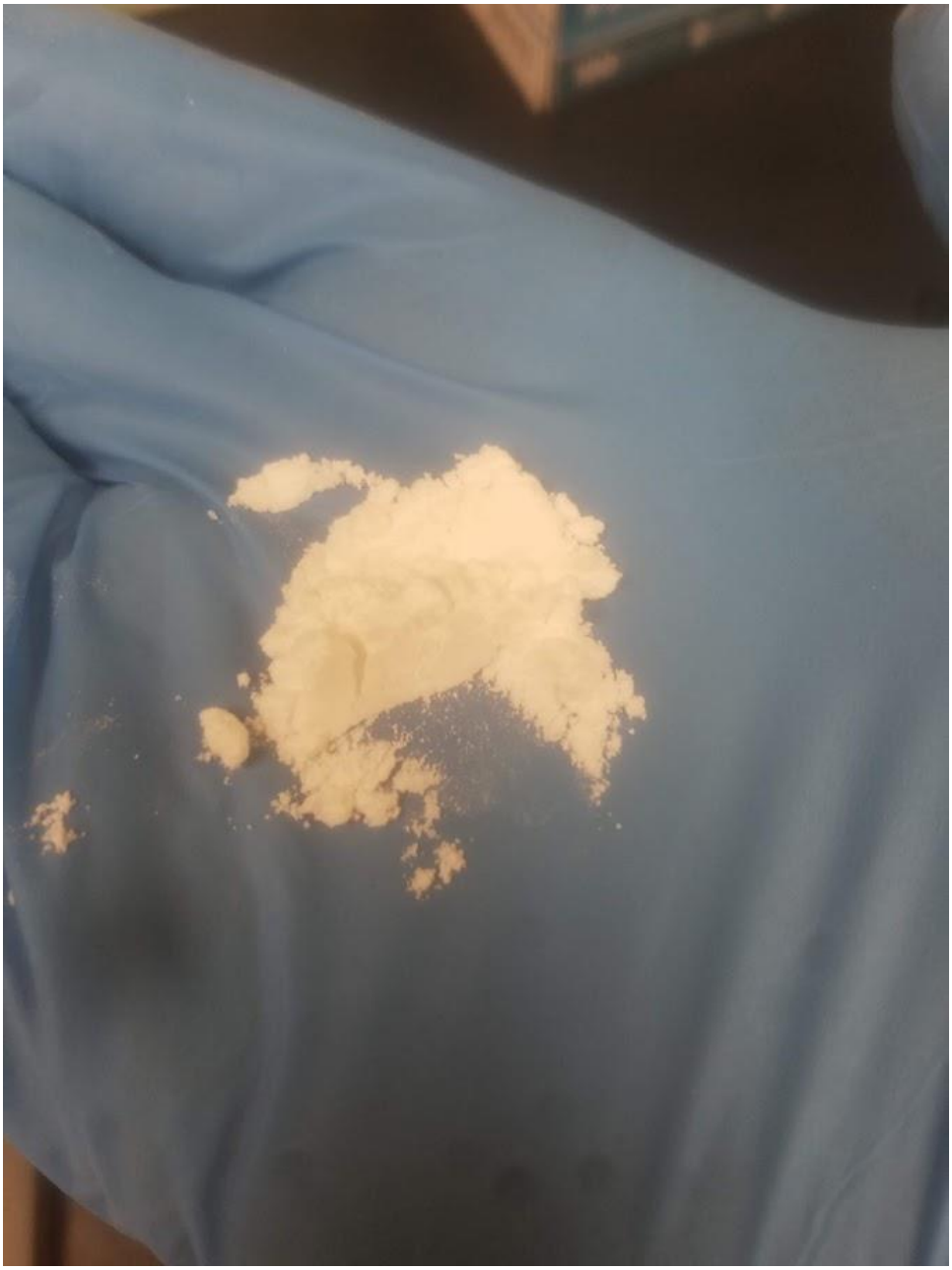

Figure 3: Carbamazepine normal view

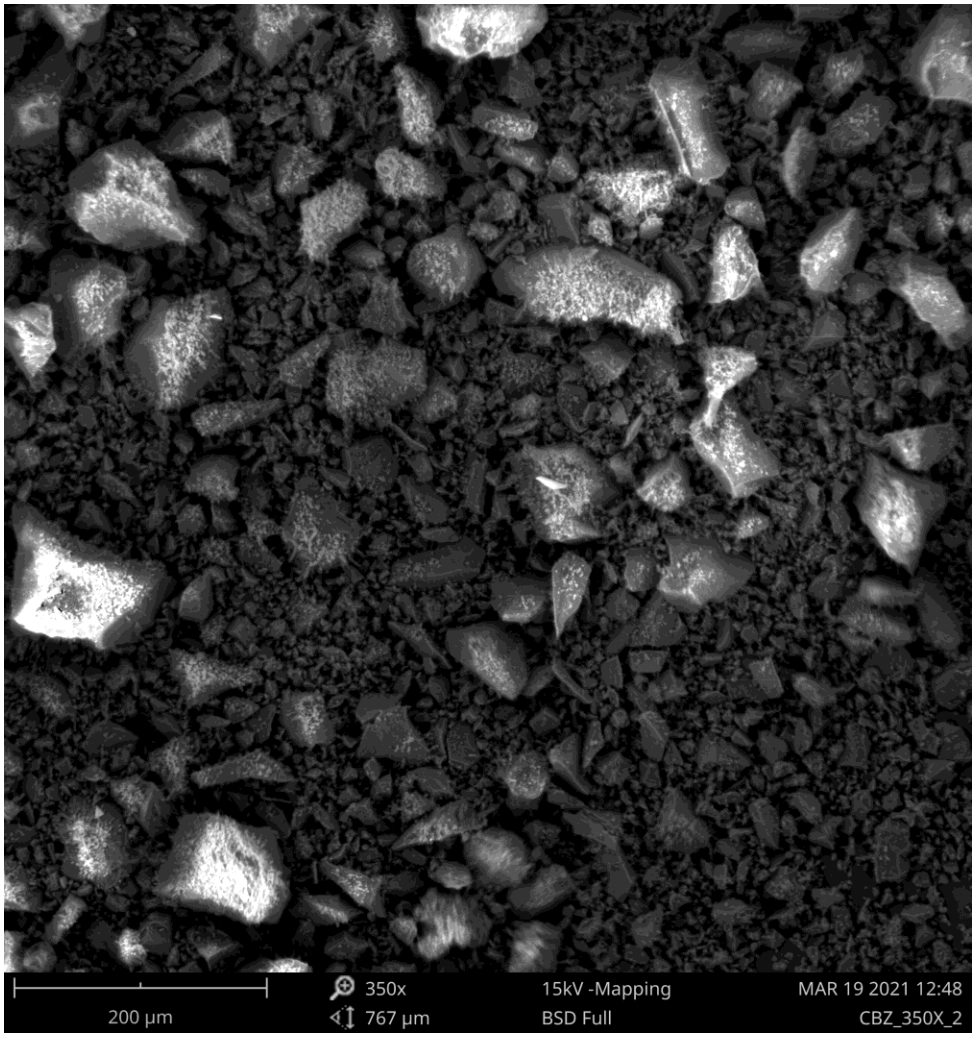

Figure 4: SEM Image of carbamazepine at 350x magnification

Candurin Ruby Red Sheen

The sheen additive used to aid the powder in absorbing the laser's energy was the Candurin® Ruby Red Sheen, silicon dioxide coated with iron oxide [45]. Of all the sheen additives, the Ruby Red and Gold products have both shown success in SLS of pharmaceuticals in instant release studies. The Ruby Red was chosen over the Gold, due

to the abundance of the Ruby Red available. Figure 5 and Figure 6 show how the powder appears normally, as well as in the SEM.

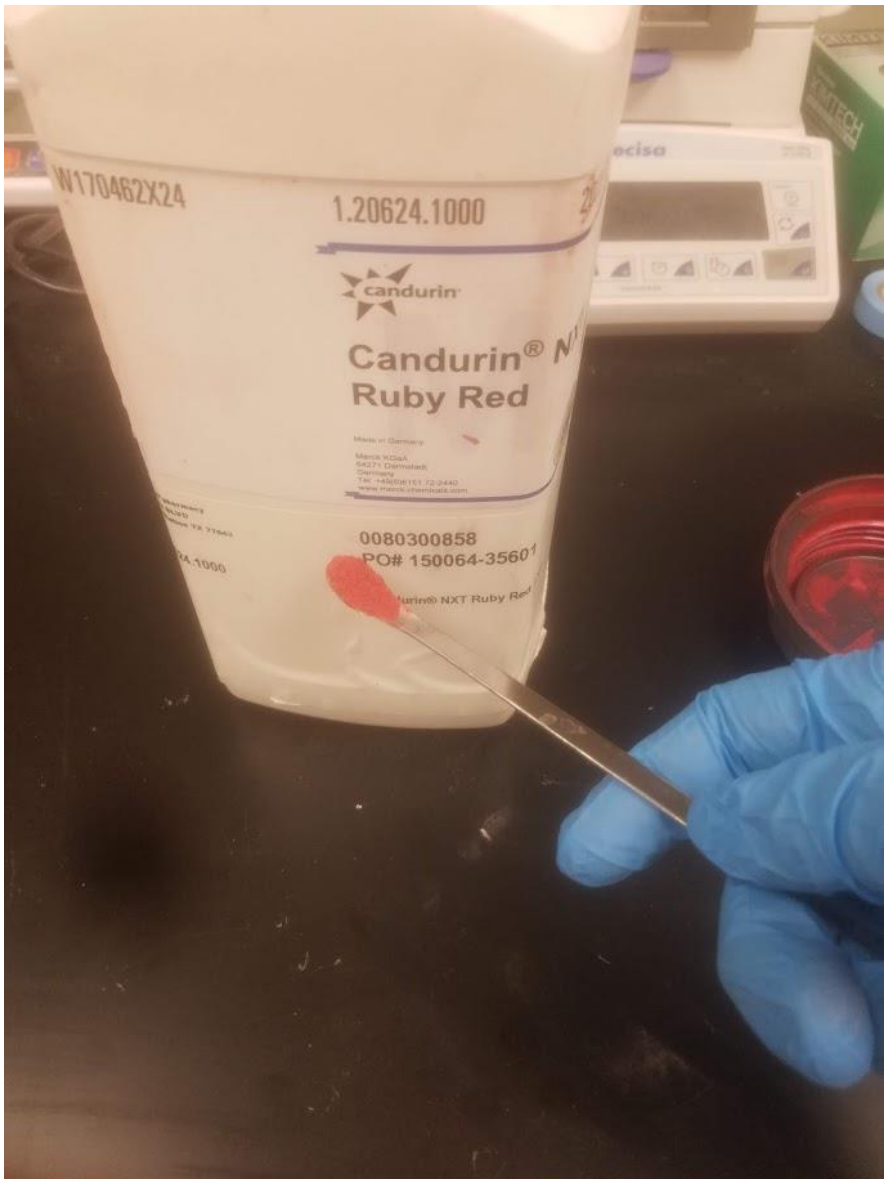

Figure 5: Sheen normal view

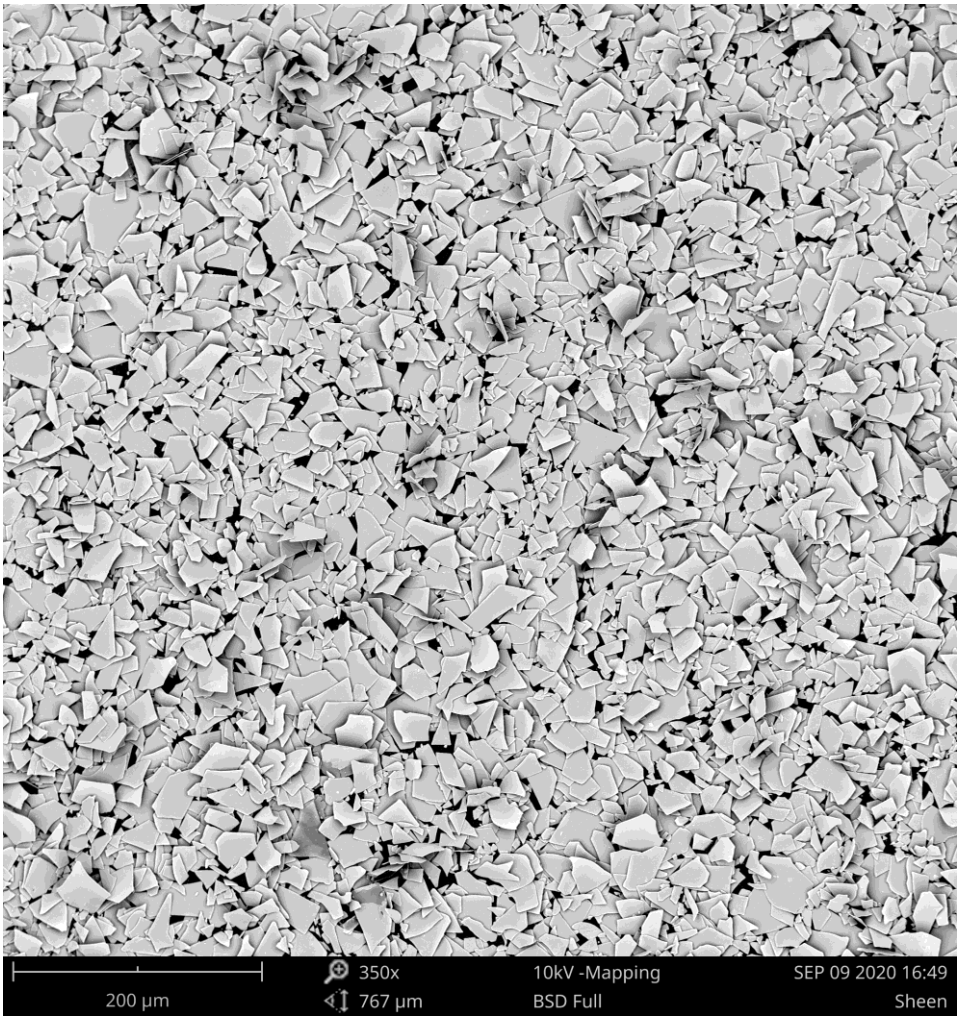

Figure 6: SEM Image of sheen at 350x magnification

Kollidon® VA64

Although Kollidon® VA64 was not chosen as the final polymer for this study, it was heavily considered and referenced when drawing conclusions about powder behavior. This polymer has already been used in direct compression, wet granulation, film-coating, and sprays in the mechanical process of pharmaceutical manufacture [42, 46]. In addition, it has been used in multiple studies regarding SLS of polymers

focusing on manufacture of pharmaceuticals [29, 31]. Kollidon® VA64 is a vinylpyrrolidone-vinyl acetate copolymer. It is soluble in both alcohol and water. In terms of disintegration, Kollidon® VA64 is used in this study for its excellent disintegration capabilities, allowing for instant release. Instant release is defined as "releasing the active ingredient immediately when it reaches the stomach [47]." However, it should be noted that Kollidon® VA64 is not limited to just instant release. When combined with other components, examples being polyacrylic acid and stearyl alcohol [46], Kollidon® VA64 can also be a suitable binder for sustained release. Kollidon® VA64 also meets the current standards to be accepted by the European Pharmacopeia, United States Pharmacopeia under "Copovidone," and the Japanese Pharmaceutical Excipients under "Copolyvidone" [46].

Methods

SLS Printing

The Sintratec Kit, shown in Figure 7, was chosen as the 3D printer for the study. The Sintratec Kit [21] allows for changes in chamber temperature, laser scan speed, and layer thickness. The chamber temperature can heat up to 150°C. The laser wavelength is 455 nm, and its max scan speed is 650 mm/s. This printer has a constant laser power of 2.3W. The printer has two bays to hold the powder mixture. Like with other powder bed fusion (PBF) printers, the Sintratec Kit moves one layer of powder from one bay to the other. Then, the laser's energy is applied. A new layer of powder is moved from the fresh powder bay to the sintering area to continue the process. The tolerance of both of

these temperatures is ± 5 °C. However, the temperature variability upon observation can deviate as much as 10 °C from the desired temperatures. This Sintratec Kit is a 3rd generation model in the Sintratec Kit line. The Sintratec software was the software used to conduct the prints. The printlet .stl files were created in Fusion360 and imported into the Sintratec Software.

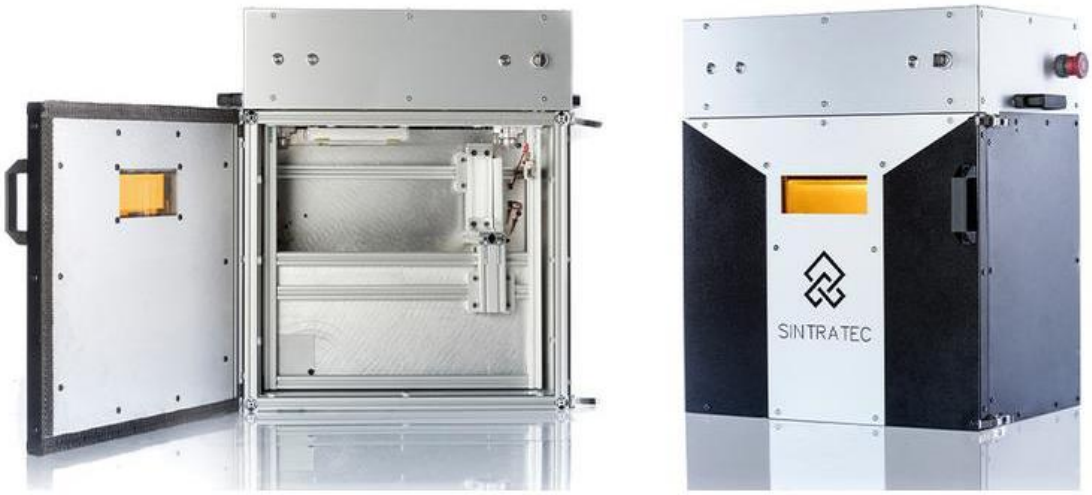

Figure 7: Sintratec SLS Printer [21]

Hardness Testing

Two different hardness testers were used to gain insight on the crushing resistance of the tablets. The first machine used was the VK 200 Tablet Hardness Tester [48], and the second machine used was the TA.XT Texture Analyzer [49]. The machines measure hardness, or rather, resistance to crushing, in kiloponds (not to be confused with a kilopound) and newtons, respectively. The VK200 and Texture Analyzer are shown by Figure 8 and Figure 9, respectively.

Figure 8: VK200 Tablet Hardness Tester

Figure 9: TA.XT Texture Analyzer
Reprinted from Reference 49

Dissolution Testing

The dissolution test was conducted to determine how much of the carbamazepine was released over a 24 hour period, as per the carbamazepine extended-release tablets USP-NF [50]. 2 mL dissolution samples at 3, 6, 12, and 24 hours were collected. The dissolution test performed was using the basket apparatus, apparatus 1, in USP 701 for dissolution [51]. The dissolution machine used was the Agilent 708-DS Dissolution Apparatus [52]. To analyze the dissolution samples, an Agilent HP 1260 series HPLC was used [53]. Each printlet formulation in the final DOE was conducted in triplicate for this test. To conduct HPLC analysis, calibrations of 5, 10, 20, 25, 50, and 100 µg CBZ in 30% ACN, 30% Methanol, 40% water solution. 15µg CBZ in the mentioned solution was chosen to be the system suitability. The calibration is shown below in Figure 10.

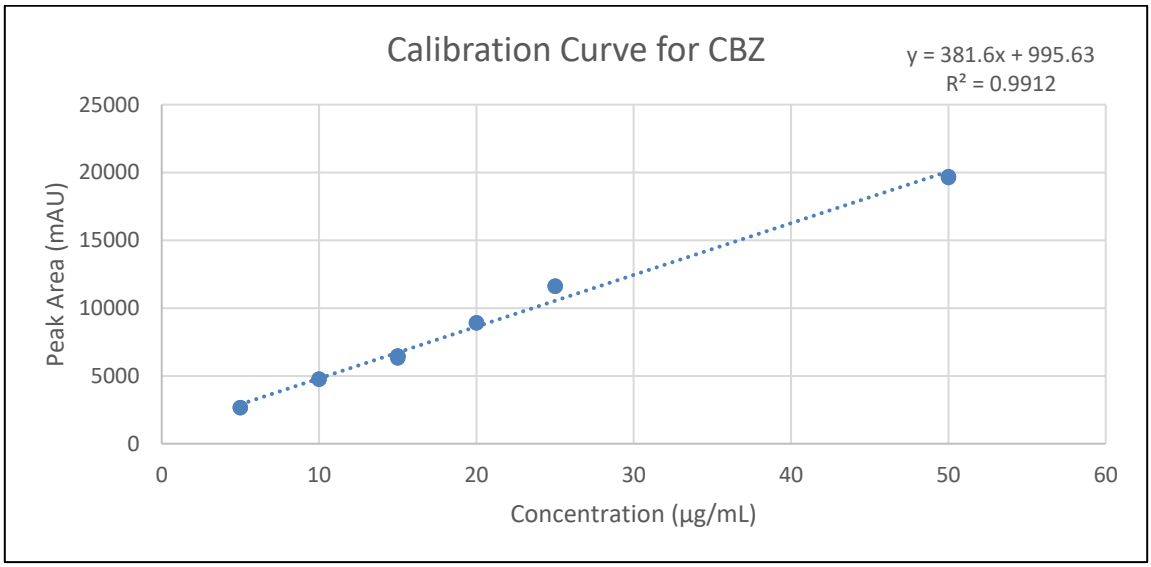

Figure 10: Calibration curve for the dissolution analysis

Each calibration and dissolution sample were run twice in the HPLC, except for the system suitability, which was run six times. The mobile phase was 35% water containing 0.1% acetic acid glacial and 65% methanol. The sample injection was 10µl, the flowrate was 1mL/minute, and the run time per injection was 10 minutes. The signal used for reporting was at a wavelength of 214 nm. OpenLab Software by Aglient Systems was the software used to acquire the data. Figure 11 and Figure 12 are photos of the dissolution equipment and the HPLC, respectively.

Figure 11: Dissolution Testing Equipment [54]
Reprinted from Reference 54

Figure 12: Agilent 1260 Infinity II HPLC used for Dissolution Analysis Reprinted from Reference 53

Scanning Electron Microscopy

SEM imaging was conducted to back the claims made by the hardness and dissolution testing. The machine used to conduct the SEM imaging was the Phenom XL Desktop SEM [55]. Magnifications of 350x, 500x, and 1000x were taken for powder and printlet comparison. Powder specimens were sprinkled onto conductive tape, and printlets were placed directly onto the sample holder. Accelerating voltages of 5, 10, and 15kV were utilized.

Testing Changes in the API/Drug Degradation

Multiple tests were conducted to investigate drug phase changes and drug degradation.

Attenuated Infrared Spectroscopy

A Nicolet iS50 FTIR Spectrometer was used to analyze the CBZ, unprinted powder, and the printlets from the final DOE [56]. The wavenumbers for analysis were between 500 – 4000 cm^{-1}, and OMNIC V9.0 software was used.

Near-Infrared Spectroscopy

The same instrument used for the FTIR also has NIR capabilities, so the Nicolet iS50 was used to conduct NIR on the CBZ, unprinted powder, and the printlets from the final DOE. The wavenumbers for analysis were between 4000 – 10000 cm^{-1}, and OMNIC V9.0 software was used.

X-Ray Diffraction

The XRD machine used is a Bruker AXS D2 Phaser. The two-theta values range is from 58.998° – -0.002°. The voltage, current, and power values were set at 30kV, 10mA, and 300W, respectively.

CHAPTER IV

RESEARCH METHODOLOGY

To understand how the process and powder parameters affect the mechanical and pharmaceutical properties of the printlets in this extended release study with Kollidon® SR and Carbamazepine, two main research questions were asked:

RQ 1: What are the influences of process and powder parameters on the mechanical and pharmaceutical performance of printlets?

RQ2: How do relative powder size-distributions affect printlet quality and performance?

Research Question 1 Tasks

Not all printing and powder parameters could be made variables in this experiment, as having too many variables could prove difficult to determine how each parameter is affecting the printing. Therefore, the process of settling on different fixed and variable parameters was broken up into tasks.

Task 1A: Determine the processing and powder fraction bounds for yielding structurally integral printlets

Task 1B: Formulate and conduct a DOE to quantify the influence of process parameters and drug percentages on printlet performance. (Hardness, dissolution rate, XRD, FTIR, NIR, SEM imaging)

Outputs: Process parameter bounds for structurally integral printlets, correlations between process/powder parameters and printlet performance.

Research Question 2 Tasks

Task 2A: Formulate and conduct a DOE with differing polymer powder size distributions.

Task 2B: Quantify the effects of relative particle sizes on the mechanical and pharmaceutical performance (hardness, SEM imaging)

Outputs: Understanding of particle size distribution effects on performance.

Overall Outcome

Relationships of process parameters and relative particle volume/size fractions on printlet mechanical and pharmaceutical performance.

CHAPTER V

INFLUENCES OF PROCESS AND POWDER PARAMETERS ON THE MECHANICAL/PHARMACEUTICAL PERFORMANCE OF PRINTLETS (RQ1)

Exploring Printer Parameter and Powder Bounds

Kollidon® SR as the Main Excipient

As mentioned, KDSR had previously been used in other areas regarding pharmacy; however, KDSR had not been used in additive manufacturing of pharmaceuticals prior to this study. Therefore, before attempting to print with the CBZ, initial prints were conducted to determine if the KDSR could even be used in SLS of pharmaceuticals. Table 1 below presents the initial printing trials of the KDSR before adding the drug to the mixture. It should be noted that these powder mixtures, as well as the powder mixtures for all prints throughout this study, contain 3% of the Ruby Red sheen by weight. Also, all powders in this study were sieved to be below 106 µm particle size.

Table 1: Initial Prints with KDSR

Print Attempt	Layer Height (µm)	Laser Speed (mm/s)	Chamber Temperature (°C)	Surface Temperature (°C)
1	100	270	100	120
2	100	250	90	110
3	150	210	100	110

Printlet attempt 1 showed that the KDSR flowed quite well in the printer. However, the surface temperature was very close (within 10 °C) to the melting point of KDSR. The powder mixture began to harden and cake with this high temperature, and during

printing, the powder mixture could be seen glistening and shimmering. In addition to the powder caking, a massive rut began to form between the two powder beds. The rut and caking phenomenon are shown in Figure 13 and Figure 14, respectively. The powder was in its glaze point at this temperature. It should also be noted that the powder in the figures below were also not properly mixed, as shown by the streaks made by the sheen; however, caking occurred on properly mixed powder, too. To prevent powder caking, lower chamber and surface temperatures had to be used. Print attempt 2 did not yield any printlets, as the drop in temperature was not compensated enough by the slower laser speed. Print 3 began to finally show that the KDSR was capable of being used in this study.

Figure 13: Rut Formed Between Powder Beds

Figure 14: Powder Caking Problem

Pushing Limits: Drug Concentration, Chamber Temperature, and Laser Speed

Before exploring the process and powder parameters in an in-depth DOE, an estimate of an upper limit of the drug concentration for that DOE needed to be established. This stage of the experiment was to qualify how each parameter affects the printing process, while the next stage of the experiment was to quantify the trends established in this stage. Previous studies [29-35] only go as high as 35% of the API in their powder mixtures. However, if changing the API amount in the powder mixture can affect the powder's flowability and printing ability, higher drug concentrations had to be explored. To compare how the CBZ affected the printing process, a familiar, at least in terms of previous studies in SLS of pharmaceuticals, percentage by weight of the API in

the powder mixture of 30% was compared to higher amounts. Additionally, printlets with the 30% CBZ powder mixture were made with different laser speeds and chamber temperatures to narrow down a more balanced range of parameters that could further be explored in the DOE. Again, each print contains 3% of the Ruby Red Sheen additive.

Table 2: Exploring Printer Parameter Bounds

Print	%CBZ	%KDSR	Chamber Temperature (°C)	Surface Temperature (°C)	Laser Speed (mm/s)	Layer Height (µm)
1	47	50	105	115	240	100
2	30	67	105	115	240	100
3	30	67	100	110	190	150
4	30	67	75	90	190	150
5	30	67	75	90	160	150
6	30	67	75	90	130	150
7	30	67	75	90	100	150
8	30	67	75	90	70	150

Print 1 was the first print conducted with the CBZ. Printlets were able to be acquired from the process; however, these printlets had to be handled with extreme caution, or they would crumble easily. Print 2 used the same printing parameters, but a lower amount of CBZ was in the mixture. These printlets had better structural properties and could be handled more easily than printlets from Print 1. This observation showed that increasing the CBZ in the powder mixture lowers the structural properties. The observation is backed by the claim that the KDSR is the only material that should be melting during printing. However, the powder mixture in Print 2, with more KDSR being present, began to cake and harden during the print. Additionally, the mechanical properties were still poor, even if they were better than in Print 1. The printlets failed to register any readings on the VK200 Tablet Hardness Tester. Therefore, the remaining

prints were conducted to improve the mechanical properties of the printlets while also working to avoid the glaze point, leading to the powder caking problem. Print 3 showed increasing mechanical properties, but powder caking still occurred. The surface and chamber temperatures at Prints 4 – 8 were low enough to solve the issue of powder caking. These prints showed a trend of increased structural integrity with slower laser speeds. Figure 15 –Figure 19 are of Prints 4 – 8, respectively. At the 190 mm/s, the highest laser speed of the three figures, the porosity of the printlets can be seen. The printlet on the right also started crumbling just after being picked up and placed onto the wax paper. The printlets with 160 mm/s exhibited similar behavior, though not as extreme. These prints suffer from a lack of sintering. The printlets made with 130 mm/s could be handled easily and were much less porous than the printlets made with 160 and 190 mm/s laser speed. Using the slower laser speeds of 100 and 70 mm/s began to burn the printlets. However, the printlets made from 100 and 70 mm/s laser speed had very good structural integrity and could not be broken by handling, shaking, or dropping. The knowledge gained from these preliminary prints was used to make the final DOE.

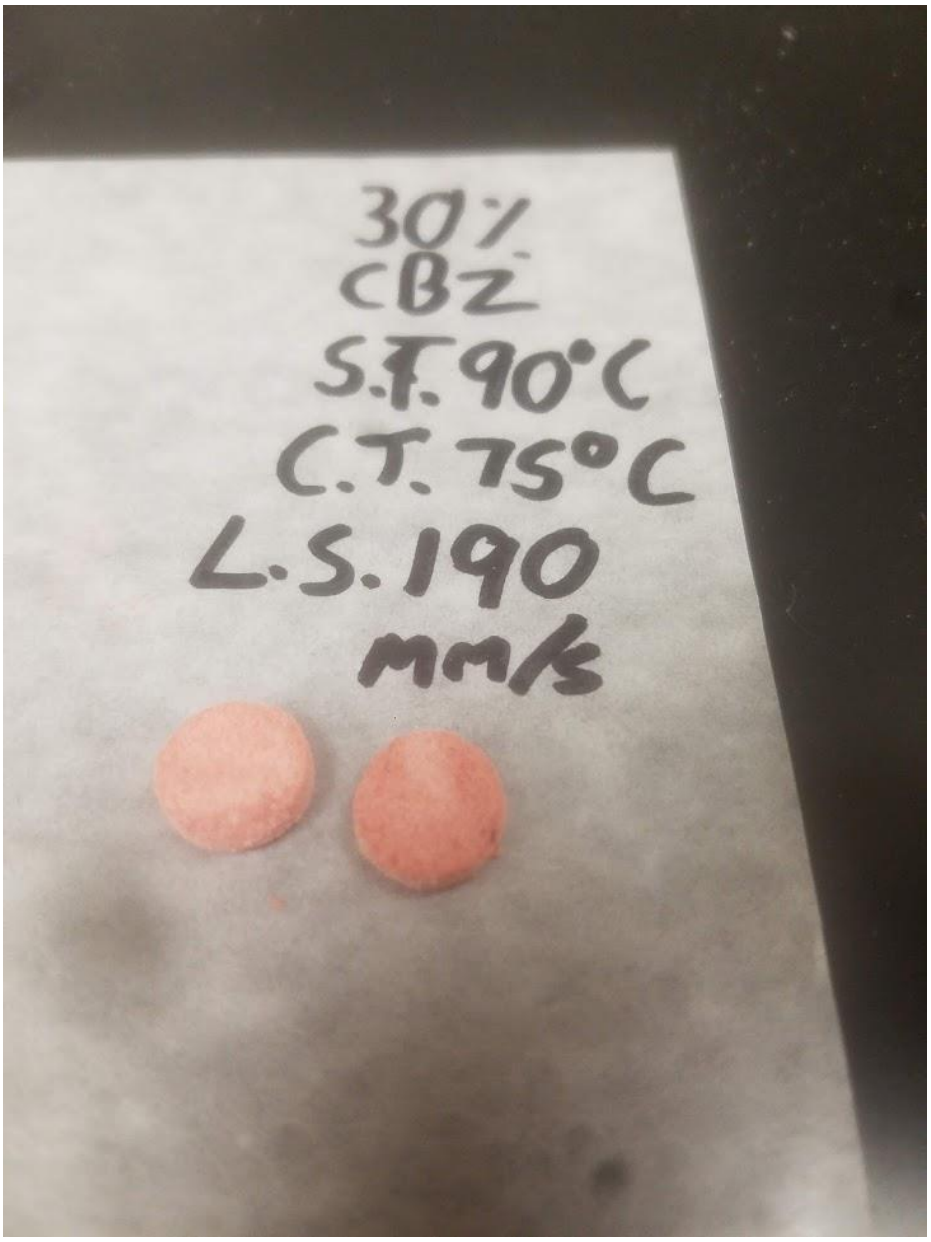

Figure 15: Comparing laser speed – 190 mm/s

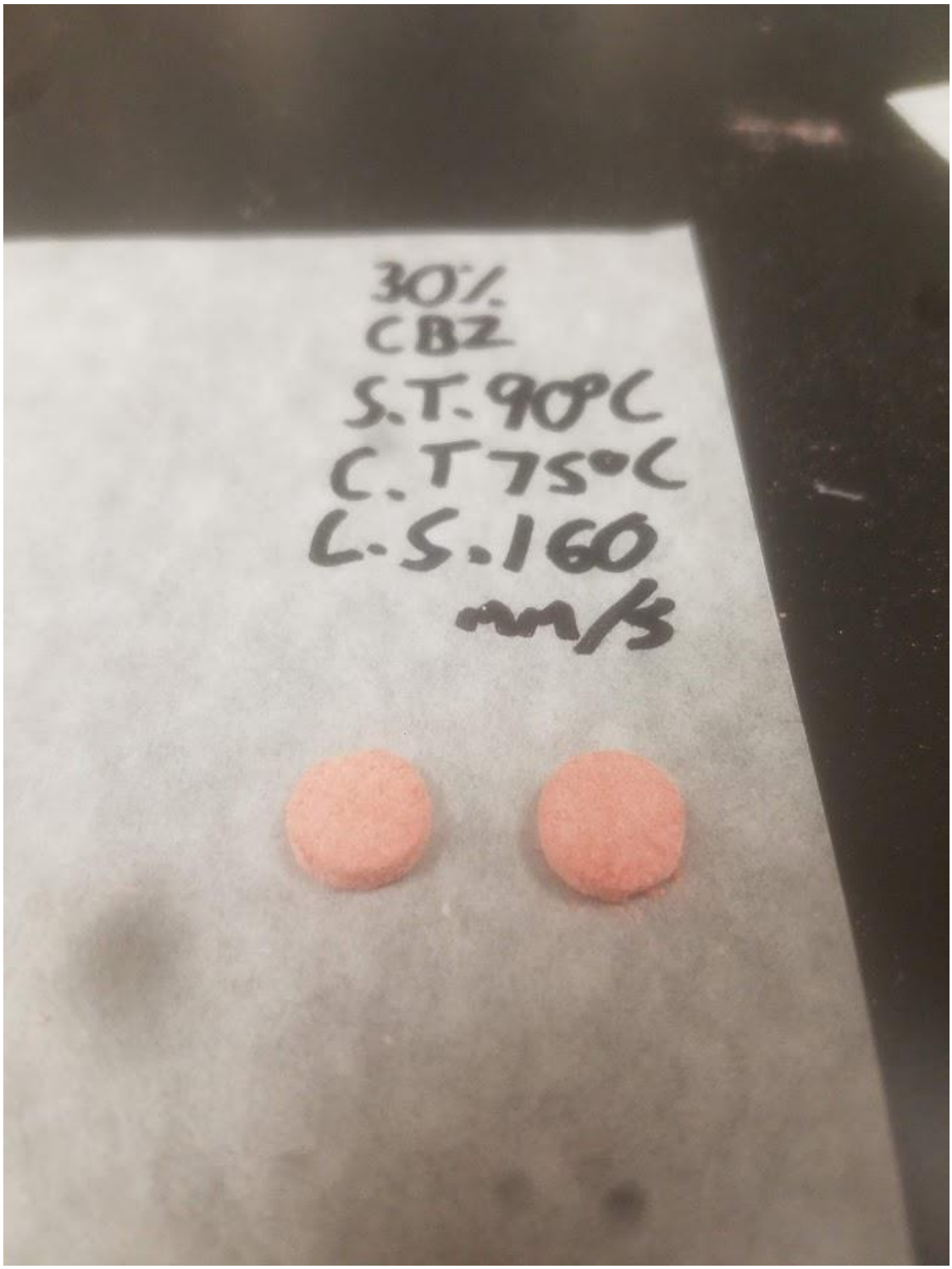

Figure 16: Comparing laser speed – 160 mm/s

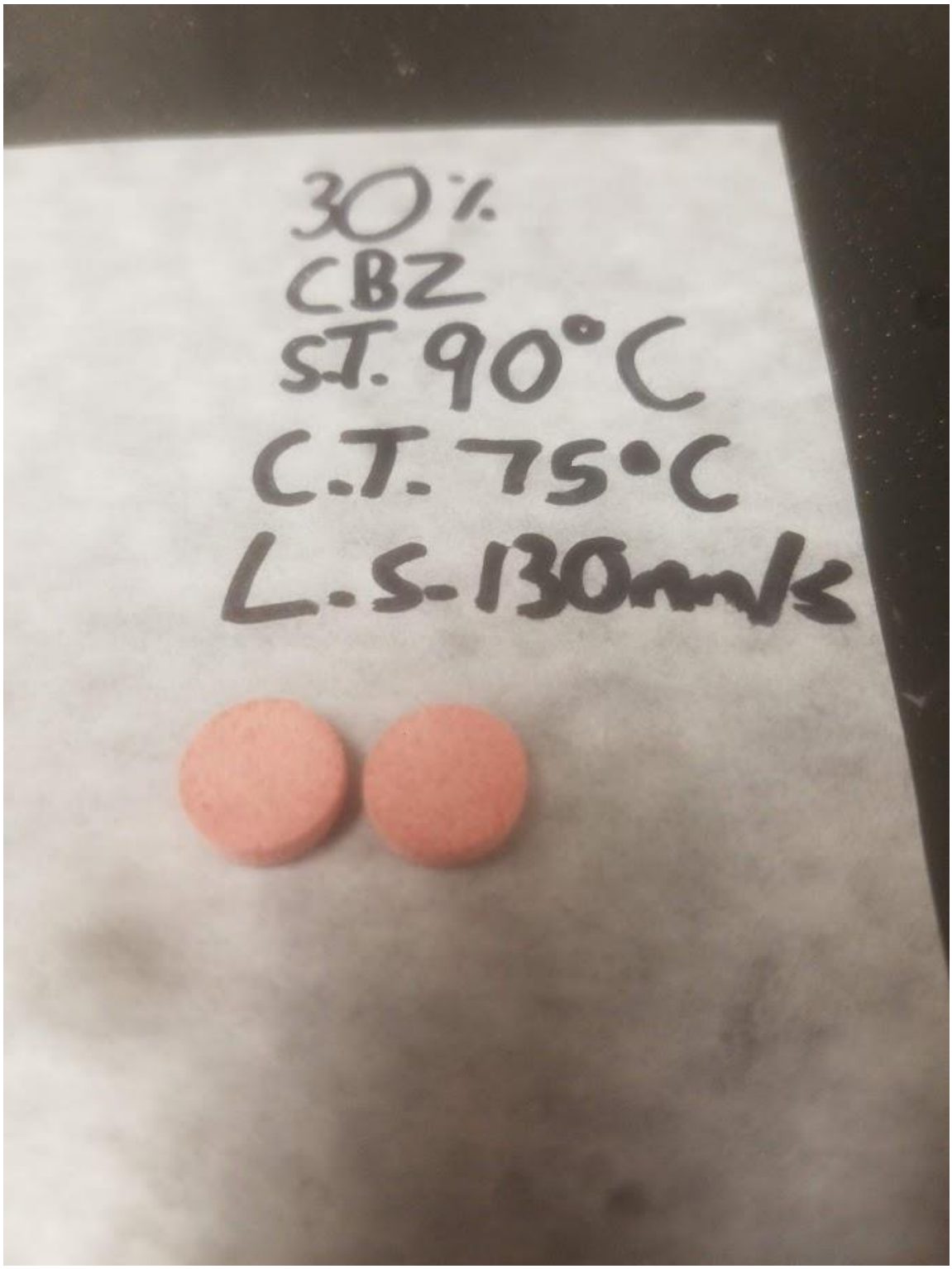

Figure 17: Comparing laser speed – 130 mm/s

Figure 18: Comparing laser speed – 100 mm/s

Figure 19: Comparing laser speed – 70 mm/s

Quantifying Process and Powder Parameters on Printlet Performance

Determining Fixed Parameters and Making the DOE

Not all process and powder parameters could be variables. Therefore, some parameters were set as constants for the remainder of the study, as shown by Table 3 below.

Table 3: Printing and powder parameters set as constants

Chamber Temperature	75 °C
Surface Temperature	90 °C
Layer Height	150 µm
Laser Hatch Distance	250 µm
Sheen Weight % in Powder	3%
Printlet Size	10 x 3 mm, circular

The chamber and surface temperatures were set as constants because of powder caking and printer variability. These temperatures reliably did not cause powder caking in the preliminary prints. Also, this parameter proved extremely hard to control, as the Sintratec Kit has a temperature variability of ± 5 °C. However, the printer would often go past this tolerance, one time going as high as 15 °C above the specified temperature. In the preliminary experiments, layer heights of 100 and 150 µm were explored. 150 µm allowed for better powder flowability and more even powder coating. The laser hatch distance, or the distance between laser passes, remained constant throughout the study, just like the sheen amount. A printlet size of 10 x 3 mm yielded tablets large enough to have CBZ amounts comparable to standard dosages, as the early printlets were 5 x 3 mm

tablets. The parameters further explored to quantify how they can influence printlet performance are shown in Table 4 below.

Table 4: Design of Experiments for exploring process and powder parameters

Final DOE	Laser Scan velocities (mm/s)		
Drug/Excipient ratio (%)	70	100	130
20/77	9 powder/laser speed combinations		
30/67			
40/57			

Although the laser energy is not the main source of energy input on SLS of pharmaceuticals, the sintering cannot occur without the laser. Also, the laser scan speed is much easier to precisely control, compared to the chamber and surface temperatures. Therefore, for varying energy input, the laser scan velocities were explored further.

The initial print involving the very high amount of CBZ (47% in the powder mixture) showed that printlets could be made with high percent of the API in the powder mixture. This initial print had very poor mechanical properties, so in order to achieve prints with enough structural integrity to conduct pharmaceutical tests, 40% CBZ in the powder mixture was set as the highest limit, which would be compared with the other powder mixtures containing lower API percentages. Approximately 20 printlets of each powder and process parameter combination were made to conduct the mechanical and pharmaceutical tests.

Mechanical Testing: Weight and Hardness Results & Analysis

After printing, printlets from each trial were weighed and tested for hardness, or crush resistance. Figure 20 shows the weight comparison of the different powder formulations and process parameters, and Table 5 displays each trial's average and standard deviations, also illustrated on Figure 20.

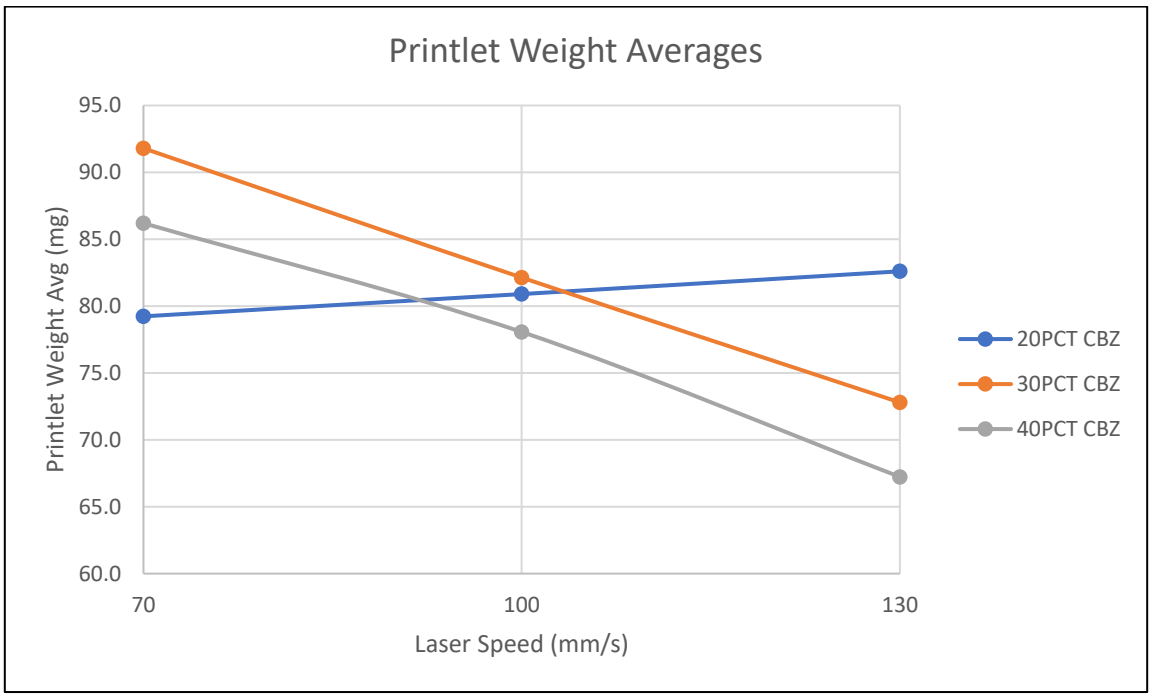

Figure 20: Printlet Weight Averages

Table 5: Averages and standard deviations of each printlet trial

Powder Formulation	Printlet Weight Average (g)	Standard Deviation of Weight (g)
20% CBZ 70 mm/s	79.2	0.40
20% CBZ 100 mm/s	80.9	3.12
20% CBZ 130 mm/s	82.6	2.42
30% CBZ 70 mm/s	91.8	3.76
30% CBZ 100 mm/s	82.1	1.17
30% CBZ 130 mm/s	72.8	1.64
40% CBZ 70 mm/s	86.2	5.84
40% CBZ 100 mm/s	78.1	9.47
40% CBZ 130 mm/s	67.2	8.07

The printlets with 20% CBZ in the powder mixture have consistent weights, with the average being around 80 grams and standard deviations of 3.12 grams or less. The 30% and 40% CBZ, however, show a decrease in weight with an increase in laser speed, not a behavior present in the 20% CBZ powder mixtures. The standard deviation in weights also increases with an increase in CBZ. The CBZ inhibits powder flowability, which can lead to inconsistent, uneven layers.

Next, the printlets' hardness was tested on the two different instruments, shown by Figure 21 and Figure 22.

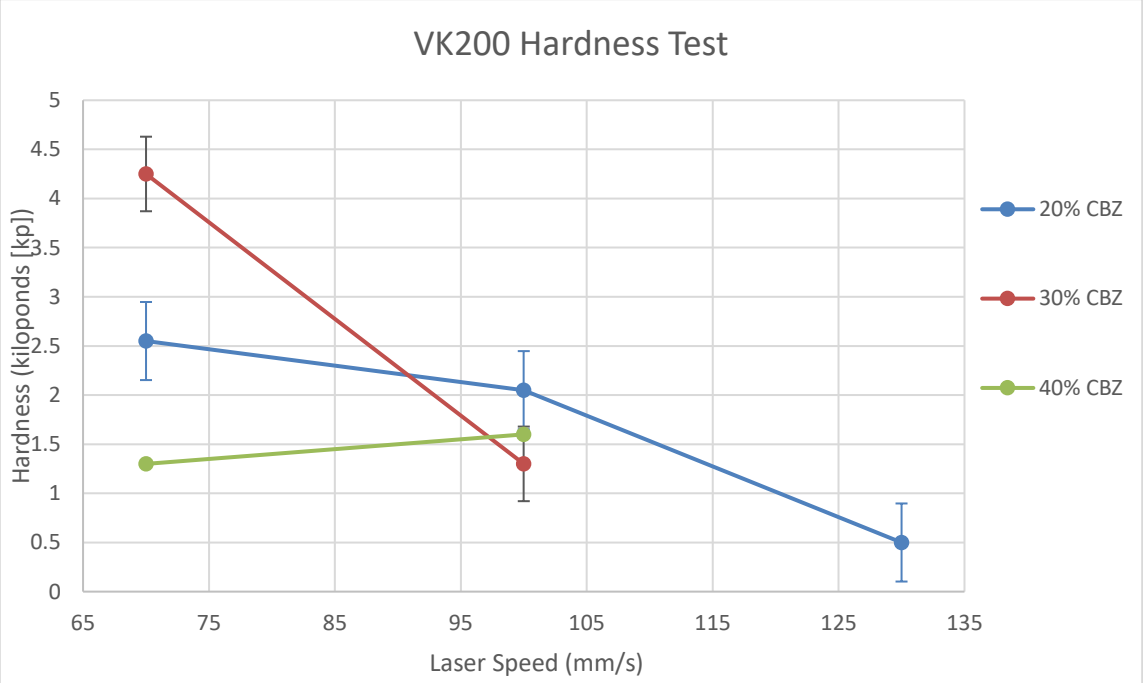

Figure 21: VK200 Hardness Test (kp)

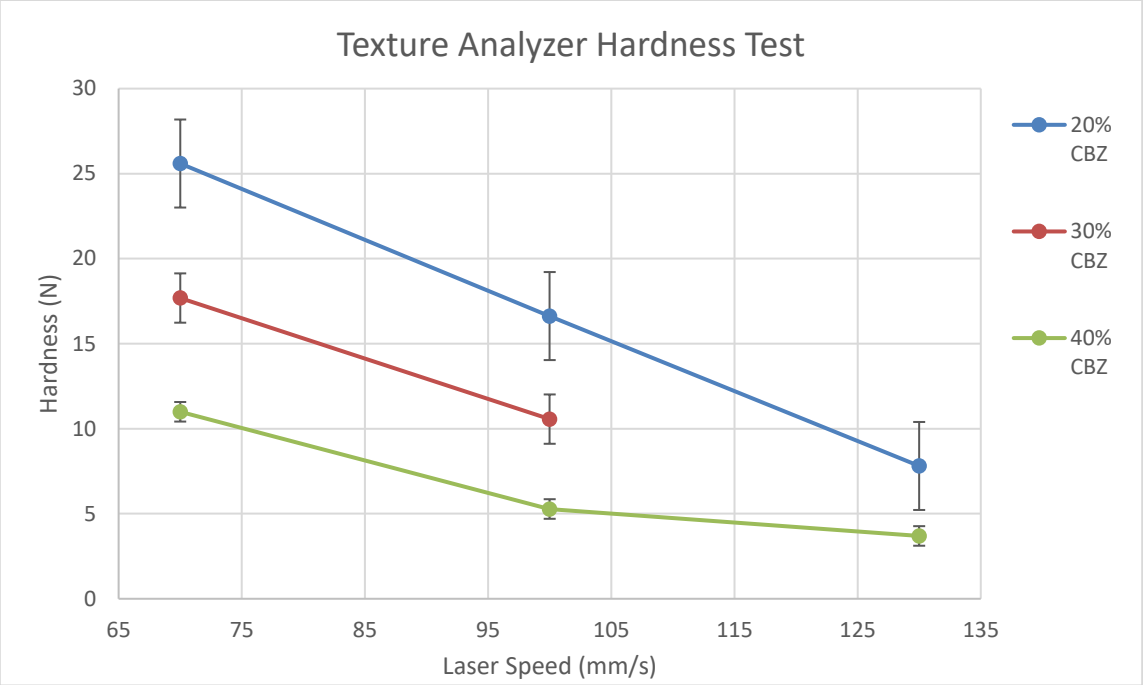

Figure 22: TA.XT Texture Analyzer Hardness Test (N)

The printlets with the higher laser speeds yield a lower hardness. Additionally, printlets with a higher CBZ in the powder mixture also have a lower hardness. The same deductions from the weight analysis, as well as the preliminary prints can be applied when analyzing the hardness. The printlets with the high laser speeds to not achieve as much sintering as printlets made with lower laser speeds. Also, printlets with a higher amount of CBZ have less excipient, KDSR, that is actually sintered. To back the claims made by the preliminary prints, weight analysis, and hardness analysis, SEM imaging was conducted on the powders and the printlets. Figure 43 – Figure 51, located in Appendix A, are SEM images of each trial from the DOE. The images also illustrate that as laser speed increases, less sintering occurs—fewer particles melt on higher laser speeds, resulting in lower hardness. Also, the images also show that number of loose

particles increases with an increase in CBZ, indicating less sintering on the higher CBZ percentages.

Dissolution Testing: Analysis of Drug Release Over Time

The dissolution test showed trends relating to drug release regarding both CBZ concentration and laser speed. Figure 23 – Figure 25 are the results of the dissolution test. The dotted lines indicate the CBZ-NF acceptable release rate in order for the printlets to pass USP testing. Each formulation's standard deviations are indicated by the brackets corresponding with the laser speed's color.

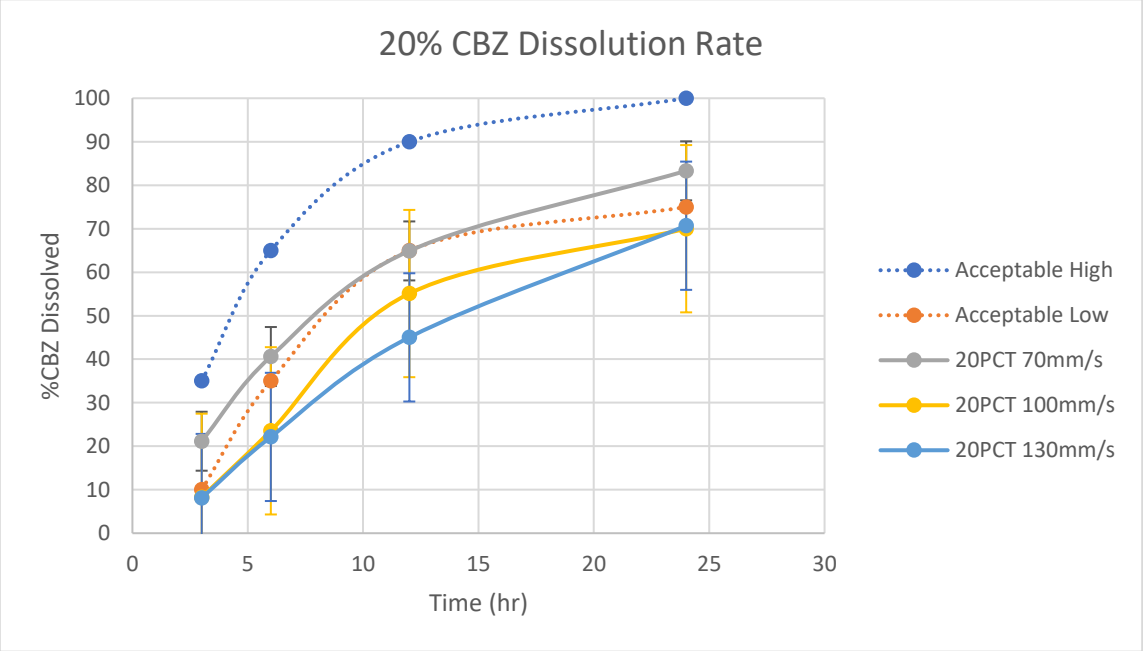

Figure 23: Analysis of drug release over time: 20% CBZ formulations

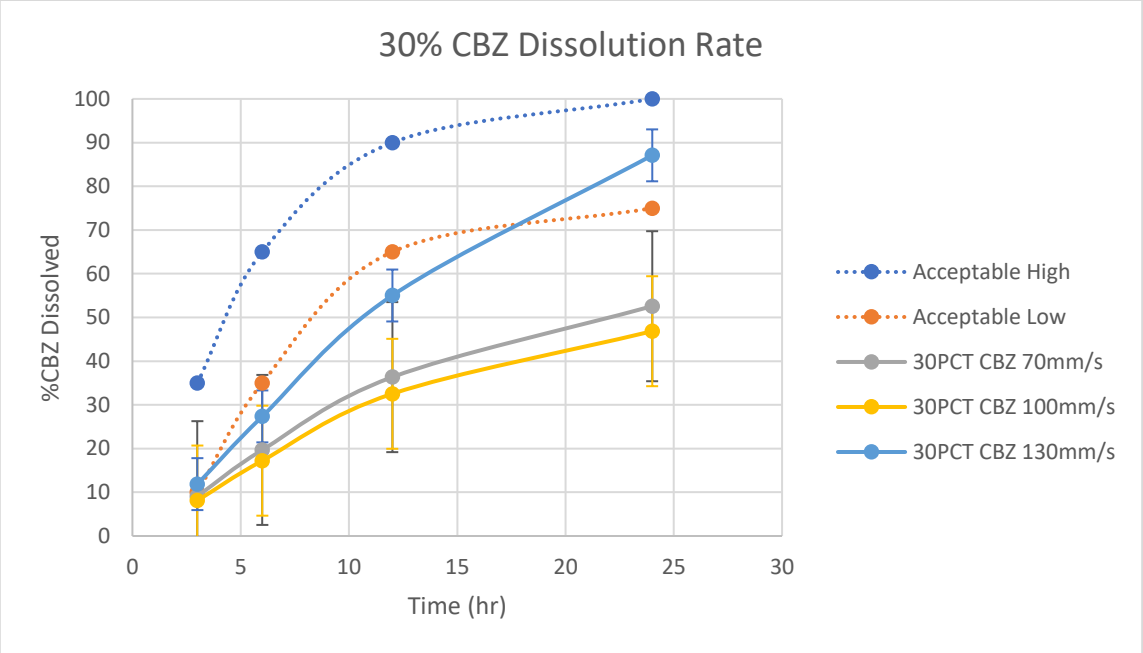

Figure 24: Analysis of drug release over time: 30% CBZ formulations

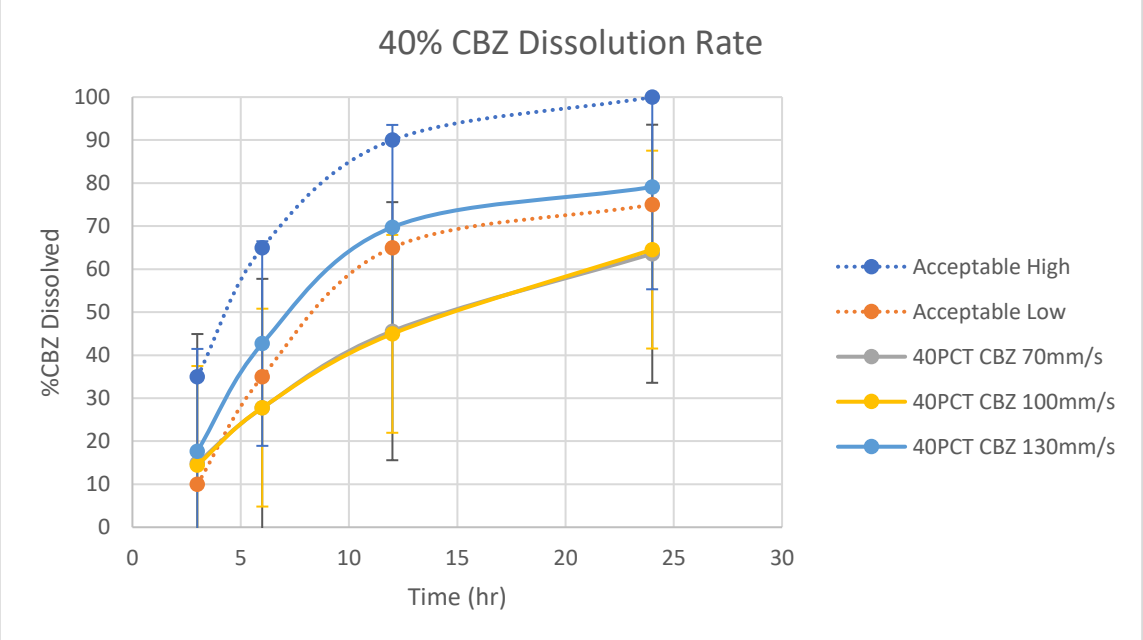

Figure 25: Analysis of drug release over time: 40% CBZ formulations

Starting with the 20% CBZ concentration, the slowest laser speed, 70 mm/s, yields the highest release rate over time. The averages also fall within the USP accepted release rate, although the standard deviations are outside the bounds. The 30% CBZ powder concentration appears to have almost a backwards trend referring to laser speed when compared to the 20% CBZ concentration powder formulation. None of the release rates of the 30% powder mixture were within the USP acceptable bounds. Finally, the 40% CBZ concentration powder mixture has the completely opposite behavior in terms of laser speed and release rate when compared to the 20% CBZ concentration. The fastest laser speed, 130 mm/s, falls within the acceptable range as per the USP standards for CBZ. However, like with the 20% CBZ 70 mm/s, the standard deviations fall outside the acceptable ranges. The change in behavior on release rate can be explained by the layer uniformity during printing and the SEM images of the unprinted powder and the printlets (Figure 40 – Figure 42), located in Appendix A.

As mentioned, when discussing the hardness, the lower CBZ formulations produced much more even layers than the higher CBZ concentration powders. Having good layer uniformity also led to more consistent energy input—on the higher drug concentrations, sometimes a previous layer could be seen underneath the new layer. This led to portions of layers being sintered twice or more.

The SEM images provide an explanation as to why the 40% CBZ powder concentration has an inverse relationship in terms of drug release when compared to the 20% CBZ. In each of the powder pictures (Figure 40 – Figure 42), the CBZ can be seen attaching and sticking to the KDSR particles. The higher the CBZ concentration, the

more CBZ can be seen sticking to the KDSR. Therefore, when the KDSR particles melt together, they may completely encapsulate the CBZ that has agglomerated on it. Even when the water-soluble portion of the KDSR dissolves, the CBZ may still be entirely surrounded in the water insoluble KDSR, preventing its release. The 30% CBZ powder mixture received the drawbacks from both the 20% and 40% CBZ formulations. The 30% CBZ powder had less uniform layers than the 20%, resulting in some areas getting sintered more than once, and the higher drug percentage caused the slower laser speeds to completely encapsulate some of the CBZ in the melted structure of the KDSR.

Examining Printlets for Drug Degradation

Before discussing the results of the tests for drug degradation, it should be noted that suspicions of drug degradation arose after analyzing the SEM images. When viewing the unprinted powder in Figure 40 – Figure 42 in Appendix A and Figure 2, Figure 4, and Figure 6, from the materials section, one can distinguish the three components used to make the powder mixture: the KDSR, the CBZ, and the metal sheen. In Figure 26 below, a printlet with 20% CBZ printed at 100 mm/s is shown.

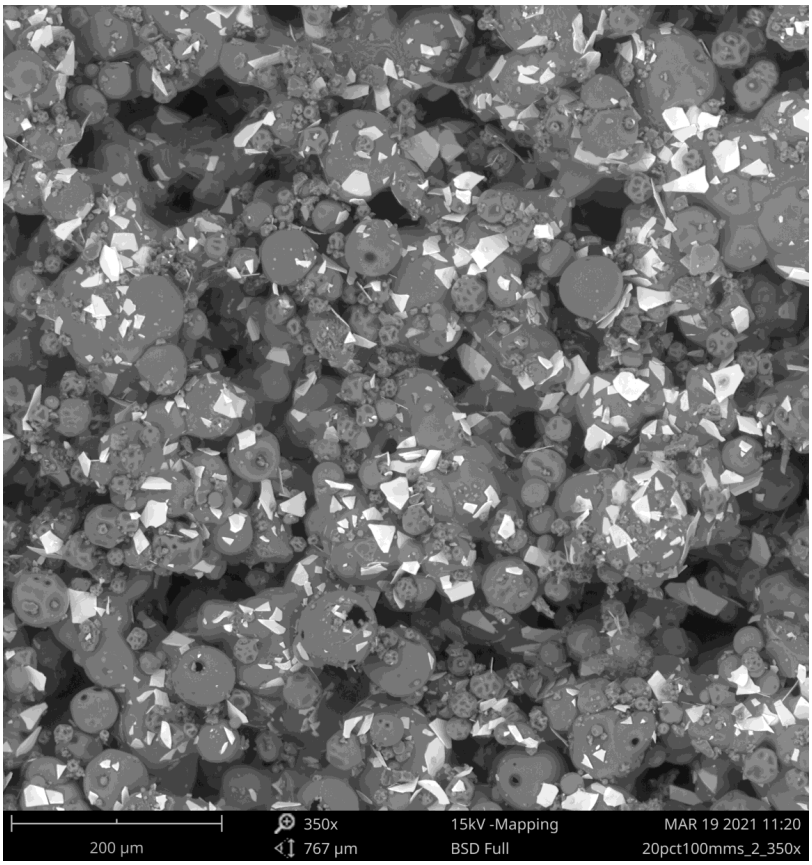

Figure 26: SEM Image of 20% CBZ, 100mm/s Printlet at 350x magnification

The KDSR, CBZ, and sheen particles can be distinguished in this picture when referencing, and no new structures appear to be present. However, on Figure 27 below, with a higher CBZ concentration (40%), a new structure appears.

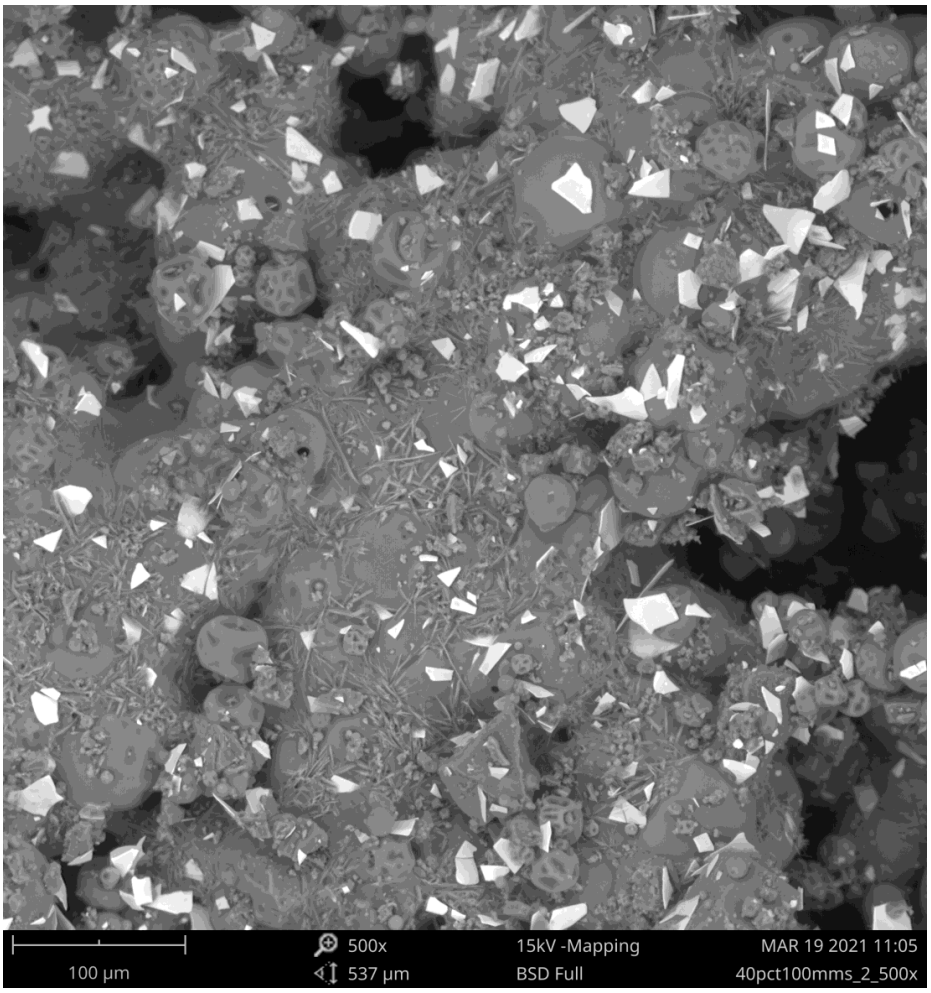

Figure 27: SEM Image of 40% CBZ, 100mm/s Printlet at 500x magnification

This printlet has a needle-like structure that is unlike any of the individual particles. The KDSR is known how it behaves when it melts—it forms the melted structure seen in all of the SEM printlet photos. However, the CBZ is not supposed to melt, but at the higher energy input of 100 mm/s and 70 mm/s, enough energy could be absorbed by the powder to melt the CBZ and form these structures. Melting the CBZ can change its properties, potentially resulting in drug degradation. This structure is

only visible on the 70 mm/s and 100 mm/s for the 40% CBZ printlets, but tests for changes in CBZ functional groups were conducted on all of the printlet trials.

Near-Infrared Spectroscopy

References to how the CBZ and KDSR appear individually are located in Appendix B as Figure 52 and Figure 53, respectively. Below in Figure 28 is the comparison of the printlets and the unprinted powder of the 40% CBZ powder mixture to the CBZ and KDSR functional groups. The 20% and 30% CBZ powder mixtures NIR photos are located in Appendix B as Figure 54 – Figure 57, as they exhibit the same trends as the 40% CBZ, though not as pronounced.

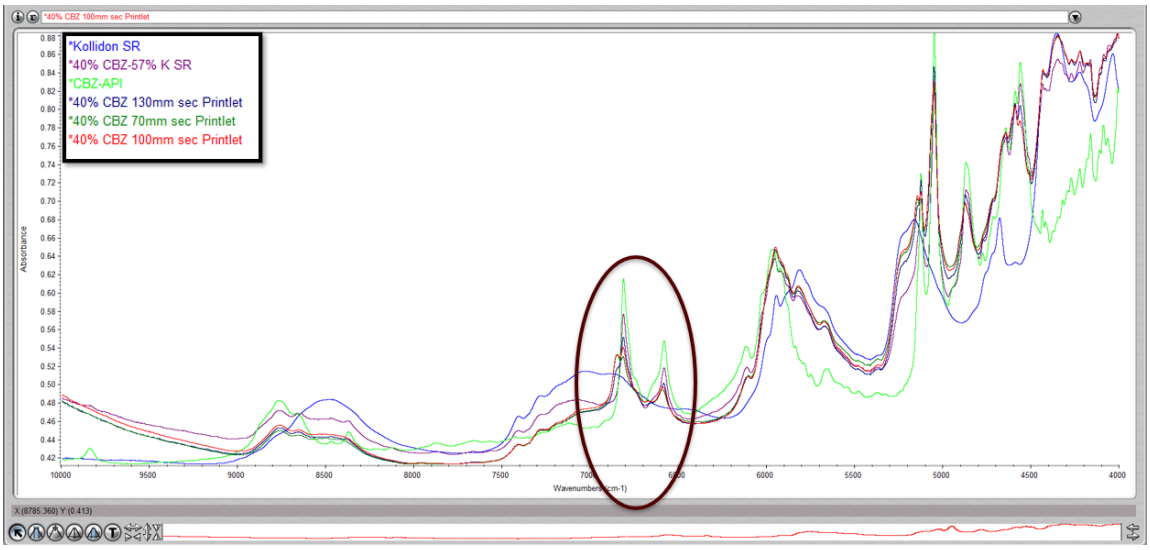

Figure 28: NIR peaks comparison of unprinted powder and printlets to the CBZ

Between wavenumbers 6000 – 7000 has been circled, as there is suspicion that the CBZ in the printlets has either degraded, or, at least, experienced a phase change.

The functional groups for the slower laser speed have changed in the circled area. Figure 29 displays a zoomed image on the area under question.

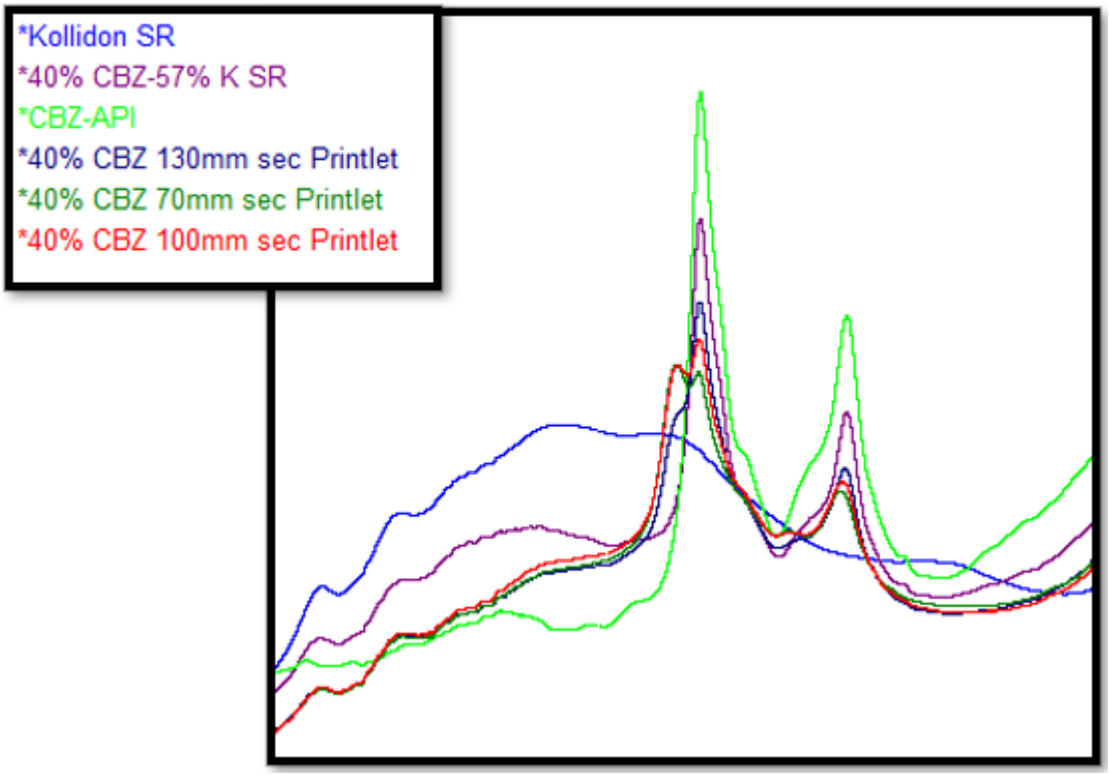

Figure 29: NIR Peak Analysis Focus

The functional groups of the 70 and 100 mm/s are significantly different than the CBZ peak, whereas the unprinted powder exhibits the same peak as the CBZ. The 130 mm/s laser speed is beginning to transition to the peaks like the 70 and 100 mm/s, but it is still close to the CBZ peak, indicating that an increase in energy input leads to a change in this functional group.

Attenuated Total Reflectance

References to how the CBZ and KDSR appear individually are located in Appendix B as Figure 58 and Figure 59.The ATR results did not show any suspicion of CBZ degradation or phase changes. The 40% CBZ concentration is shown below as Figure 30. The 20% and 30% CBZ concentrations are located in Appendix B as Figure 60 and Figure 61 .

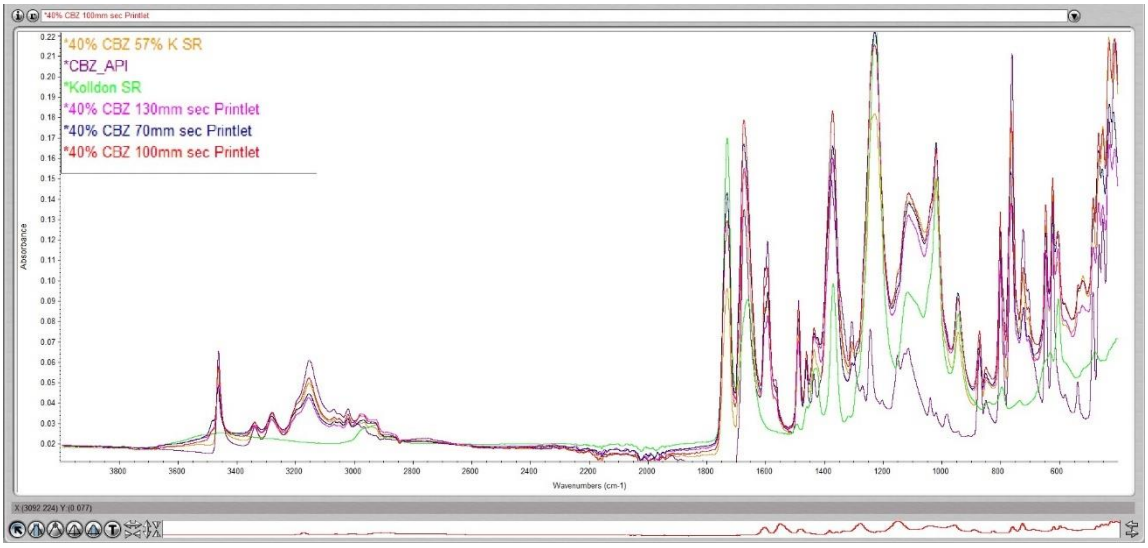

Figure 30: ATR of 40% CBZ Concentration

Each peak from the unprinted powder and the printlets of the three laser speeds all align with the peaks of the CBZ.

X-ray Diffraction

In order to show the comparison of the unprinted powder and printlets' peaks to the peaks of the CBZ, the graph must cut off the tops of the peaks of the CBZ. Therefore, an uncropped reference of the CBZ functional groups for the XRD is in Appendix B as Figure 62. Also, the 20% and 30% CBZ concentration samples produced similar results as the 40%, so they will be located in Appendix B as Figure 63 and Figure 64, respectively. Below is the 40% CBZ peak comparison for the XRD.

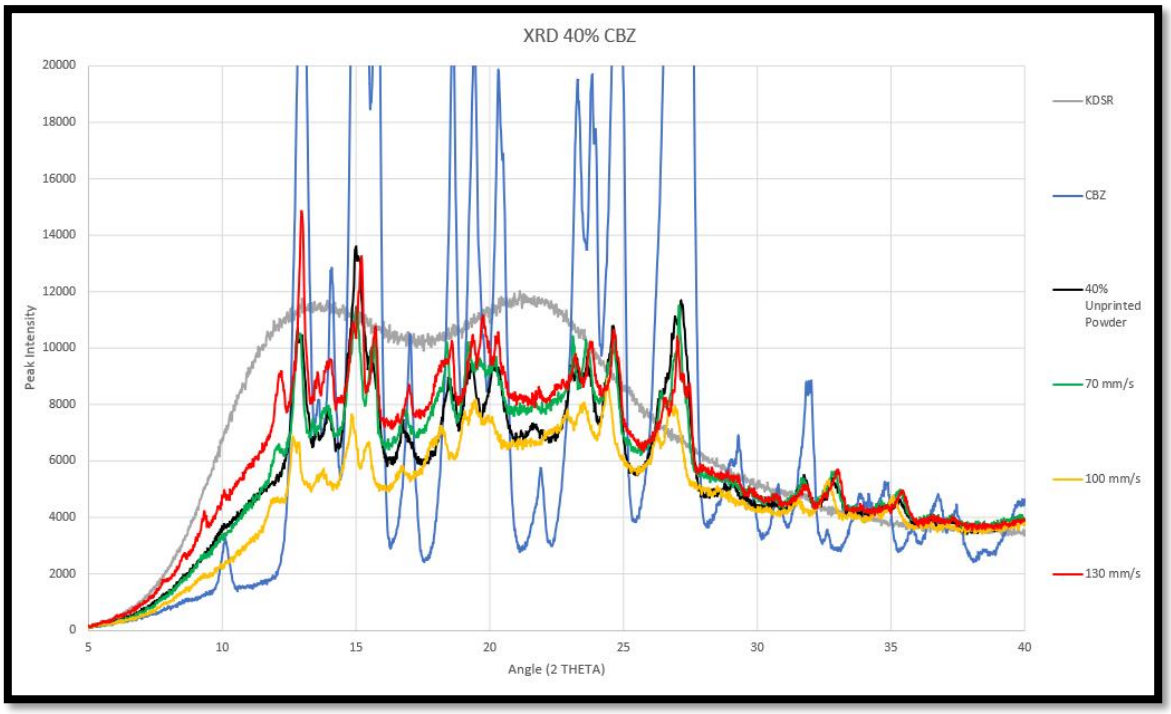

Figure 31: 40% CBZ XRD peak comparison

The unprinted powder exhibits peaks in the same locations as the CBZ, so if the CBZ does not experience a change in crystallinity for the printlets, then it should appear as the unprinted powder does. However, each printlet, especially the 70 and 100 mm/s

laser speed printlets, yield quite different peaks, specifically between the angle range of 15 – 25, as shown by Figure 32.

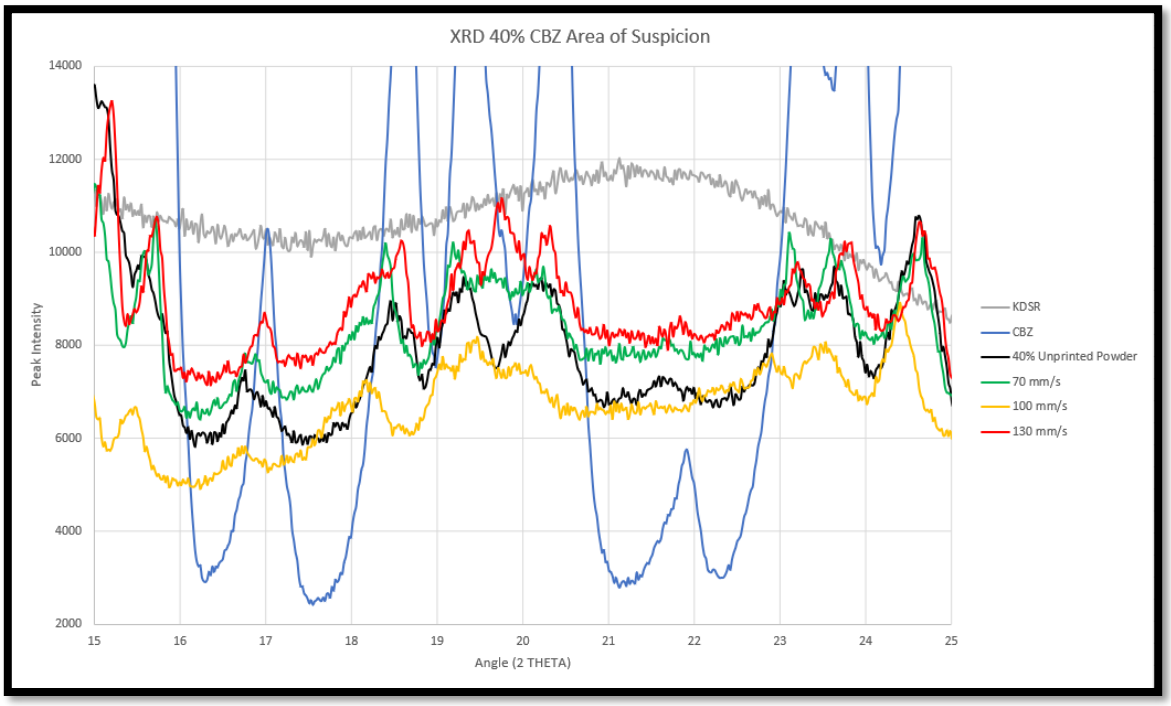

Figure 32: 40% CBZ Area of Potential Degradation

The unprinted powder can be seen correctly following the peaks of the CBZ. However, the printlets show peaks in multiple incorrect ways. Focusing on the three peaks in the middle (between the 18 – 21 angle), the 70 mm/s printlets are unaligned and appear much less defined than the unprinted powder or the CBZ, indicating a potential change to amorphous structure. The 100 mm/s printlets have the least-defined peaks out of any of the printlets in this area, also indicating a change to an amorphous structure. Finally, the 130 mm/s peaks are in line with the unprinted powder and the CBZ, and they are

more defined than the 70 and 100 mm/s printlet. However, a fourth new peak has emerged, indicating a change in the material structure.

Summary of Observations and Deductions

The bulk heating, or the chamber and surface temperature, can affect the powder flowability during the printing process. If the bulk heating is too high, the powder reaches its glaze point, causing it to cake and harden. Printing with KDSR should be conducted below the glaze point to have successful prints. A surface temperature heating of 90 °C is 40 °C below the KDSR melting point, and no powder caking occurred at this temperature.

The laser speed affects both the mechanical and pharmaceutical properties of the printlets. Having a slower laser speed (higher energy input) yields higher mechanical properties, but the slower laser speeds can also potentially degrade the drug.

CHAPTER VI

EFFECTS OF RELATIVE POWDER SIZE DISTRIBUTION ON PRINTLET QUALITY AND PERFORMANCE (RQ2)

Making the DOE: Powder Formulation and Relative Size Distributions

Choosing the powder was largely based on the performance of the formulations from RQ1. The highest CBZ concentration was chosen (40%), as the dosage from the printlets made from this formulation were closest to standard dosages. Although AM is desired to be used in the specialized areas of prescription strength, the USP testing is conducted at standard dosages, so achieving a dose close to standard was an important factor when deciding which powder to pick. The medium laser speed, 100 mm/s, was chosen, in order to achieve good layer fusion while not burning the printlets, like with the 70 mm/s. The same constants used in RQ1 were also used here, shown in Table 3.

Choosing the relative particle sizes was based on both RQ1 and previous studies conducted with particle size influence on SLS of polymers. Previous studies are in agreement that having smaller particle sizes increases flowability up until a certain point, where particle agglomeration occurs, and flowability is actually inhibited by smaller particle sizes. However, depending on the study, the recommendation for the lower limit on particle size can differ [12, 29]. Also, the materials used in previous studies SLS of pharmaceuticals did not include KDSR. Because the maximum particle size was 106 μm in RQ1, the decision was made to split the particle sizes down the middle to have three different printlets to compare, as shown in Table 6. The SEM images of these powders can be seen in Figure 33 – Figure 35. It should be noted that the operator was

different for Figure 34 than for Figures 33 and 35, which is why the pictures may appear quite different. The operator for Figures 33 and 35 sprayed the powder with compressed air to prevent it coming loose in the SEM.

Table 6: Particle Sizes Chosen

Particle Size	Range
Small	0 – 53 µm
Large	50 – 106 µm
Full Distribution (already completed from RQ1)	0 – 106 µm

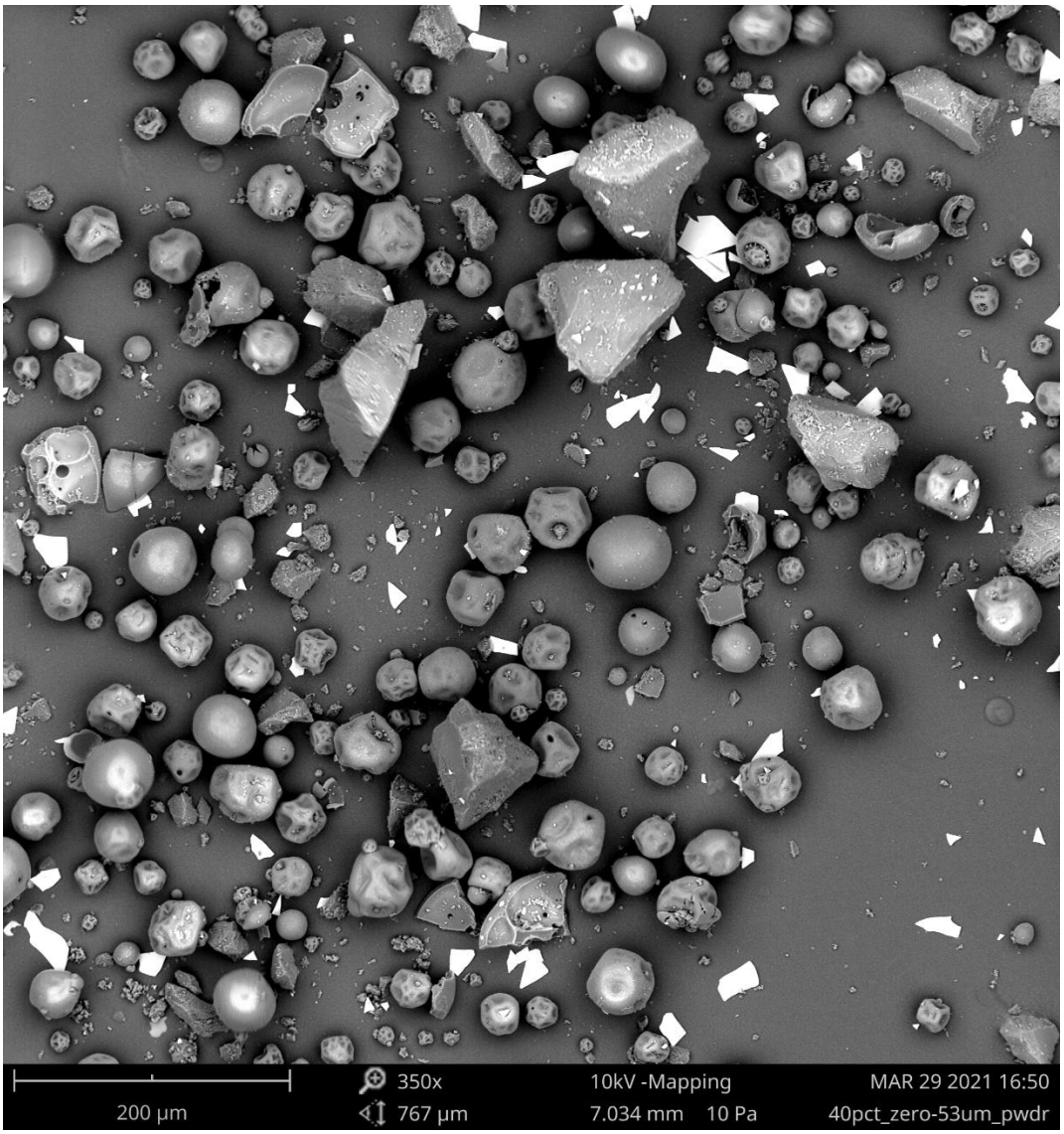

Figure 33: SEM Image of the unprinted powder with the small particle size distribution (0 - 53 µm) at 350x magnification. The powder is 40% CBZ concentration.

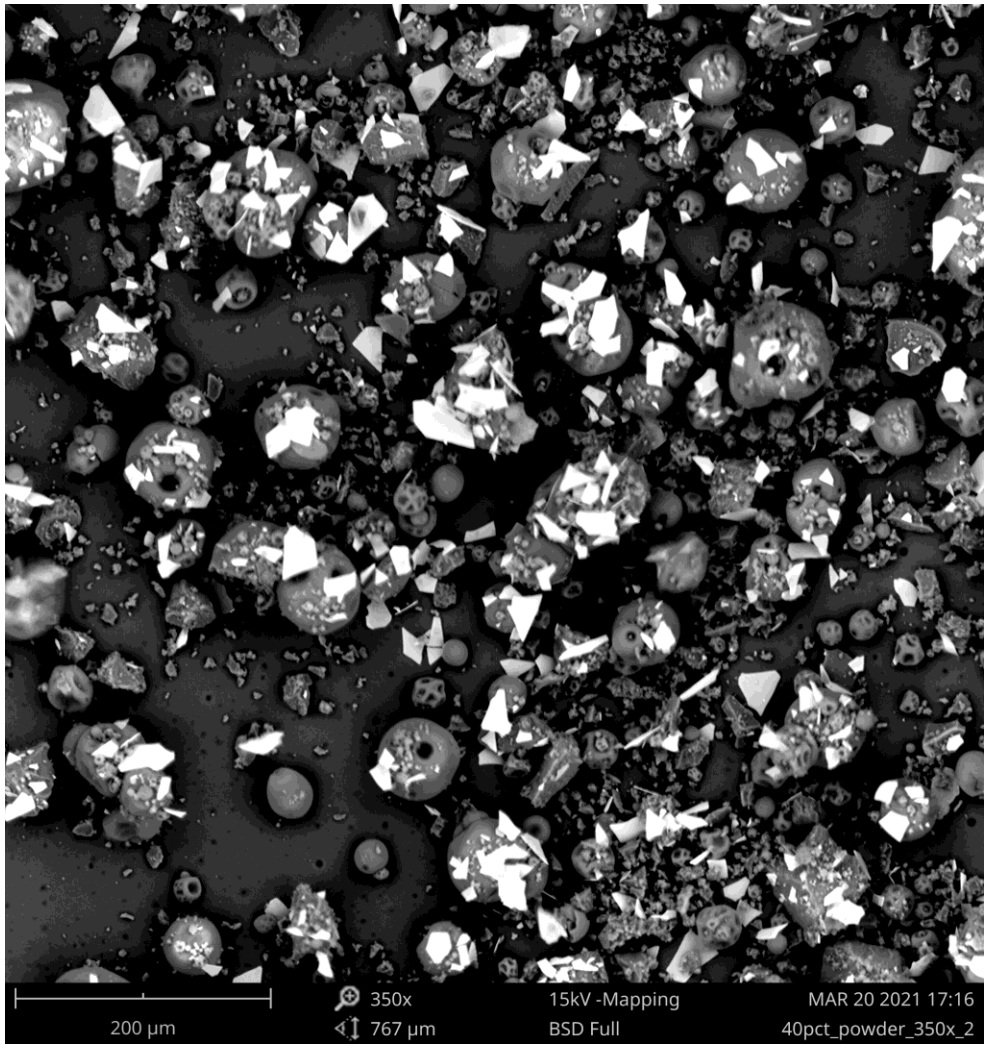

Figure 34: SEM Image of the unprinted powder with the full particle size distribution (0 - 106 µm) at 350x magnification. The powder is 40% CBZ concentration.

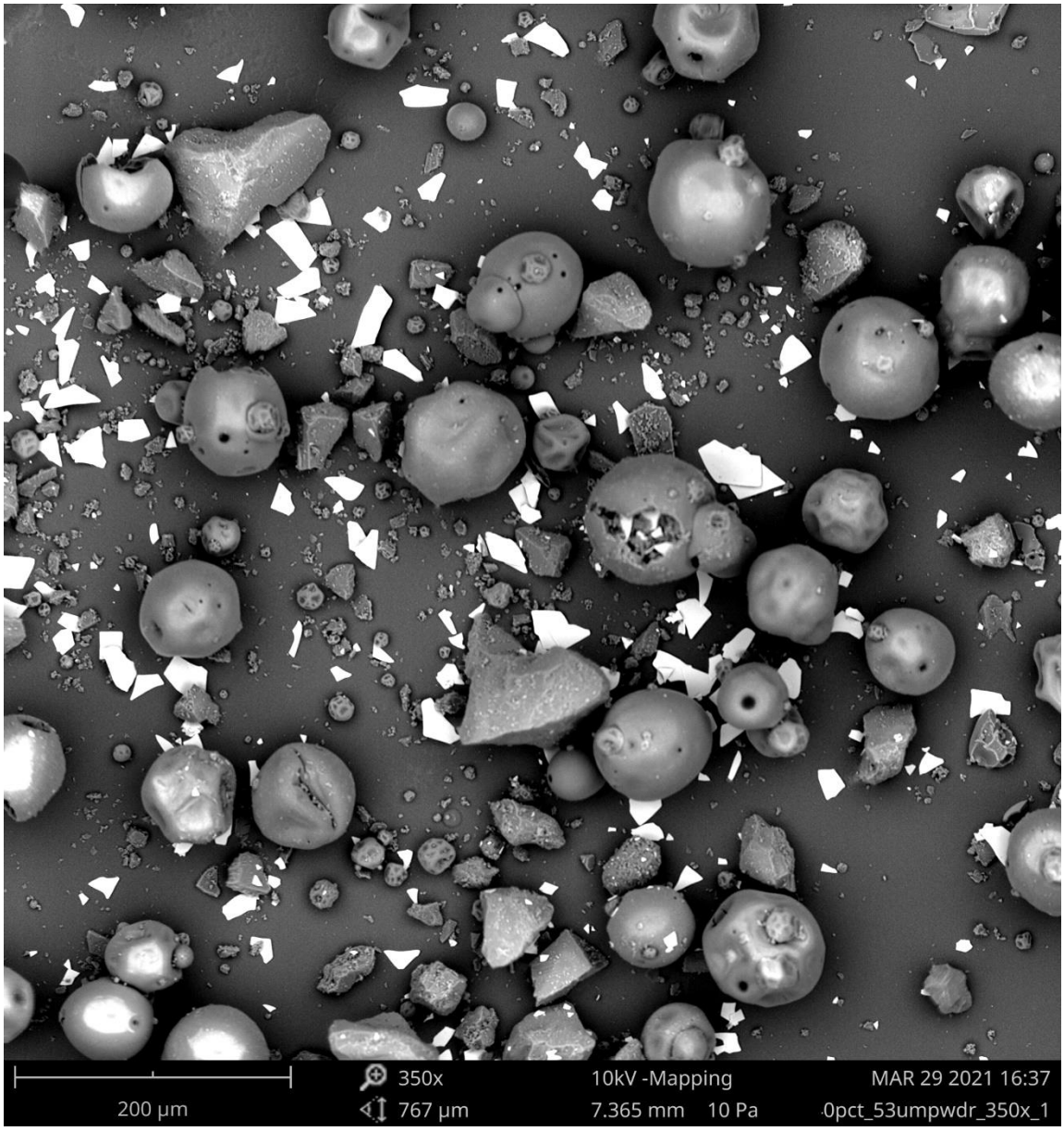

Figure 35: SEM Image of the unprinted powder with the large particle size distribution (53 - 106 µm) at 350x magnification. The powder is 40% CBZ concentration.

Quantifying the Effects of Different Particle Size Distributions

The printlet hardness comparison is show below in Table 7 and Figure 36.

Table 7: Hardness Values of Differing Particle Size Distributions

40% CBZ, 57% KDSR, 3% Sheen w/ 100mm/s Laser Speed	Hardness (N)
0 - 53µm	<2
0 - 53µm	<2
0 - 106µm	5
0 - 106µm	5.56
53 – 106µm	5.07
53 – 106µm	7.66

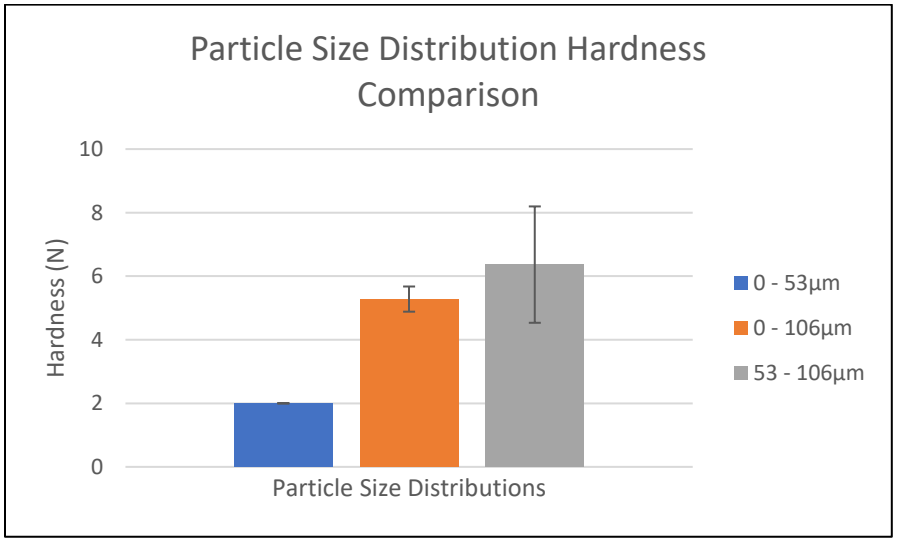

Figure 36: Hardness Value Averages and Standard Deviations of Differing Particle Size Distributions

The printlets with smaller particle size (0 - 53µm) had agglomeration issues while printing when compared to the larger particles (53 - 106µm) and the full distribution (0 – 106µm). Additionally, the printlets with smaller particle size were significantly more porous than the printlets with larger particles or the even distribution. The agglomeration and resulting porosity are reflected by the hardness values, yielding a significantly lower hardness for the smallest particle size distribution. The SEM photos in Figure 37 – Figure 39 can further back these claims. The SEM images also illustrate how different each printlet's melted structure appears. While the small particle range (0 – 53 µm) has severe porosity, indicated by the large gaps below the surface that can be seen, the structure that is present has excellent fusion. The large particle size distribution (53 – 106 µm) has decent fusion and significantly less porosity than the small particle size. The full particle size distribution (0 – 106 µm) appears to have similar fusion and porosity as the large particle size distribution. The flowability of the full distribution was inhibited slightly by the small particles, reflected by the drop in hardness when compared to the large particle size distribution.

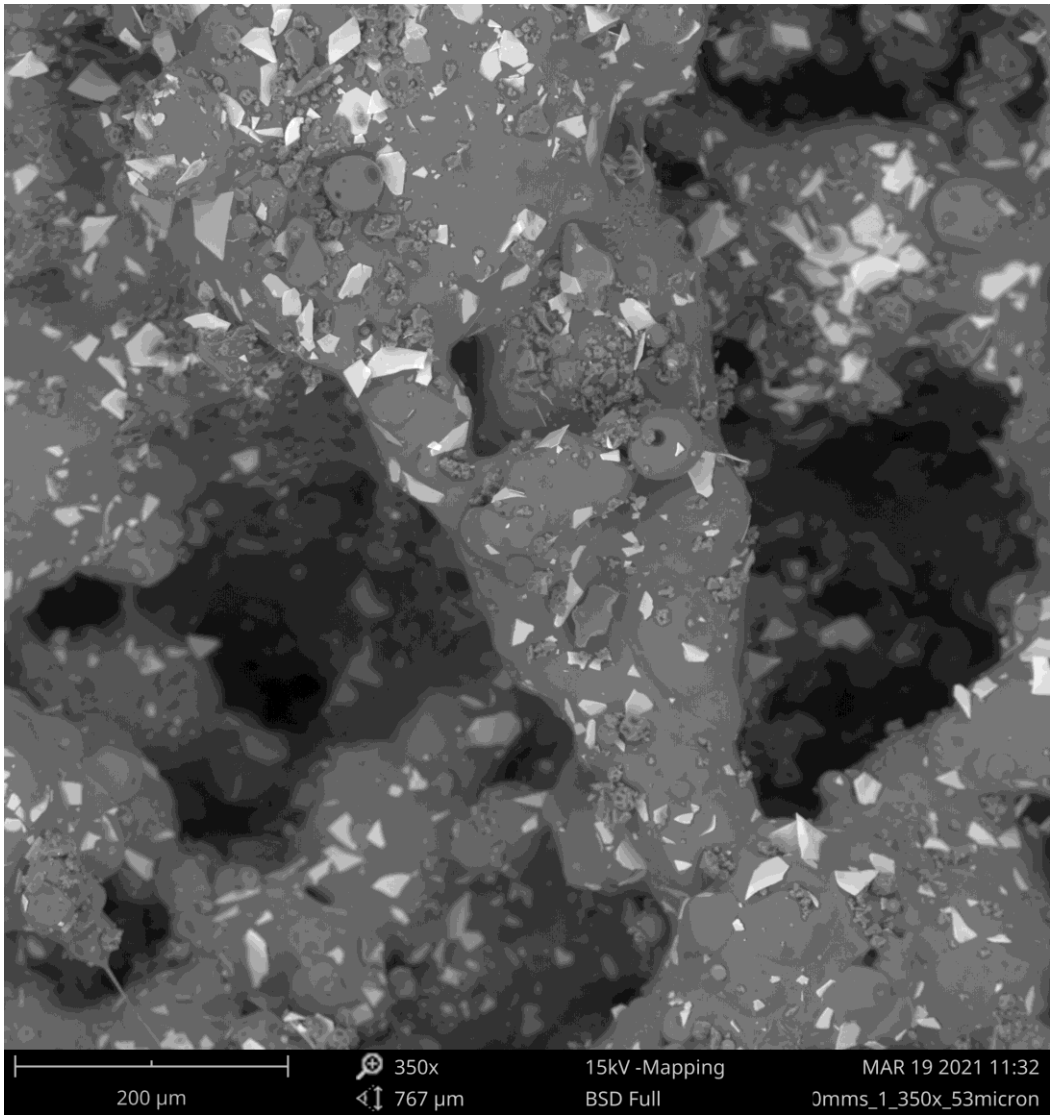

Figure 37: SEM Image of printlet with the smallest particle size distribution, 0 - 53µm. Powder and process parameters: 40% CBZ, 100mm/s

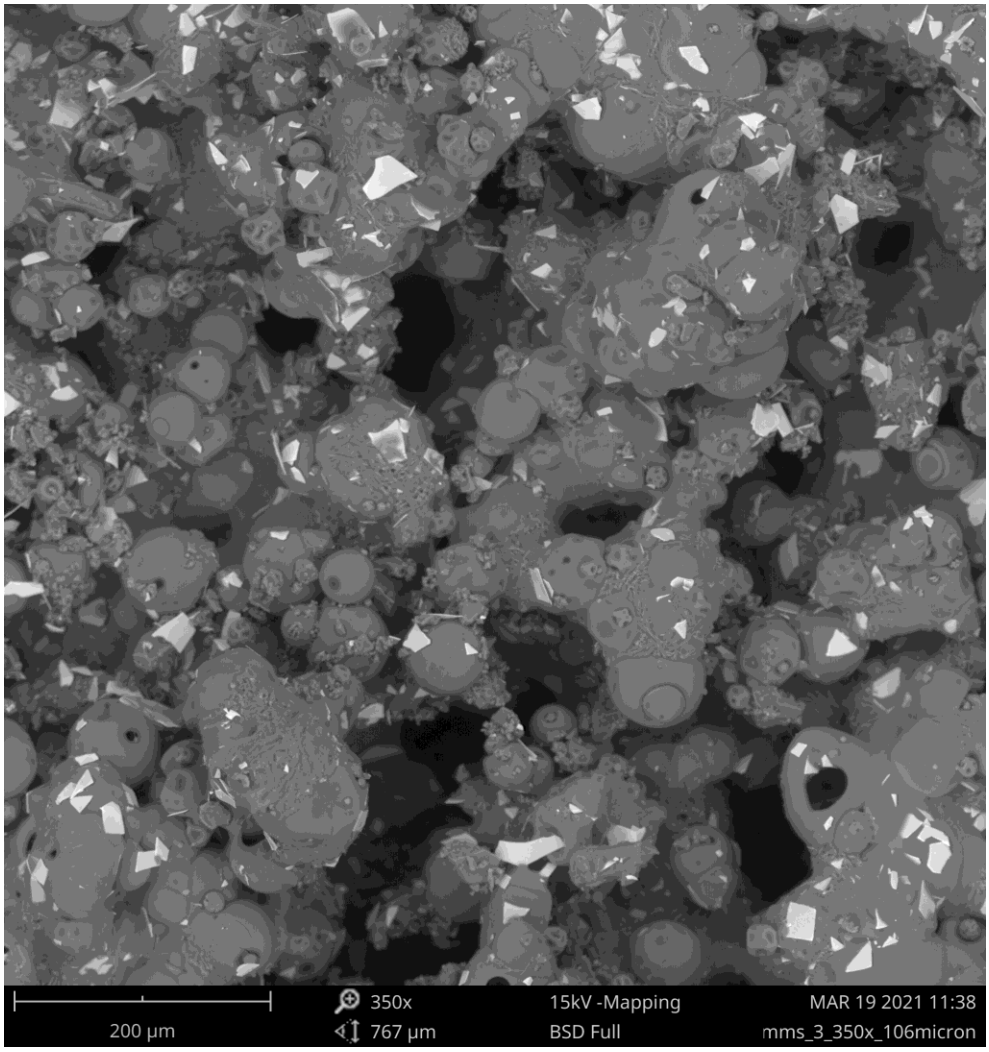

Figure 38: SEM Image of printlet with the large particle size distribution, 53 - 106µm. Powder and process parameters: 40% CBZ, 100mm/s

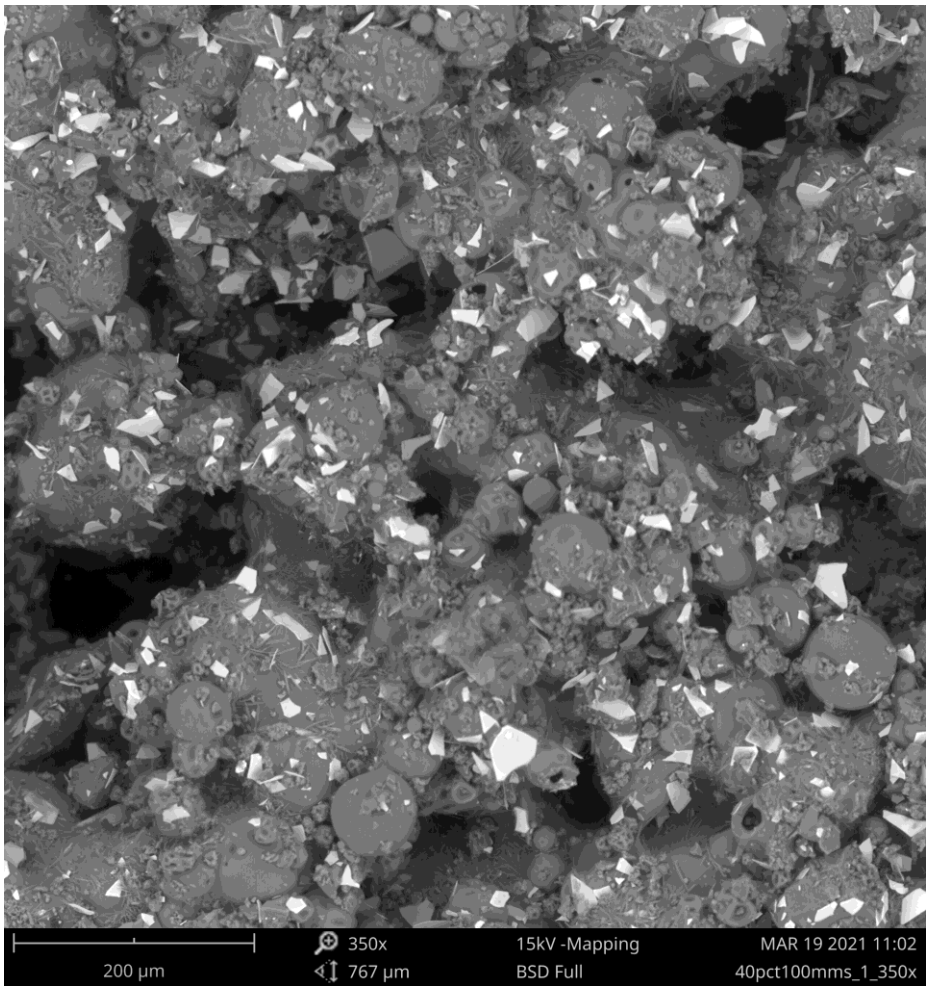

Figure 39: SEM Image of printlet with the full particle size distribution, 0 - 106µm. Powder and process parameters: 40% CBZ, 100mm/s

Summary of Deductions and Observations

The small particle size distribution (0 – 53 µm) experienced agglomeration, leading to inhibited flowability. The same behavior of the small particles present in the full powder size distribution (0 – 106 µm), also agglomerated during printing, inhibiting flowability. The lower flowability led to a decrease in mechanical properties.

CHAPTER VII

CONCLUSIONS

Impact of Process Parameters on Printlets

The bulk heating and the laser speed have significant effects on the manufacturability and the properties of the printlets, both mechanical and pharmaceutical.

Chamber and Surface Temperature

The chamber and surface temperature largely affect the powder flowability, as they control whether powder caking occurs or not (Figure 14). The powder caking began to occur ~100 °C, approximately 30 °C below the melting point of the KDSR. Printing with KDSR should be conducted just below the glaze point. With the variability in the Sintratec Kit's bulk heating, 90 °C is a reliable surface temperature that can be used to prevent the powder caking.

Laser Speed

The laser speed influences both the mechanical and pharmaceutical properties of the printlets. A higher laser speed (lower energy input) sacrifices mechanical strength for the benefit of preserving the carbamazepine. SEM images and hardness testing provide evidence of the mechanical properties trend. The dissolution testing, NIR, ATR, XRD, and SEM imaging provide evidence of the drug degradation, or at least a change in drug crystallinity, especially at lower laser speeds.

Impact of Powder Parameters on Printlets

Changing the amount of API (drug) in the powder mixture, as well as having different relative particle size distributions influences the printing process, greatly affecting the mechanical properties of the printlets.

Carbamazepine Concentration

Increasing the concentration of the CBZ in powder mixture inhibited the flowability of the powder mixture. The jagged, non-spherical CBZ particles stuck to KDSR particles, affecting the processing and performance. Examining the changes in CBZ concentration in the powder and changes in laser speed results in an inverse trend: when powder flowability is high, the highest energy input yields the best dissolution, and when powder flowability declines, the lower energy input yields the best dissolution. The two trials that were within the acceptable release rate for dissolution were the complete opposites in the DOE: the lowest drug concentration with the slowest laser scan speed (highest energy input) and the highest drug concentration with the fastest laser scan speed (lowest energy input).

Relative Particle Sizes

The smallest particle size powder (0 – 53 μm) led to agglomeration issues when printing, inhibiting flowability. This agglomeration caused the printlets to have high porosity. The agglomeration was present in the full particle size distribution (0 – 106

μm), inhibiting the its flowability, resulting in a lower hardness than the larger (53 – 106 μm) particle size distribution (Table 7, Figure 36).

Altogether, a fine balance must be achieved between all of the printing and powder parameters to produce printlets with acceptable mechanical properties while still achieving acceptable drug release without drug degradation.

Future Work

Further study is required in order to produce printlets that release the API in a more repeatable, reliable manner. Therefore, now that the printing properties of KDSR have been explored, other additives can be considered to add into the powder mixture. These additives could be to enhance API release rate, improve flowability, prevent powder caking, or even change how effectively the powder absorbs the laser energy.

One area of SLS rarely discussed in SLS studies [12] and is not explicitly explored is the subject of recycling the powder. An investigation on powder flowability, drug release rate, and drug degradation regarding recycled powder is an unexplored topic.

As mentioned in the knowledge gaps, one parameter not considered until this study's conclusion was the effect humidity can have on the powder during storing, mixing, and printing.

Finally, for SLS of pharmaceuticals, a change in laser power has not been explored, other than changing the laser scan speed. All studies involving SLS of pharmaceuticals use the Sintratec Kit [21], which has a constant laser power of 2.3W. However, the effect of a different laser, whether a different constant power or a pulse laser, has not been explored.

REFERENCES

[1] Spritam® FDA label. Accessed on May 15, 2020. https://www.accessdata.fda.gov/drugsatfda_docs/label/2017/207958s004lbl.pdf.

[2] "LFA Rotary Tablet Presses." Retrieved March 24, 2020, from https://www.lfatabletpresses.com/products/rotary-tablet-presses.

[3] USP (2017). "Harmonization Standards." from https://www.usp.org/harmonized-standards/pdg/general-chapters.

[4] E. Heidari, M.A. Sobati, S. Movahedirad, Dynamics of particle wetting in wet granulation: Micro-scale analysis, International Journal of Heat and Mass Transfer, 146 (2020) 118853.

[5] S. Shanmugam, Granulation techniques and technologies: recent progresses, BioImpacts, 5 (2015) 55-63.

[6] R. Eyjolfsson, Design and Manufacture of Pharmaceutical Tablets, in, Academic Press, 2015.

[7] F. Osei-Yeboah, C.C. Sun, Validation and applications of an expedited tablet friability method, International Journal of Pharmaceutics, 484 (2015) 146-155.

[8] I. Akseli, J. Xie, L. Schultz, N. Ladyzhynsky, T. Bramante, X. He, R. Deanne, K.R. Horspool, R. Schwabe, A Practical Framework Toward Prediction of Breaking Force and Disintegration of Tablet Formulations Using Machine Learning Tools, Journal of Pharmaceutical Sciences, 106 (2017) 234-247.

[9] Z. Rahman, N.A. Charoo, M. Kuttolamadom, A. Asadi, M.A. Khan, Chapter 46 - Printing of personalized medication using binder jetting 3D printer, in: J. Faintuch, S. Faintuch (Eds.) Precision Medicine for Investigators, Practitioners and Providers, Academic Press, 2020, pp. 473-481.

[10] W.E. Katstra, R.D. Palazzolo, C.W. Rowe, B. Giritlioglu, P. Teung, M.J. Cima, Oral dosage forms fabricated by Three Dimensional Printing™, Journal of Controlled Release, 66 (2000) 1-9.

[11] "Stereolithography (SLA) 3D Printing – Simply Explained." All3DP, 26 Feb. 2020, all3dp.com/2/stereolithography-3d-printing-simply-explained/.

[12] C.A. Chatham, T.E. Long, C.B. Williams, A review of the process physics and material screening methods for polymer powder bed fusion additive manufacturing, Progress in Polymer Science, 93 (2019) 68-95.

[13] Y. Zhou, S. Xi, Y. Huang, M. Kong, Q. Yang, G. Li, Preparation of near-spherical PA12 particles for selective laser sintering via Plateau-Rayleigh instability of molten fibers, Materials & Design, 190 (2020) 108578.

[14] L.C.Y. Chan, N.W. Page, Particle fractal and load effects on internal friction in powders, Powder Technology, 90 (1997) 259-266.

[15] S. Ziegelmeier, P. Christou, F. Wöllecke, C. Tuck, R. Goodridge, R. Hague, E. Krampe, E. Wintermantel, An experimental study into the effects of bulk and flow behaviour of laser sintering polymer powders on resulting part properties, Journal of Materials Processing Tech., 215 (2015) 239-250.

[16] M. Schmid, A. Amado, K. Wegener, Polymer Powders for Selective Laser Sintering (SLS), AIP Conference Proceedings, 1664 (2015) 1.

[17] S. Haeri, Y. Wang, O. Ghita, J. Sun, Discrete element simulation and experimental study of powder spreading process in additive manufacturing, Powder Technology, 306 (2017) 45-54.

[18] J. Choren, V. Gervasi, T. Herman, S. Kamara, J. Mitchell, SLS powder life study, Solid Freeform Fabrication Symposium, (2001).

[19] S. Dadbakhsh, L. Verbelen, O. Verkinderen, D. Strobbe, P. Van Puyvelde, J.-P. Kruth, Effect of PA12 powder reuse on coalescence behaviour and microstructure of SLS parts, European Polymer Journal, 92 (2017) 250-262.

[20] I. Gibson, D. Shi, Material properties and fabrication parameters in selective laser sintering process, Rapid Prototyping Journal, 3 (1997) 129-136.

[21] "Sintratec Kit." Retrieved 24 March 2020, from https://sintratec.com/product/sintratec-kit/. in.

[22] A.H. Espera, Jr., A.D. Valino, J.O. Palaganas, L. Souza, Q. Chen, R.C. Advincula, 3D Printing of a Robust Polyamide-12-Carbon Black Composite via Selective Laser Sintering: Thermal and Electrical Conductivity, in, 2019.

[23] Candurin® NXT Ruby Red. 120624. Merck Group. Darmstadt, Germany. 6 September 2020.

[24] "Gold Sheen Powder Candurin®." Retrieved 24 March 2020, from https://www.ingredientdepot.com/products/candurin-gold-sheen.

[25] D. Drummer, D. Rietzel, F. Kühnlein, Development of a characterization approach for the sintering behavior of new thermoplastics for selective laser sintering, Physics Procedia, 5 (2010) 533-542.

[26] M. Pavan, M. Faes, D. Strobbe, B. Van Hooreweder, T. Craeghs, D. Moens, W. Dewulf, On the influence of inter-layer time and energy density on selected critical-to-quality properties of PA12 parts produced via laser sintering, Polymer Testing, 61 (2017) 386-395.

[27] J. Schneider, S. Kumar, Multiscale characterization and constitutive parameters identification of polyamide (PA12) processed via selective laser sintering, Polymer Testing, 86 (2020).

[28] Z. Hadi, Investigation into crystallinity and degree of particle melt in selective laser sintering, 2011.

[29] S.F. Barakh Ali, E.M. Mohamed, T. Ozkan, M.A. Kuttolamadom, M.A. Khan, A. Asadi, Z. Rahman, Understanding the effects of formulation and process variables on the printlets quality manufactured by selective laser sintering 3D printing, International Journal of Pharmaceutics, 570 (2019) 118651.

[30] N. Allahham, F. Fina, C. Marcuta, L. Kraschew, W. Mohr, S. Gaisford, A.W. Basit, A. Goyanes, Selective Laser Sintering 3D Printing of Orally Disintegrating Printlets Containing Ondansetron, in, 2020.

[31] A. Awad, A. Yao, S.J. Trenfield, A. Goyanes, S. Gaisford, A.W. Basit, 3D Printed Tablets (Printlets) with Braille and Moon Patterns for Visually Impaired Patients, in, 2020.

[32] F. Fina, A. Goyanes, S. Gaisford, A.W. Basit, Selective laser sintering (SLS) 3D printing of medicines, International Journal of Pharmaceutics, 529 (2017) 285-293.

[33] A. Atheer, F. Fabrizio, J.T. Sarah, P. Pavanesh, G. Alvaro, G. Simon, W.B. Abdul, 3D Printed Pellets (Miniprintlets): A Novel, Multi-Drug, Controlled Release Platform Technology, Pharmaceutics, 11 (2019) 148-148.

[34] F. Fina, C.M. Madla, A. Goyanes, J. Zhang, S. Gaisford, A.W. Basit, Fabricating 3D printed orally disintegrating printlets using selective laser sintering, International Journal of Pharmaceutics, 541 (2018) 101-107.

[35] C. Funkhouser, S.F. Barakh Ali, L. Richardson, Z. Rahman, M. Khan, M. Kuttolamadom, Thermal Influence on Printlet Quality in the Selective Laser Sintering of Pharmaceutical Formulations, in, 2020.

[36] V. M, A.S. J, H. D, N.T. T, Mechanical characterization of the Poly lactic acid (PLA) composites prepared through the Fused Deposition Modelling process, Materials Research Express, 6 (2019) 105359.

[37] K. Wudy, S. Greiner, M. Zhao, D. Drummer, Selective laser beam melting of polymers: In situ and offline measurements for process adapted thermal characterization, Procedia CIRP, 74 (2018) 238-243.

[38] A. Goyanes, A.B.M. Buanz, G.B. Hatton, S. Gaisford, A.W. Basit, 3D printing of modified-release aminosalicylate (4-ASA and 5-ASA) tablets, European Journal of Pharmaceutics and Biopharmaceutics, 89 (2015) 157-162.

[39] S. Morales-Planas, J. Minguella-Canela, J. Lluma-Fuentes, J. Antonio Travieso-Rodriguez, A.-A. Garcia-Granada, Multi Jet Fusion PA12 Manufacturing Parameters for Watertightness, Strength and Tolerances, in, 2018.

[40] A. Wegner, G. Witt, Process monitoring in laser sintering using thermal imaging, 22nd Annual International Solid Freeform Fabrication Symposium - An Additive Manufacturing Conference, SFF 2011, (2011).

[41] Badamid PA12 H. Baden, Germany. Accessed 3 April 2020. https://www.bada.de/download/public/share/public/shop/22/product/Safety-data-sheet-Badamid-PA12-H.pdf

[42] T.R. Jagtap P, Shendge R. A brief review on Kollidon. JDDT [Internet]. 15Mar.2019 [cited 29Jun.2020];9(2):493-00. Available from: http://jddtonline.info/index.php/jddt/article/view/2539.

[43] S.H. Song, B.R. Chae, S.I. Sohn, D.W. Yeom, H.Y. Son, J.H. Kim, S.R. Kim, S.G. Lee, Y.W. Choi, Formulation of controlled-release pelubiprofen tablet using Kollidon® SR, International Journal of Pharmaceutics, 511 (2016) 864-875.

[44] BASF (2020). "Kollidon® SR." Retrieved 13 July 2020, from https://pharmaceutical.basf.com/global/en/drug-formulation/products/kollidon-sr.html.

[45] “CARBAMAZEPINE TABLETS, USP.” U.S. National Library of Medicine, National Institutes of Health May, 2010.

[46] BASF, Kollidon® VA64, in, BASF, Ludwigshafen, Germany, 2000.

[47] BASF (2020). "Functional solutions for formulations with sustained drug release." Retrieved 1 September 2020.

[48] “VK 200 Tablet Hardness Tester Operator’s Manual.” Https://Www.agilent.com/Cs/Library/Usermanuals/Public/70-9015h_vk_200_op_man.Pdf, Nov. 2010, www.agilent.com/cs/library/usermanuals/public/70-9015h_vk_200_op_man.pdf.

[49] “TA.XTplusC Texture Analyser.” Stable Micro Systems, www.stablemicrosystems.com/TAXTplus.html.

[50] Carbamazepine Extended-Release Tablets. USP43-NF38 - 746, USP42-NF37 - 728, USP41-NF36 - 689. Accessed 1 April 2021.

[51] USP, Harmonization Standards, in, 2017.

[52] “708-DS Dissolution Apparatus.” Agilent, www.agilent.com/en/product/dissolution-testing/dissolution-apparatus/708-ds-dissolution-apparatus.

[53] “1260 Infinity II LC System.” Agilent, www.agilent.com/en/product/liquid-chromatography/hplc-systems/analytical-hplc-systems/1260-infinity-ii-lc-system.

[54] http://www.bostonlabco.com/uploads/2/4/5/1/24519591/s652753007727812206_p418_i2_w640.jpeg.

[55] “Phenom XL.” Nanoscience Instruments, 9 Dec. 2020, www.nanoscience.com/products/scanning-electron-microscopes/phenom-xl/.

[56] “Nicolet iS50 FTIR Spectrometer.” Thermo Fisher Scientific - US, www.thermofisher.com/us/en/home/industrial/spectroscopy-elemental-isotope-

analysis/molecular-spectroscopy/fourier-transform-infrared-ftir-spectroscopy/ftir-instruments/ftir-spectrometers/nicolet-iS50-ftir-spectrometer.html.

APPENDIX A

SEM IMAGES

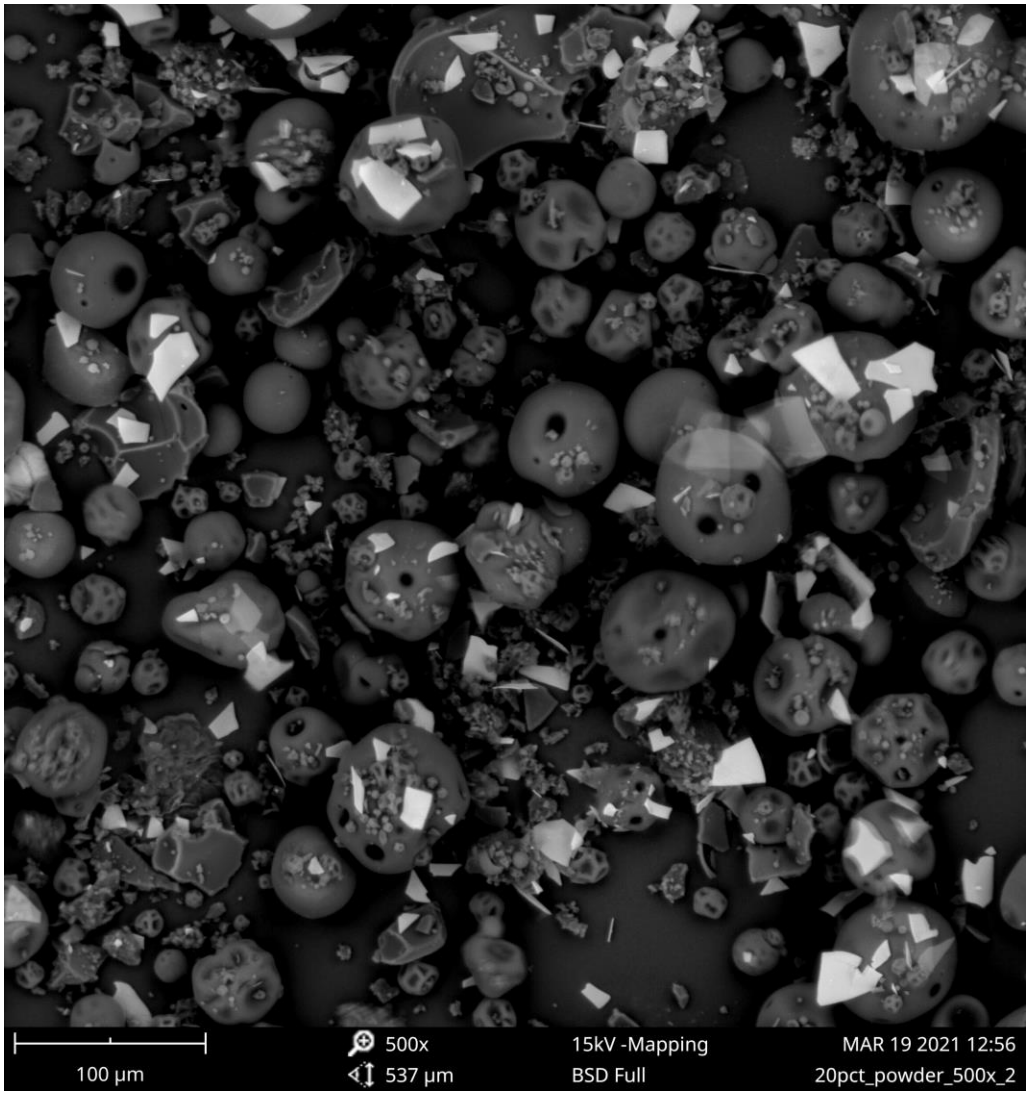

Figure 40: SEM Image of 20% CBZ Unprinted Powder at 500x magnification

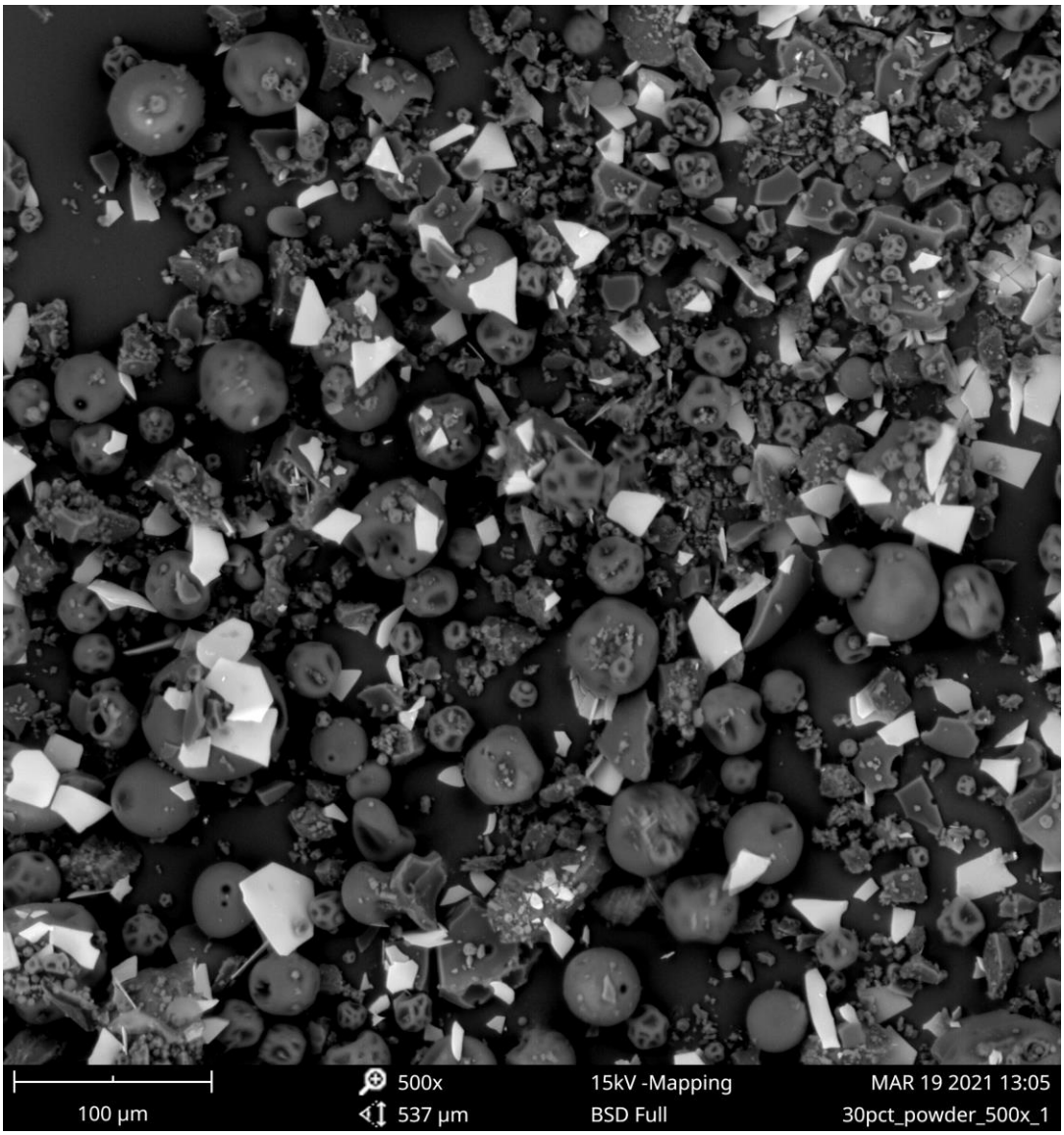

Figure 41: SEM Image of 30% CBZ Unprinted Powder at 500x magnification

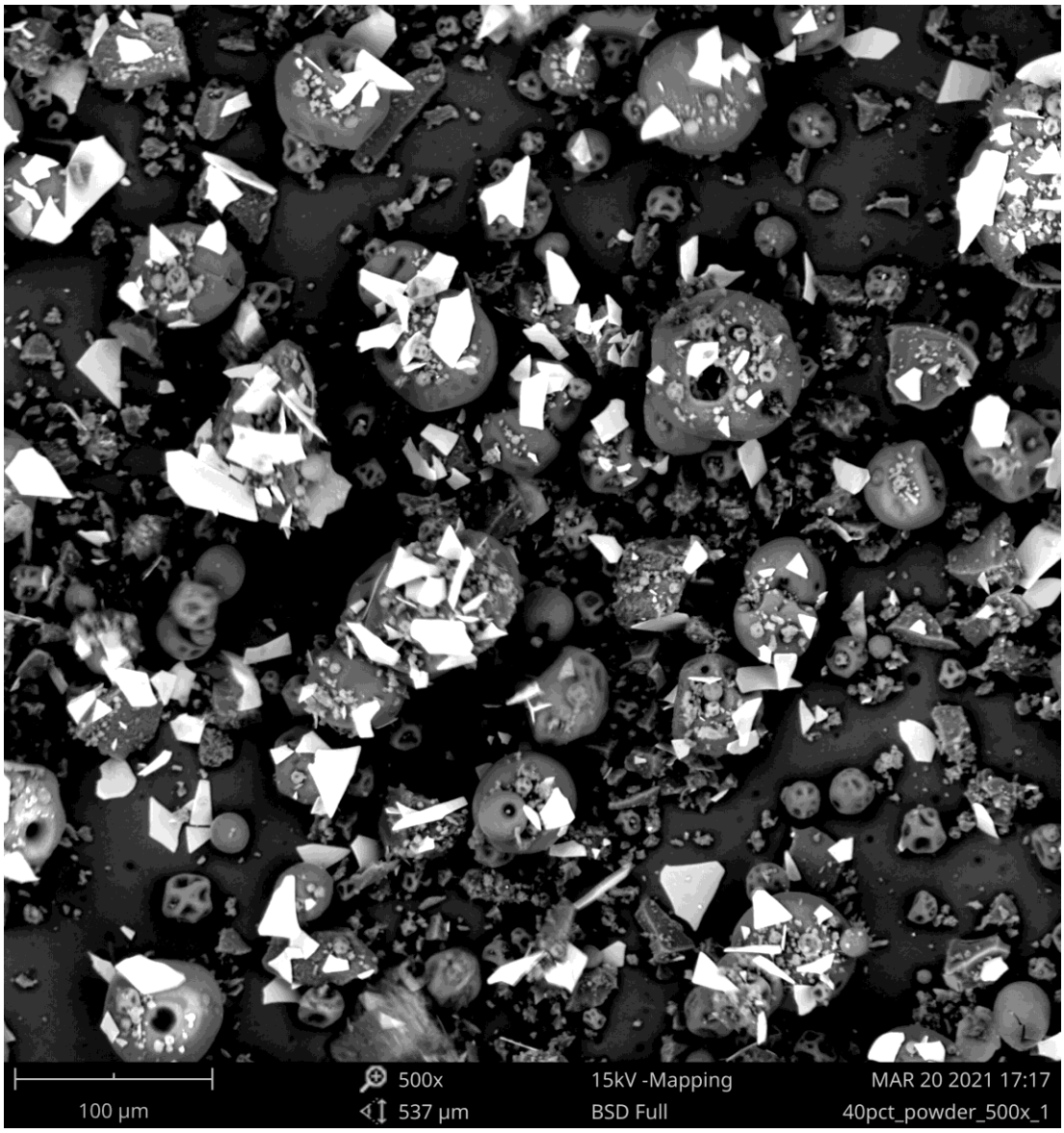

Figure 42: SEM Image of 40% CBZ Unprinted Powder at 500x magnification

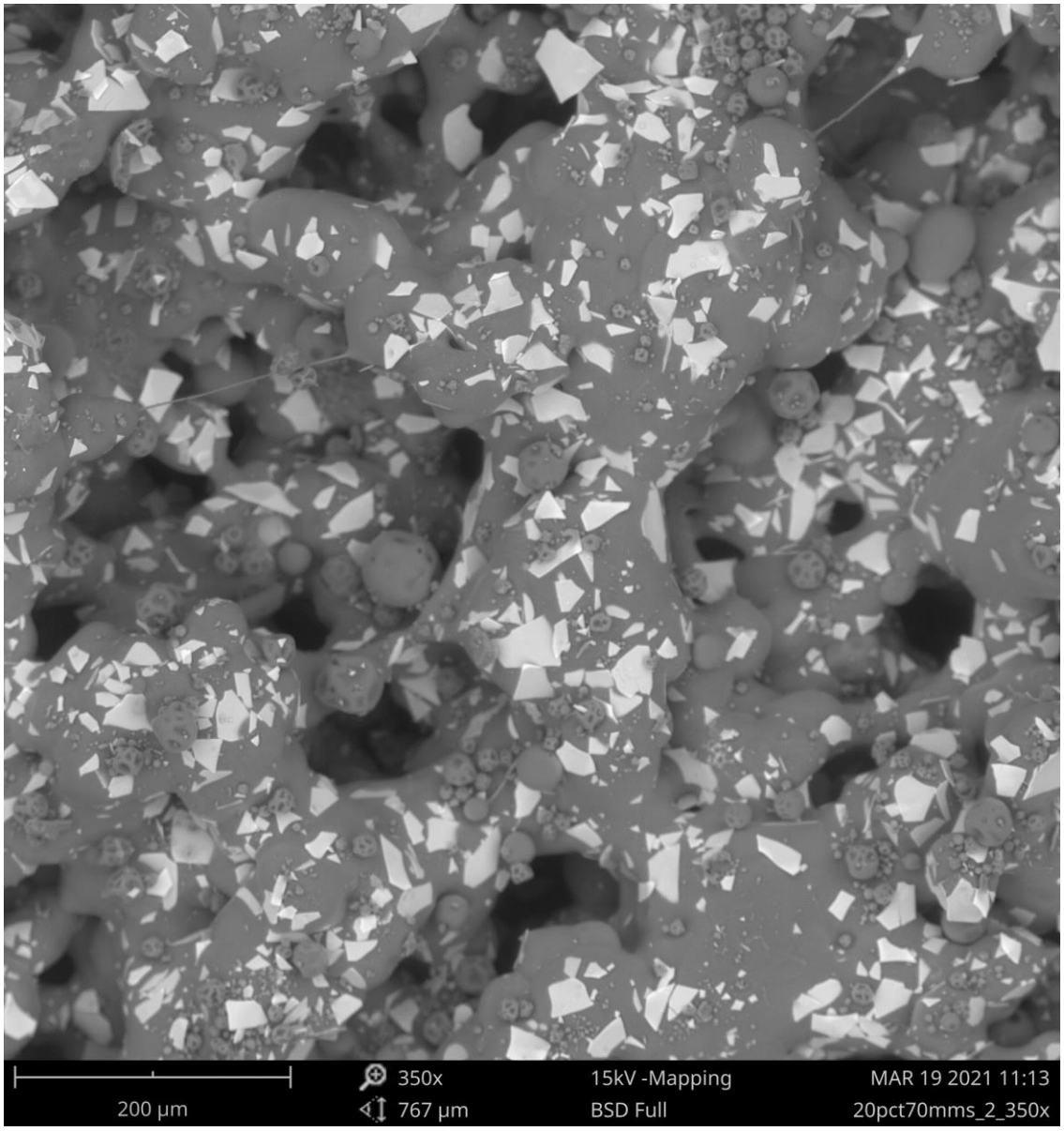

Figure 43: SEM Image of 40% CBZ, 70mm/s Printlet at 350x magnification

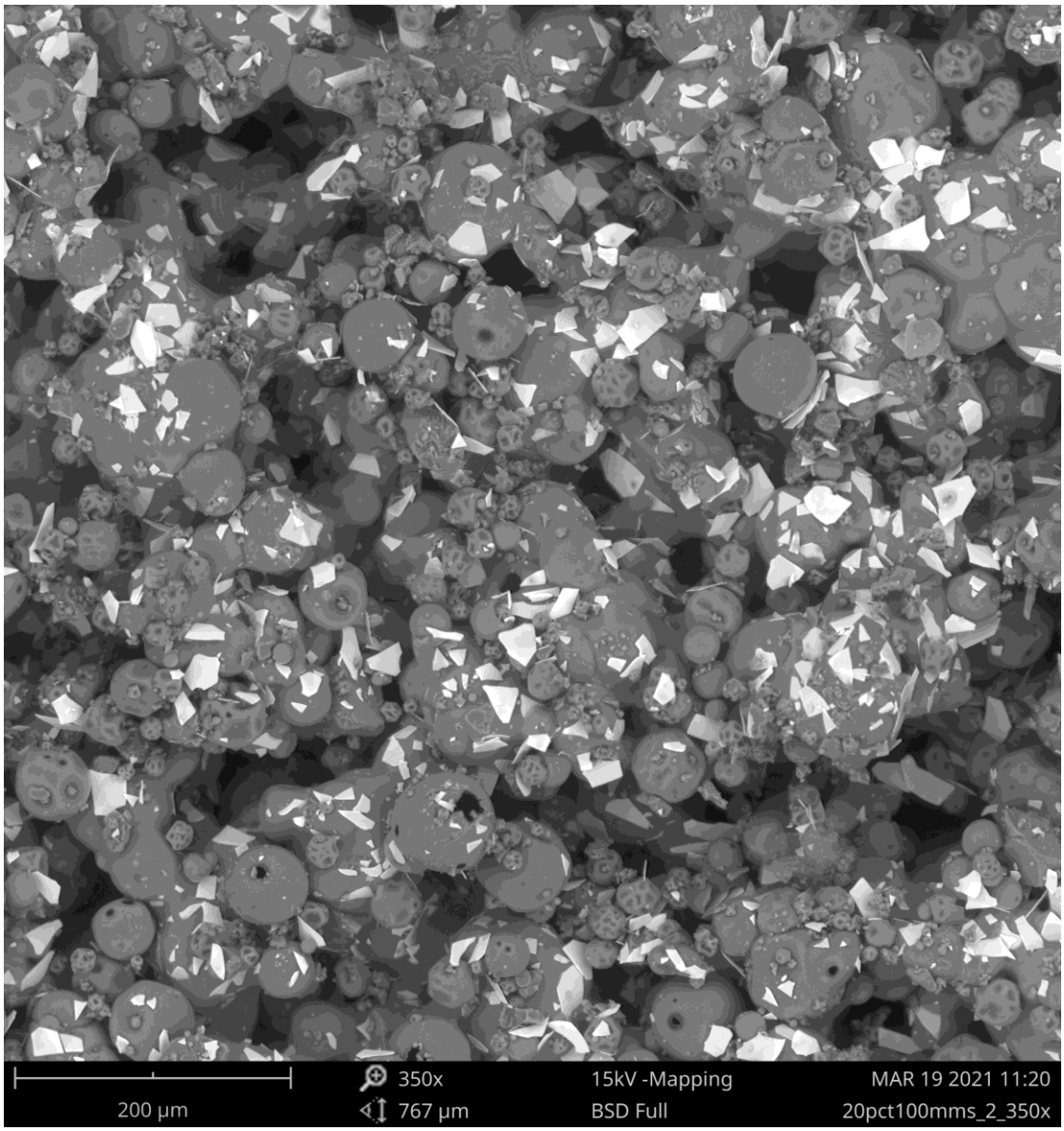

Figure 44: SEM Image of 40% CBZ, 100mm/s Printlet at 350x magnification

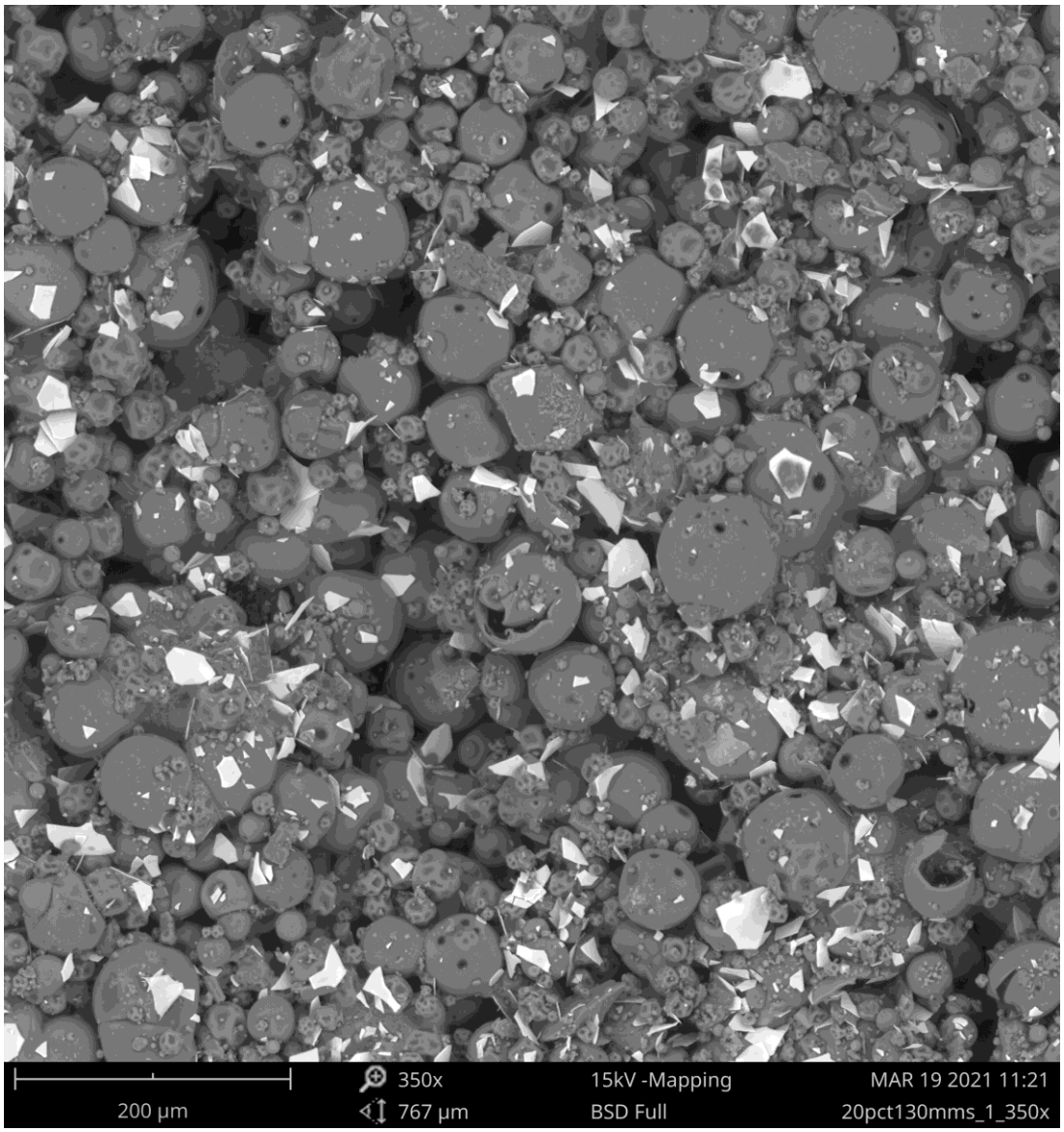

Figure 45: SEM Image of 40% CBZ, 130mm/s Printlet at 350x magnification

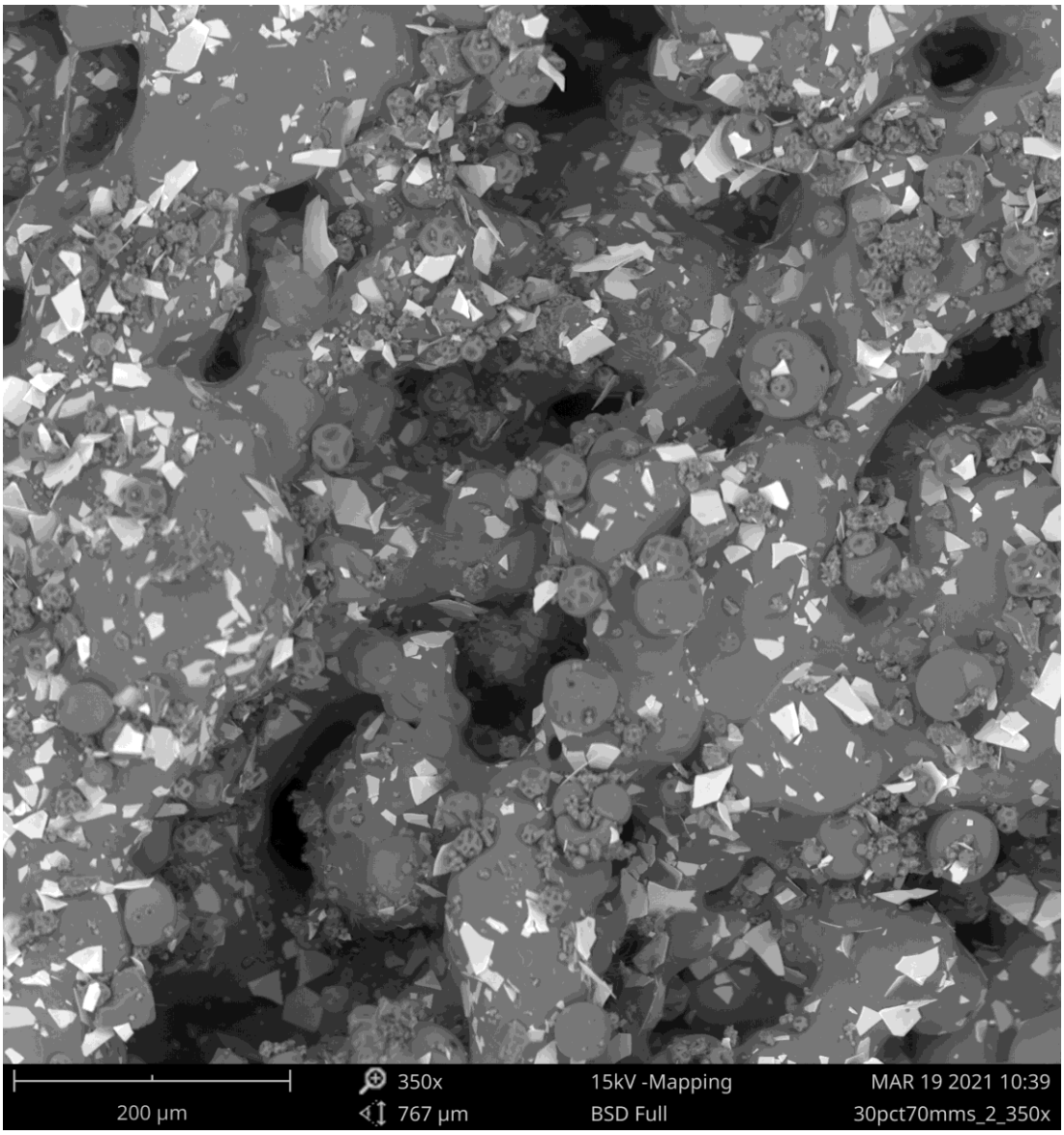

Figure 46: SEM Image of 30% CBZ, 70mm/s Printlet at 350x magnification

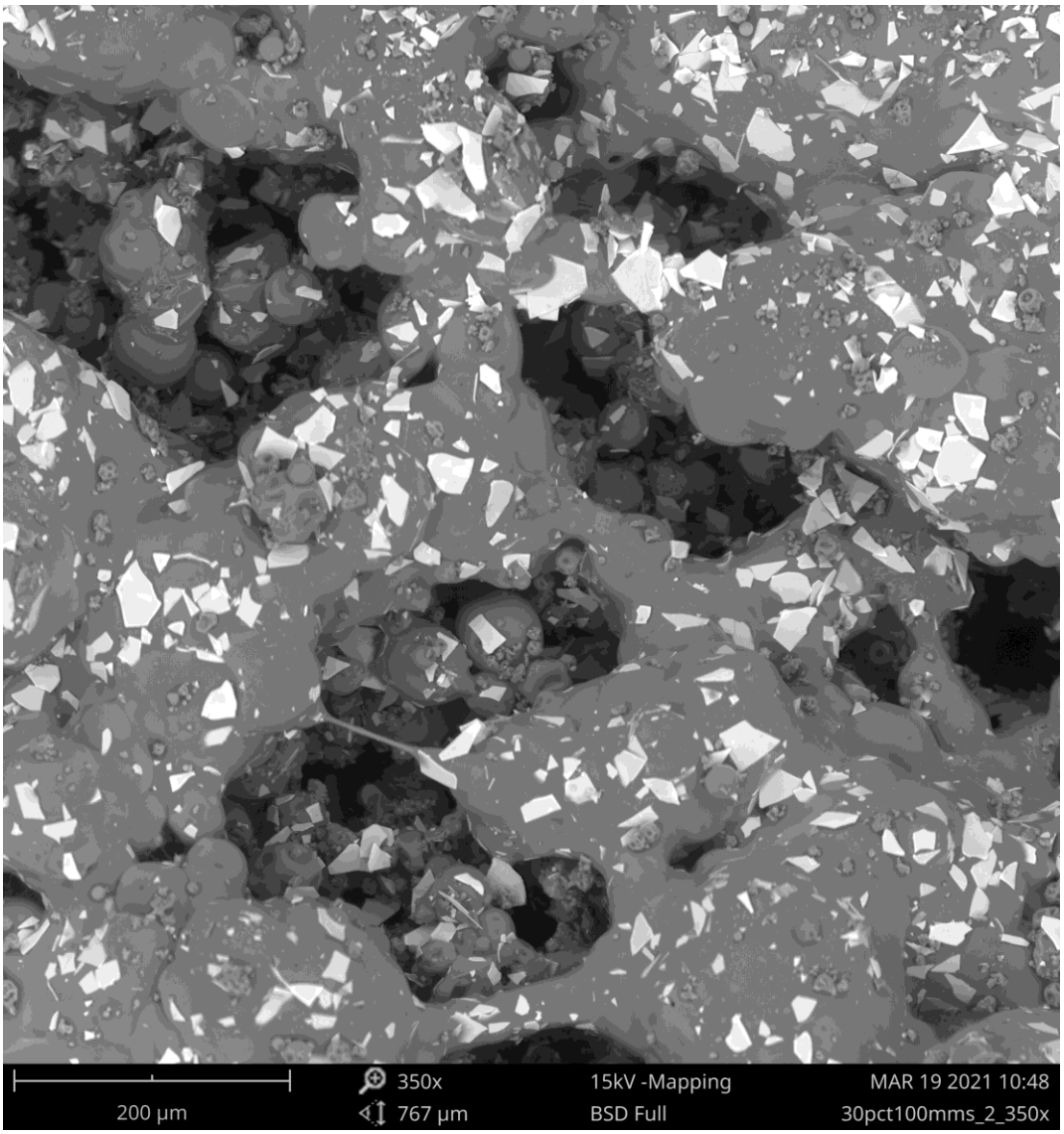

Figure 47: SEM Image of 30% CBZ, 100mm/s Printlet at 350x magnification

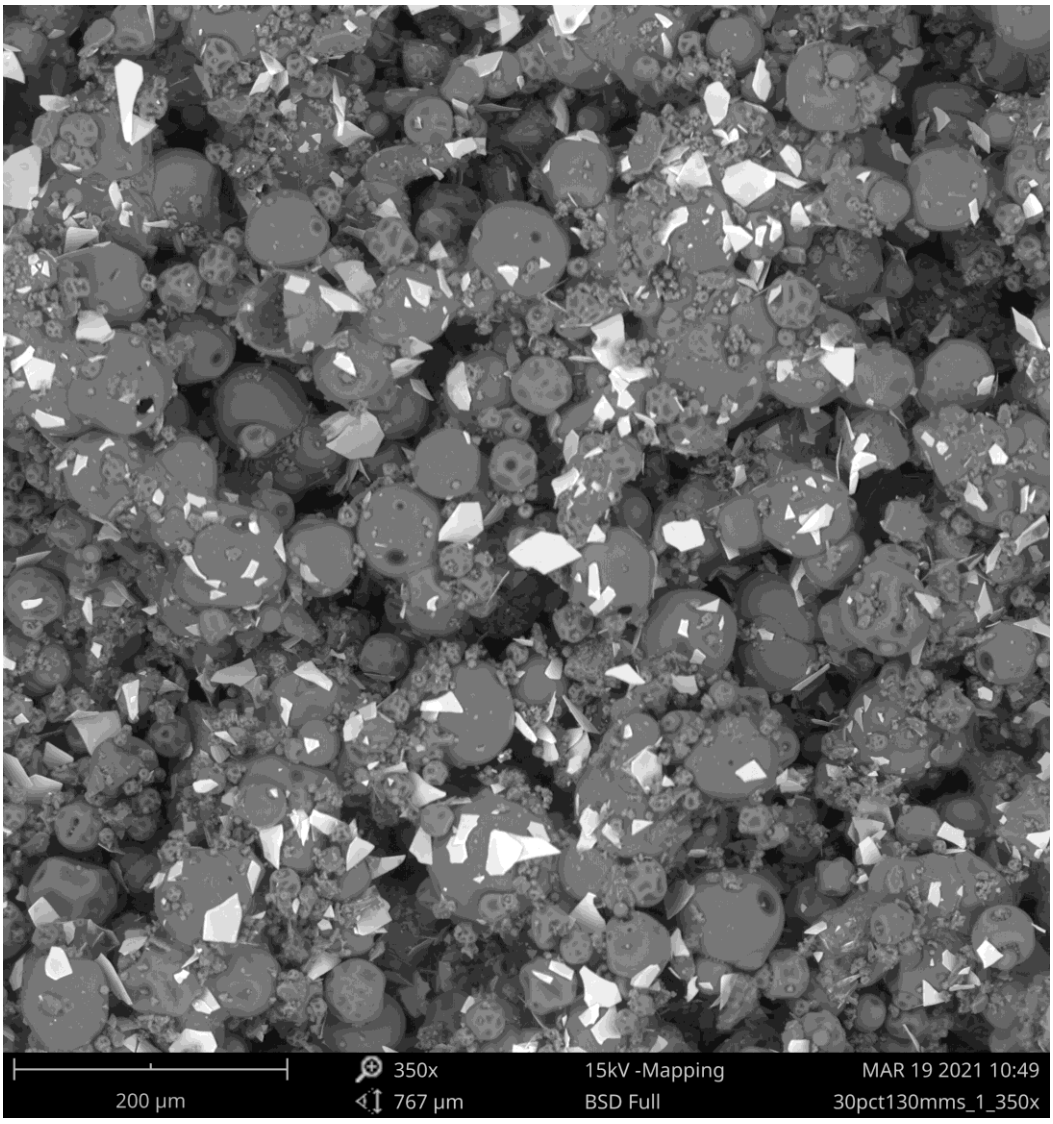

Figure 48: SEM Image of 30% CBZ, 130mm/s Printlet at 350x magnification

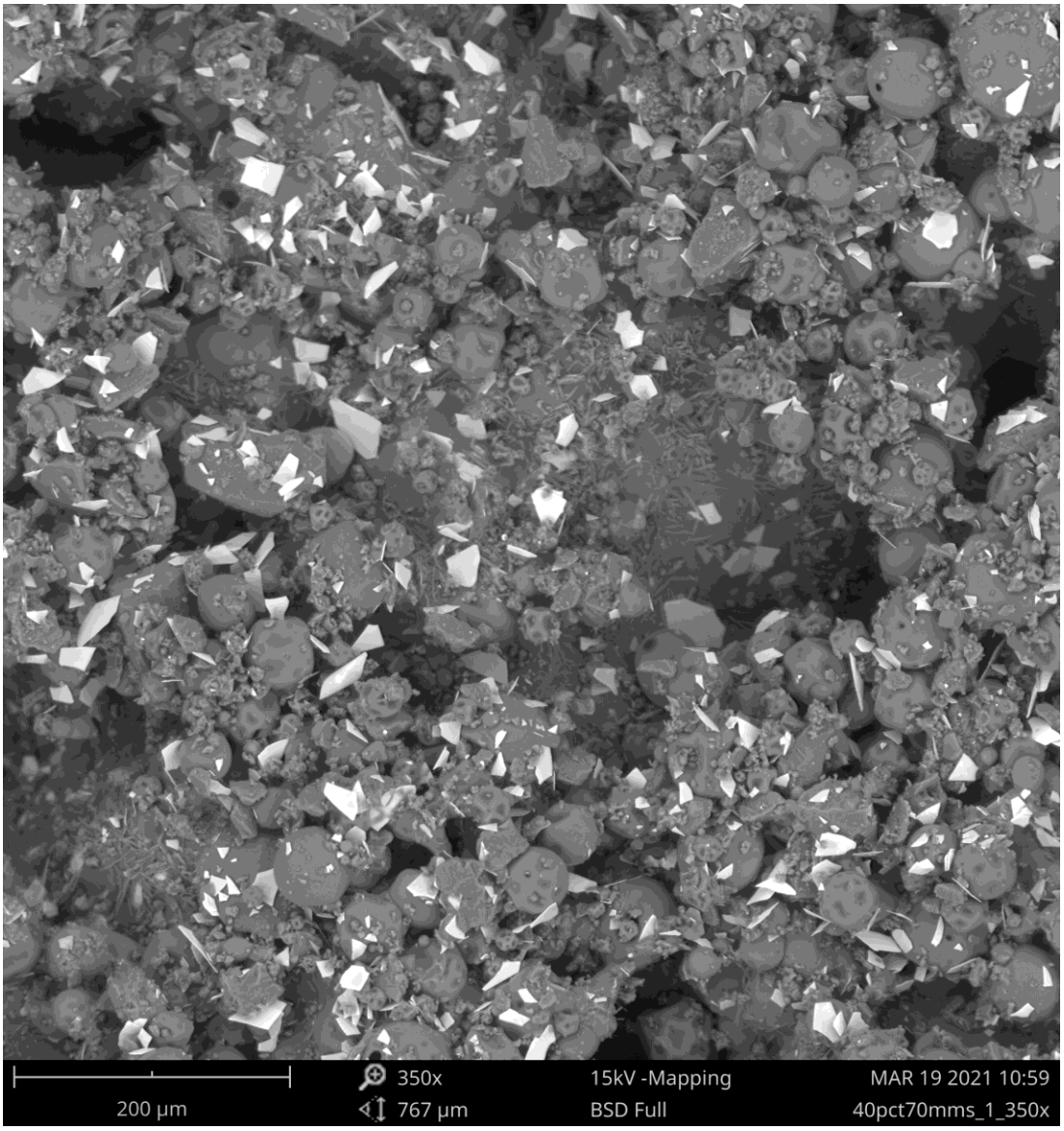

Figure 49: SEM Image of 40% CBZ, 70mm/s Printlet at 350x magnification

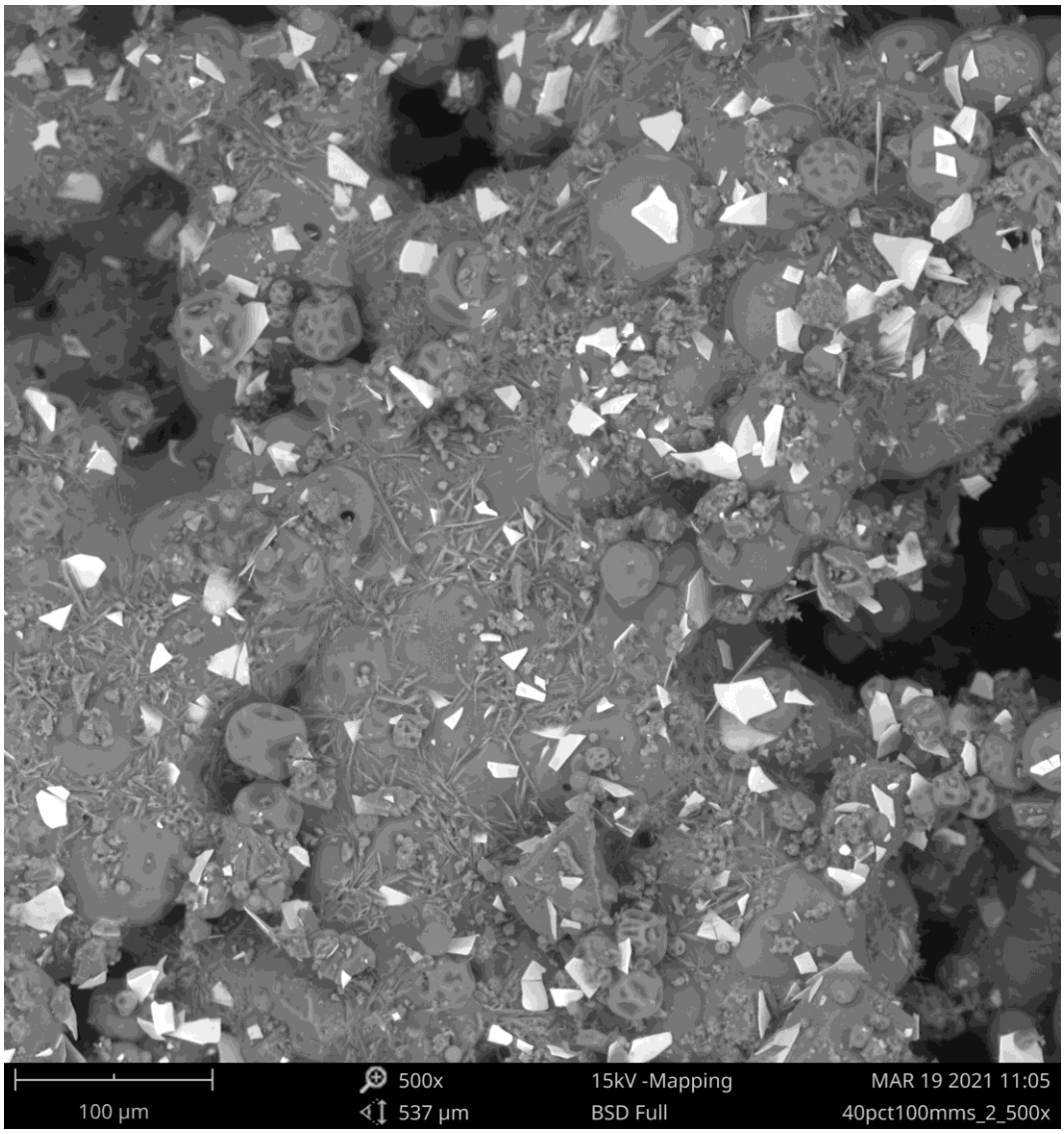

Figure 50: SEM Image of 40% CBZ, 100mm/s Printlet at 350x magnification

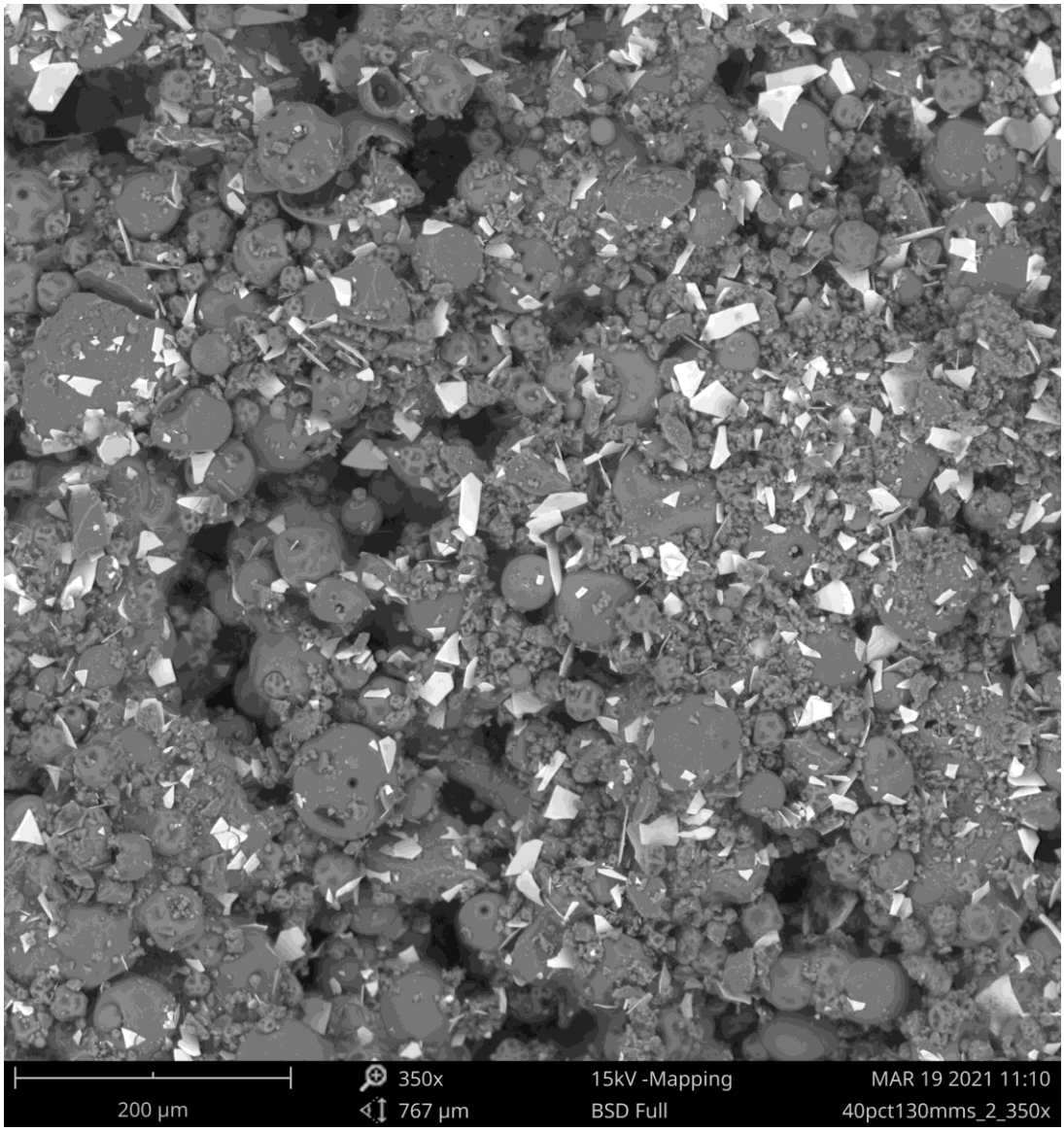

Figure 51: SEM Image of 40% CBZ, 130mm/s Printlet at 350x magnification

APPENDIX B:

NIR, ATR, AND XRD IMAGES

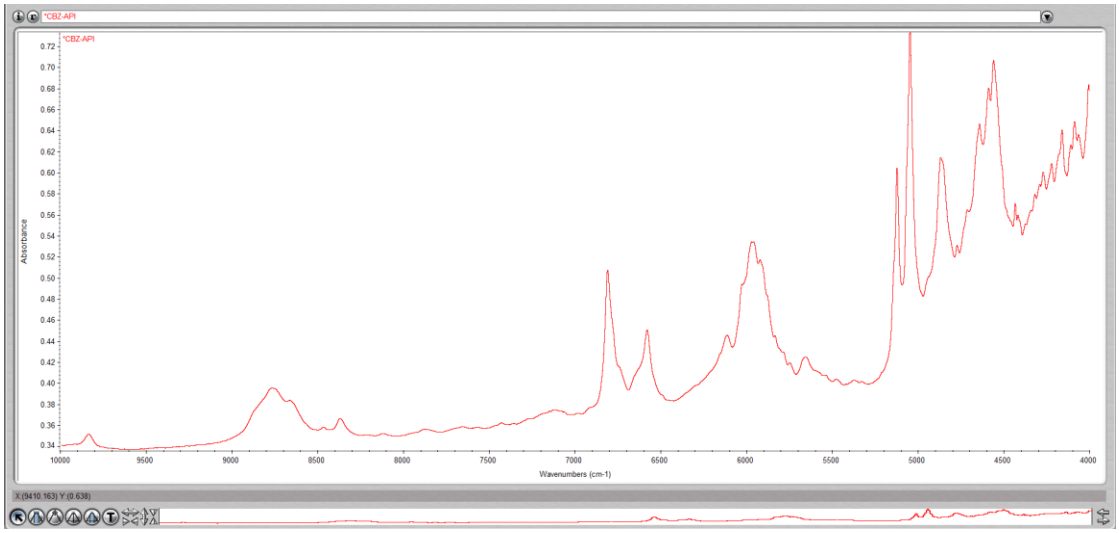

Figure 52 NIR: CBZ Functional Groups

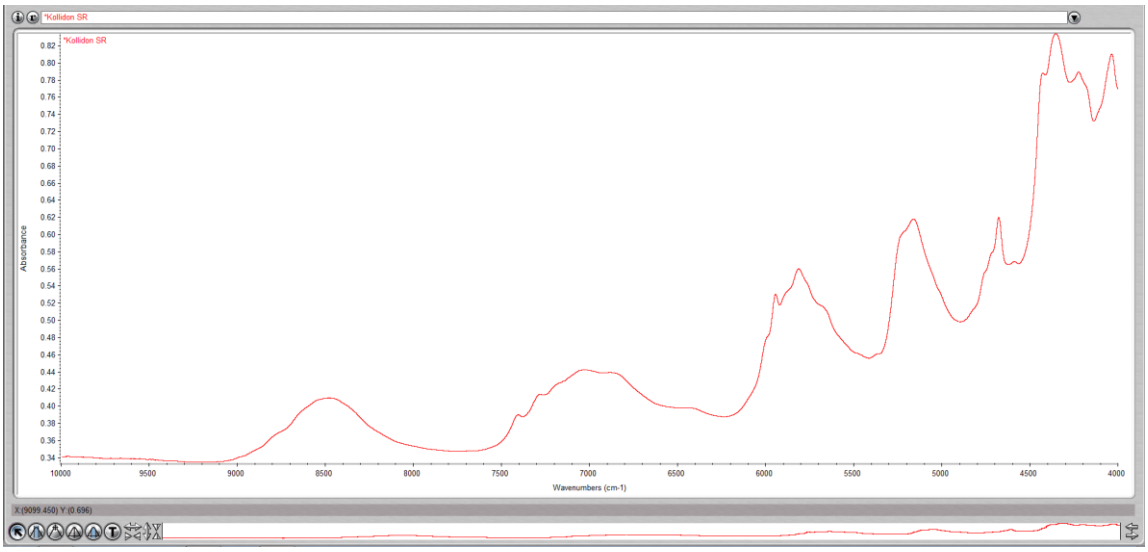

Figure 53: NIR KDSR Functional Groups

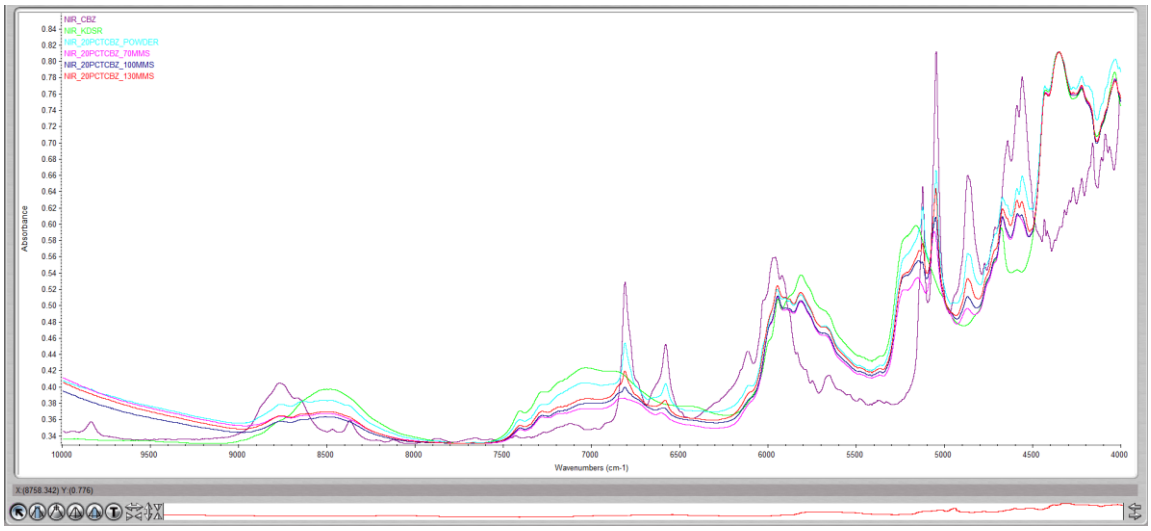

Figure 54: NIR 20% CBZ Functional Groups Comparison

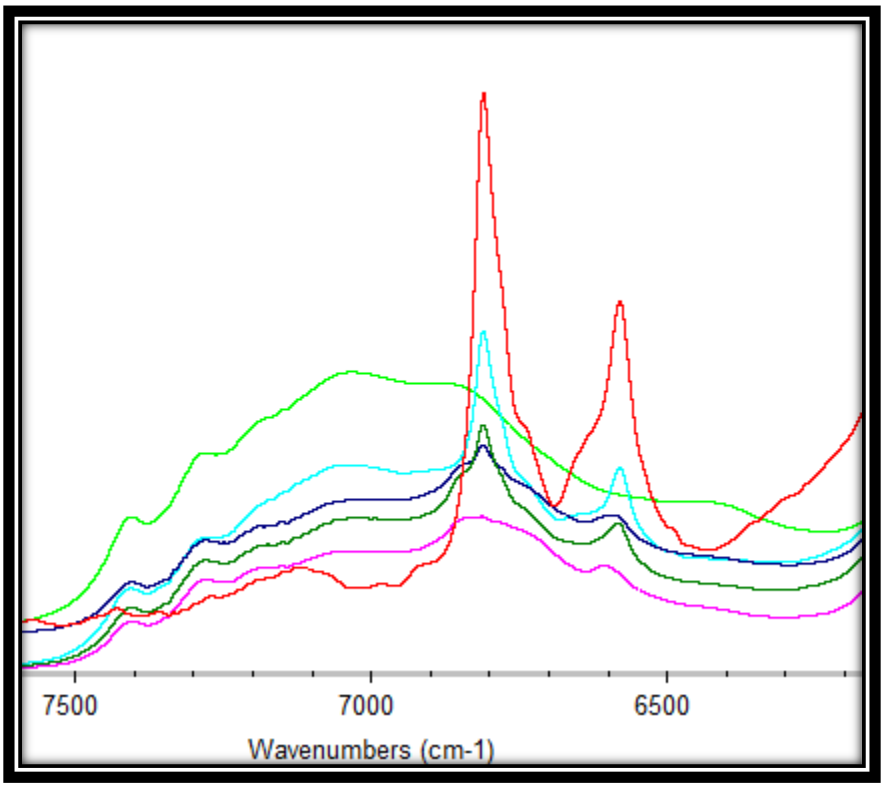

Figure 55: NIR 20% CBZ Peak Changes

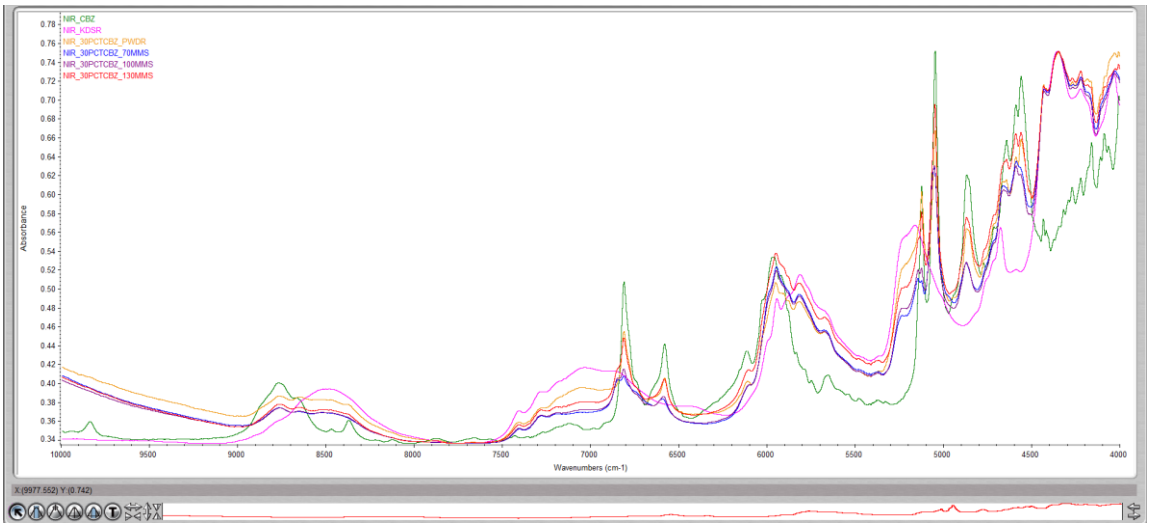

Figure 56: NIR 30% CBZ Functional Groups Comparison

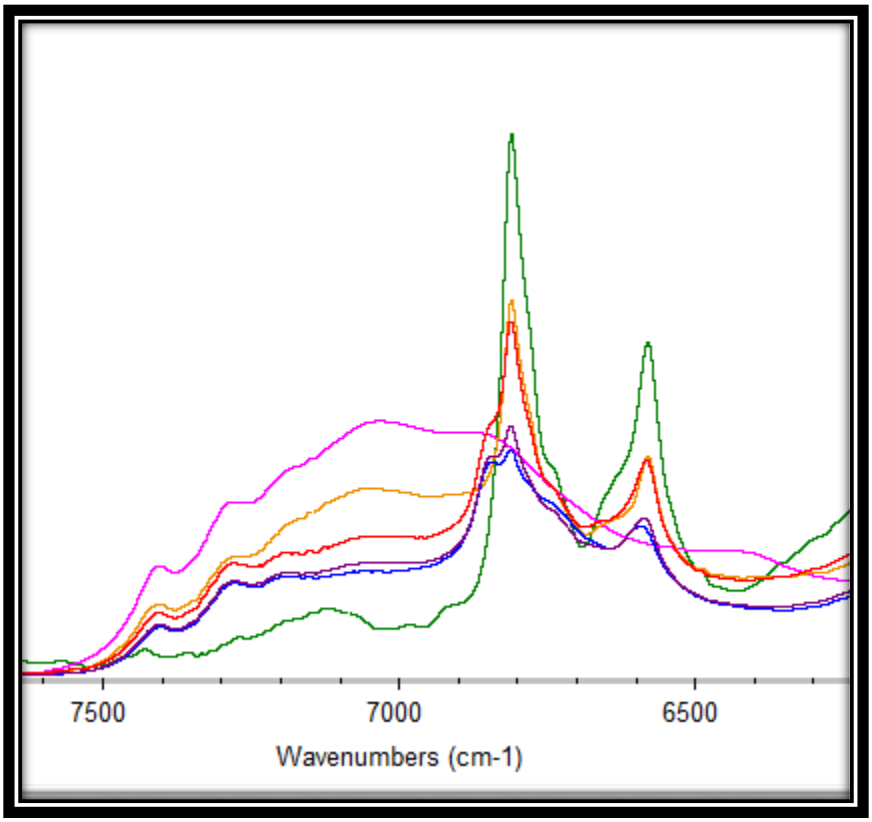

Figure 57: NIR 30% CBZ Peak Changes

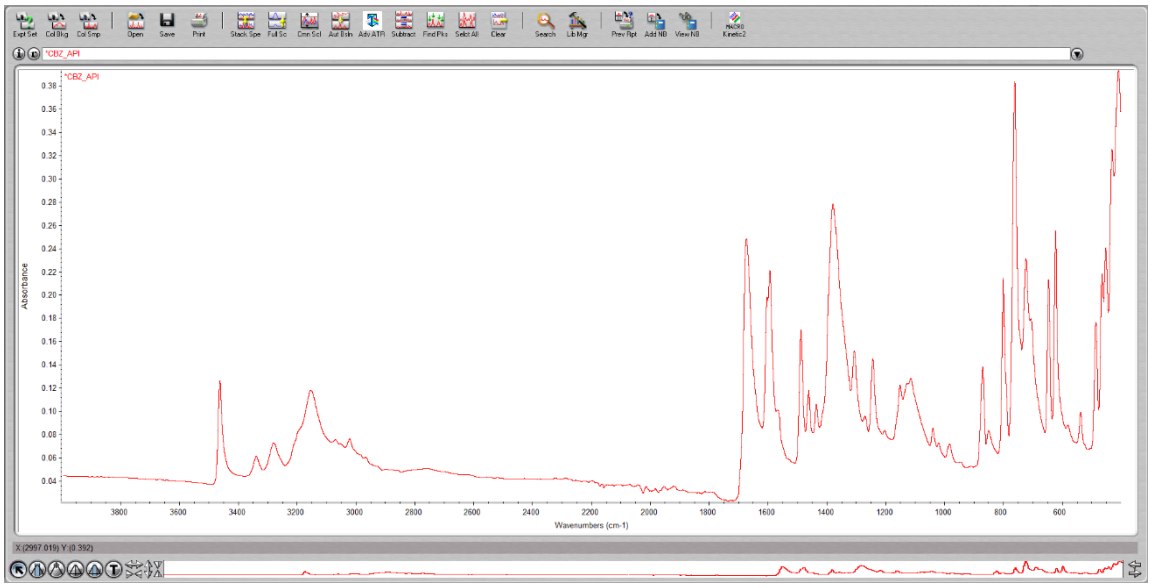

Figure 58: ATR Functional Groups of the CBZ

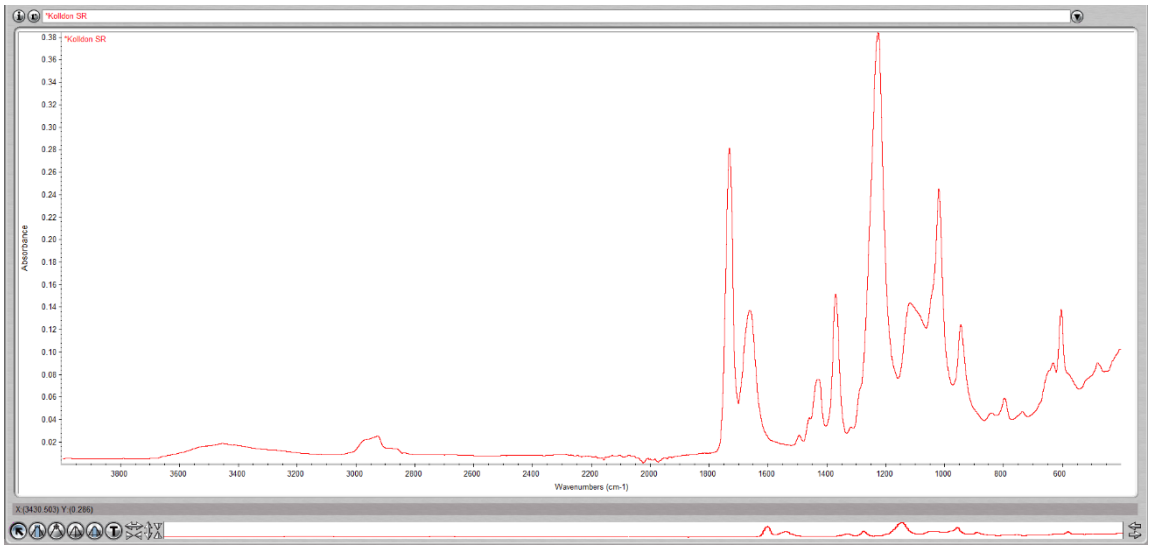

Figure 59: ATR Functional Groups of the KDSR

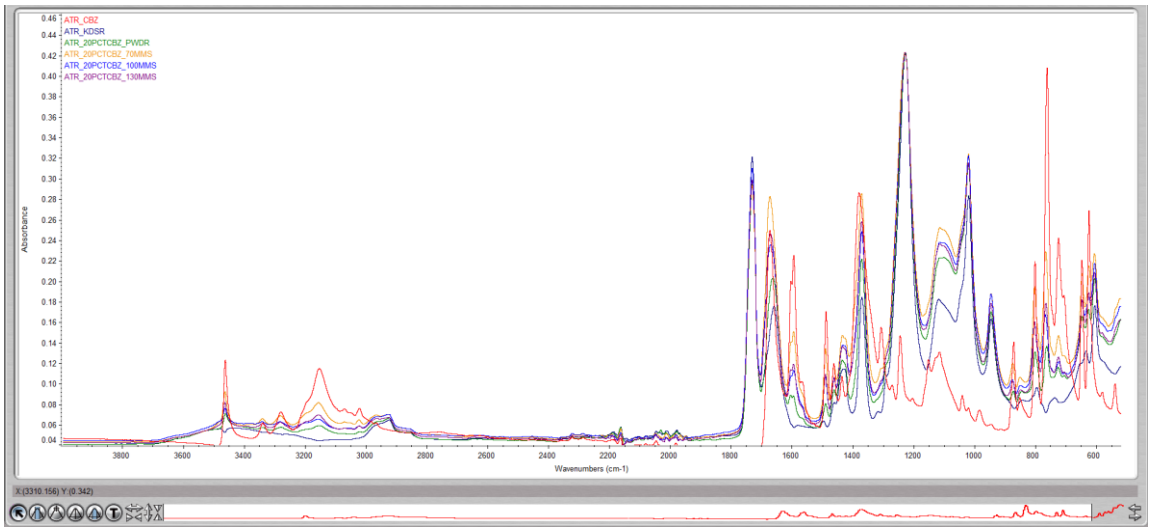

Figure 60: ATR of 20% CBZ Concentration

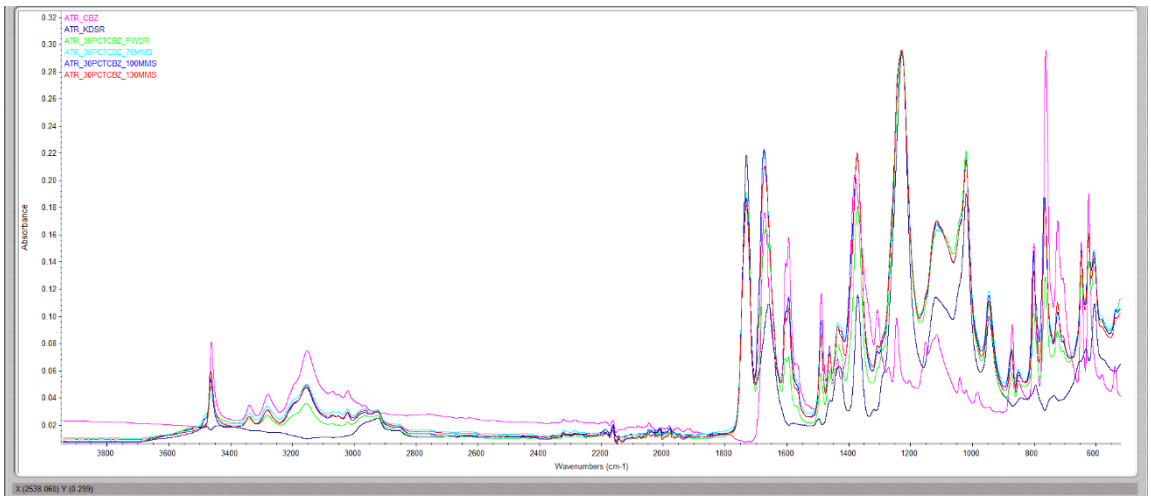

Figure 61: ATR of 30% CBZ Concentration

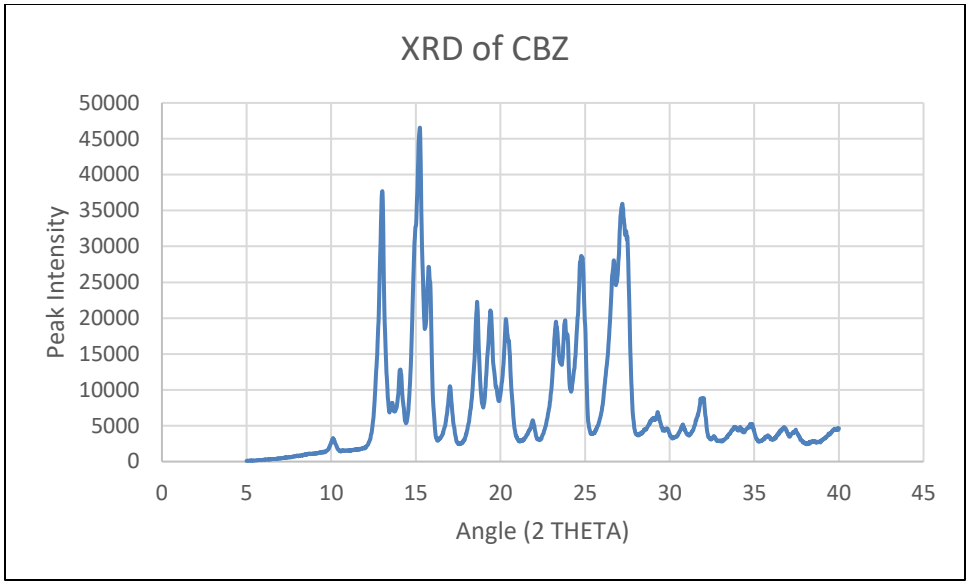

Figure 62: CBZ functional groups for XRD

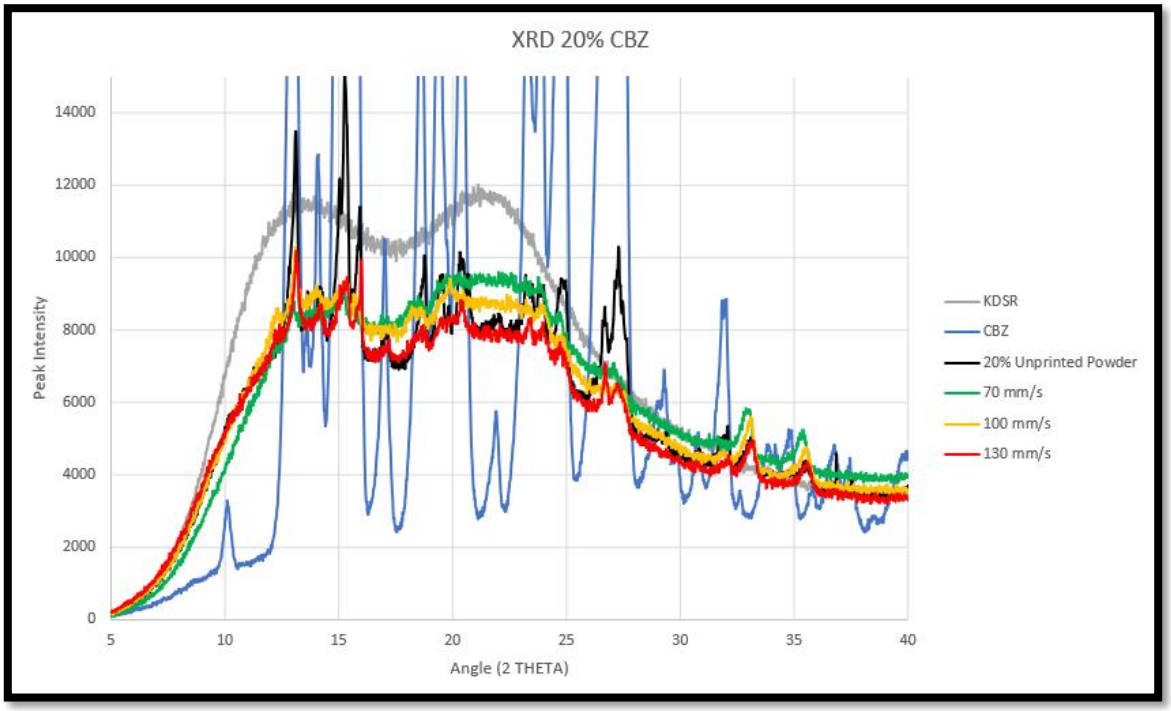

Figure 63: 20% CBZ XRD peak comparison

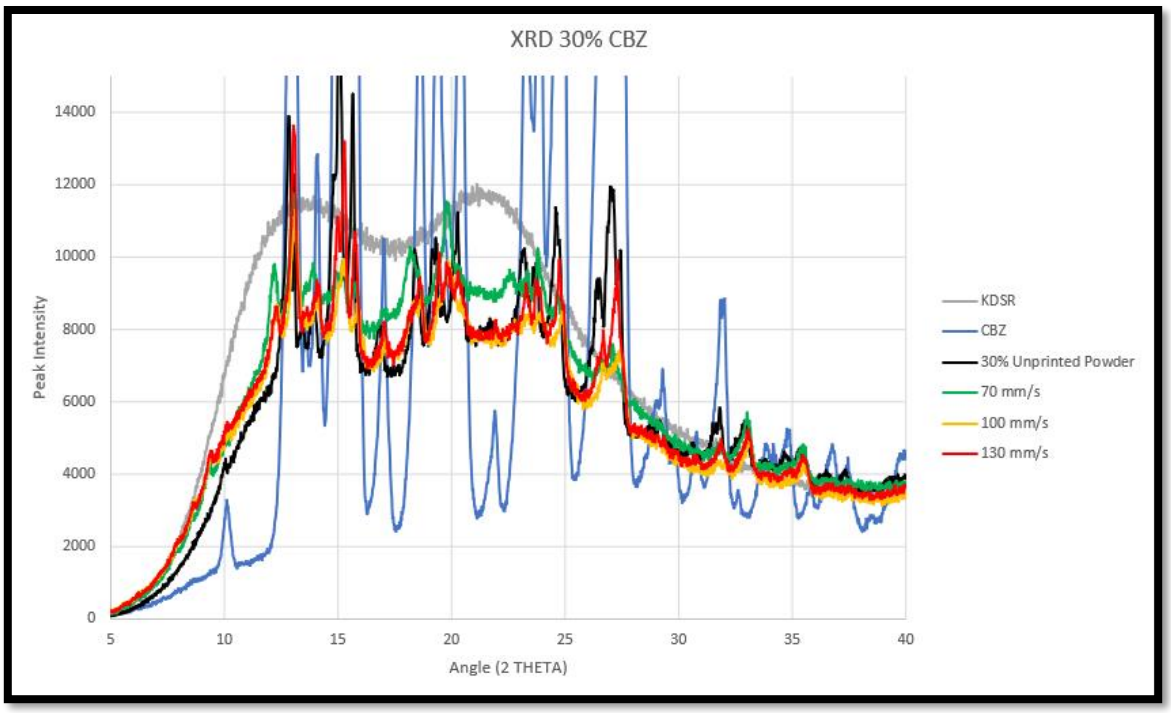

Figure 64: 30% CBZ XRD peak comparison